NASA CR-134914

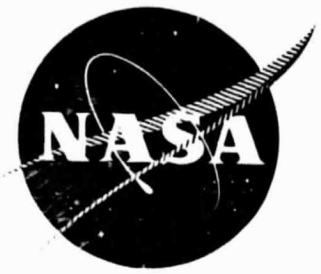

QUIET CLEAN SHORT-HAUL EXPERIMENTAL ENGINE (QCSEE)

Under-the-Wing Engine Simulation Report

by

Advanced Engineering & Technology Programs Department
Group Engineering Division

GENERAL ELECTRIC COMPANY

Prepared For

National Aeronautics and Space Administration

NASA Lewis Research Center
Contract No. NAS3-18021

TABLE OF CONTENTS

LIST OF ILLUSTRATIONS

LIST OF ILLUSTRATIONS (Continued)

LIST OF ILLUSTRATIONS (Concluded)

LIST OF TABLES

SUMMARY

This report describes the hybrid computer simulations of the General Electric QCSEE Under-the-Wing (UTW) experimental engine and control system. The system includes a variable-pitch fan, active inlet Mach number control, and a digital electronic control. The primary purpose of the simulations has been to develop a control system design with the following objectives:

- Fast engine thrust response for powered-lift operations.
- Fast thrust reversing capability.
- Accurate, steady-state and fast response control of the engine where thrust variations are maintained within acceptable limits.

Two hybrid simulations of the engine are used, one for forward thrust operation and one for forward to reverse thrust operation. The hybrid simulations for the engines and the control use both analog and digital computer equipment. The analog is used primarily for dynamics and the digital for function generation.

Simulation results for throttle bursts from 62 to 100 percent net thrust predict that the experimental engine will meet the thrust response requirement of 62 to 95 percent thrust in one second. When transients are made from takeoff to maximum reverse thrust through stall, results predict that the experimental engine will achieve maximum reverse thrust in less than 1.5 seconds; for the conditions investigated, safe engine operation is predicted for these transients. Simulation results for transients from takeoff to maximum reverse through flat pitch predict excessive fan speed; the indication is that a design change to the control logic is needed to reduce peak fan speed during these transients. Since reverse thrust transients through stall have been selected as the primary mode, the decision has been to delay changing the control logic design until there is adequate fan test data in the flat pitch mode.

SUMMARY

This report describes the hybrid computer simulations of the General Electric QCSEE Under-the-Wing (UTW) experimental engine and control system. The system includes a variable-pitch fan, active inlet Mach number control, and a digital electronic control. The primary purpose of the simulations has been to develop a control system design with the following objectives:

- Fast engine thrust response for powered-lift operations.
- Fast thrust reversing capability.
- Accurate, steady-state and fast response control of the engine where thrust variations are maintained within acceptable limits.

Two hybrid simulations of the engine are used, one for forward thrust operation and one for forward to reverse thrust operation. The hybrid simulations for the engines and the control use both analog and digital computer equipment. The analog is used primarily for dynamics and the digital for function generation.

Simulation results for throttle bursts from 62 to 100 percent net thrust predict that the experimental engine will meet the thrust response requirement of 62 to 95 percent thrust in one second. When transients are made from takeoff to maximum reverse thrust through stall, results predict that the experimental engine will achieve maximum reverse thrust in less than 1.5 seconds; for the conditions investigated, safe engine operation is predicted for these transients. Simulation results for transients from takeoff to maximum reverse through flat pitch predict excessive fan speed; the indication is that a design change to the control logic is needed to reduce peak fan speed during these transients. Since reverse thrust transients through stall have been selected as the primary mode, the decision has been to delay changing the control logic design until there is adequate fan test data in the flat pitch mode.

INTRODUCTION

The major purpose of the QCSEE Program is to develop and demonstrate the technology required for propulsion systems for quiet, clean, and economical commercial STOL aircraft. Two of the elements of this comprehensive program are to provide the digital electronic engine control technology required to control a variable-pitch fan engine and to improve engine thrust response.

The UTW experimental engine propulsion system is currently being developed. Three key features of this system are a gear driven, variable-pitch fan, an active inlet duct Mach number control, and a digital electronic control with a 4000 word core memory. The variable-pitch capability of the fan is utilized in both steady-state and transient control of the engine in the forward thrust mode. Engine thrust reversal is achieved by pitch angle changes which reverse the fan tip airflow. The inlet duct Mach number control maintains a nominal 0.79 Mach number at the throat of the inlet during high power, forward thrust operation. Maintaining the inlet Mach number is needed to meet engine noise goals. The digital electric control contains the necessary logic to achieve fast, stable, and safe engine operation in both forward and reverse thrust modes.

Two hybrid simulations of the UTW variable-pitch fan engine have been used to develop the design for the digital electronic control. One has been used for design studies concerned with forward thrust operation; the second has been used for studies concerned with reverse thrust operation. These simulations have provided the capability to analyze and predict the stability and transient response of the engine and control system in each of the above thrust modes.

The analytical models for the UTW variable-pitch fan engine in the forward and the reverse thrust operating modes include the F101 core engine and low pressure turbine; the UTW variable-pitch fan is driven by this low pressure turbine through a main reduction gear. The analytical models for hydromechanical components in the nozzle area, fuel, and compressor stator controls are based on current technology and test experience. Dynamic testing of the advanced fan pitch actuation system is scheduled for completion in late 1977; therefore, experimental verification of the model for the fan pitch actuation system is pending.

The hybrid simulations of the UTW engine and controls were constructed at the General Electric AEG Dynamic Analysis Simulation Center. The simulations were implemented on an Electronic Associates, Inc. 690 Hybrid Computing System. The engine simulation for forward thrust operation was verified by a comparison with cycle deck data from the QCSEE preliminary technical requirements. The simulation for reverse thrust operation in the transition region between forward and reverse is based on a limited amount of GE and NASA test data from engines with similar fans; it is expected that data from future testing of the QCSEE UTW fan will provide the means for verifying this simulation.

The next section of this report summarizes key characteristics of the UTW engine and also describes the general structure of the control system. This is followed by a discussion of the analytical model, which is the mathematical representation of the engine and control system. This section describes the models for the UTW engine in the forward and reverse thrust modes and also the dynamic models for the fan speed, inlet duct Mach number, engine pressure ratio, and the core compressor stator controls. Next, the hybrid simulation is discussed: techniques used in simulating the analytical model and details on verifying the simulation are presented. The remainder of this report contains simulation results for forward and reverse thrust transients at the sea level static, standard day condition.

The UTW hybrid simulation has been used to simulate the effect of selected frictions, backlashes, deadbands, etc. to predict steady state hunting of the control system. The simulation also has been used to predict the transients which would be caused by selected control failures.

UTW EXPERIMENTAL PROPULSION SYSTEM

Engine

The UTW experimental propulsion system, shown in Figure 1, features: a composite high Mach (accelerating) inlet; a gear-driven, variable-pitch fan with composite fan blades; a composite fan vane-frame; a treated fan duct with an acoustic splitter ring; a variable geometry fan exhaust nozzle; an advanced (F101) core and low pressure turbine; a treated core exhaust nozzle; top-mounted engine accessories; and a digital electronic control system combined with a hydromechanical fuel control.

The UTW experimental propulsion system is designed to provide 81,398 N (18,300 lb) of uninstalled thrust and 77,395 N (17,400 lb) of installed thrust at takeoff on a 305.6 K (90° F) day.

The fundamental design criterion which established the engine design approach was the fan engine cycle required to meet the noise objective. The fan and core exhaust pressure ratios were dictated by jet-flap noise constraints. Analysis indicates that, when scaled in accordance with the specified ground rules, the engine will meet all of the program noise objectives.

The fan is a low pressure ratio (1.27), low tip speed [289.6 m/sec (950 ft/sec)] configuration sized to provide 405.5 kg/sec (894 lb/sec) of corrected airflow, at takeoff power setting. It contains 18 composite, variable-pitch fan blades and is driven by the F101 low pressure turbine through a main reduction gear. The fan is capable of blade pitch change from forward to reverse thrust through either flat pitch or stall pitch. The fan variable-pitch actuation and control systems are designed to move the blades from their forward thrust position to reverse in 0.80 to 0.95 seconds.

The fan exhaust nozzle is a variable-area, four-flap design capable of area change from takeoff to cruise, as well as opening to a flared position to form an inlet in the reverse thrust mode. The nozzle flaps are hydraulically actuated.

Control System

The UTW engine control system controls four variables (engine pressure ratio, fan speed, inlet duct Mach number, and compressor stator angle) to achieve an optimum balance between thrust, fuel consumption, noise, exhaust pollution goals, and transient response. Control of engine pressure ratio, fan speed, and inlet duct Mach number is achieved by manipulating fuel flow, fan blade pitch angle, and exhaust nozzle area, respectively.

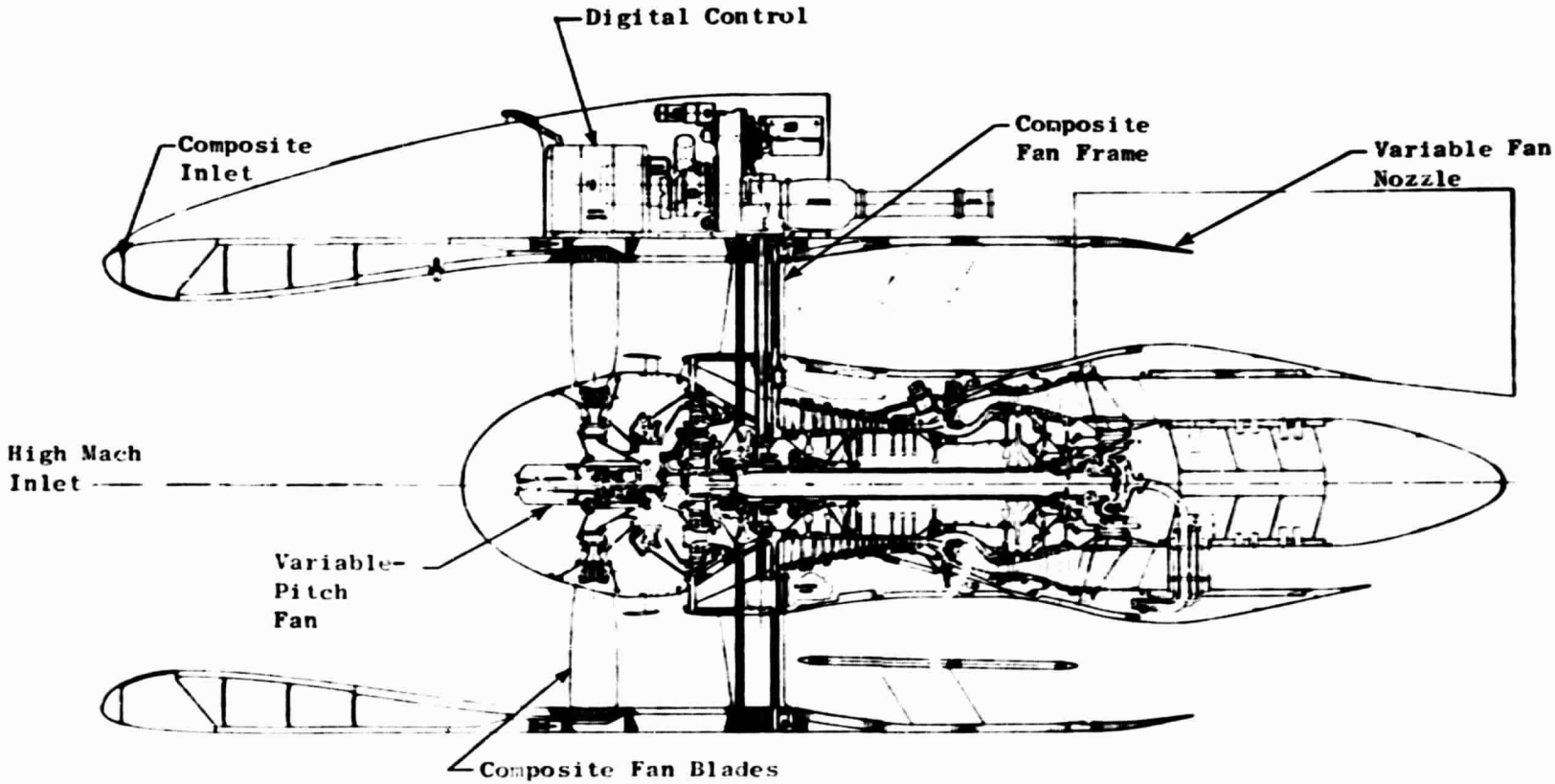

Figure 1. UTW Experimental Propulsion System.

The design incorporates two basic control components, an engine-mounted digital electronic control designed specifically for the QCSEE, and a modified F101 hydromechanical fuel control. The digital electronic control provides the primary control and limiting of engine variables. It modifies the fuel flow demand of the hydromechanical fuel control, which also acts as a backup and provides acceleration and deceleration limits.

The primary design requirements for the overall control system are:

- Thrust control throughout specified flight map with minimum pilot workload
- Fast thrust response

  1.0 second from 62% to 95% forward thrust

  1.5 seconds from takeoff to maximum reverse thrust
- Specified noise and pollution goals

The general structure of the control system is shown in Figure 2. The digital electronic control is the heart of the system and controls the manipulated variables in response to commands representing those which would be received from an aircraft propulsion system computer. The system includes a hydromechanical control which incorporates an electro-hydraulic servovalve through which the digital control maintains primary control of the fuel flow. The fuel-operated servomechanisms in the hydromechanical control serve primarily as backup fuel-controlling elements and acceleration/deceleration limits although they are the primary controlling elements for the core compressor stators.

An F101 fuel pump is used for supplying engine fuel, for operating servomechanisms in the hydromechanical control, and for providing a source of high pressure fuel for operation of the actuators which position the core compressor stator vanes. A variable-displacement, constant-pressure hydraulic pump supplies fluid for operation of the actuators which position the fan nozzle and the hydraulic motor which drives the variable-pitch actuation mechanisms.

The experimental system includes both automatic and manual operating modes. The automatic mode provides integrated control of engine variables to permit exploration of steady-state and transient characteristics of the engine. The manual mode and several partial-automatic/partial-manual modes provide experimental flexibility to allow independent manipulation of controlled variables so that engine characteristics can be completely mapped.

The definition of the automatic control mode was made primarily on the basis of a tolerance analysis. This analysis used a computer program which evaluated many potential modes. The modes were evaluated relative to the accuracy with which they maintain key engine variables when subjected to typical control and engine manufacturing tolerances, sensing tolerances, and

The design incorporates two basic control components, an engine-mounted digital electronic control designed specifically for the QCSEE, and a modified F101 hydromechanical fuel control. The digital electronic control provides the primary control and limiting of engine variables. It modifies the fuel flow demand of the hydromechanical fuel control, which also acts as a backup and provides acceleration and deceleration limits.

The primary design requirements for the overall control system are:

- Thrust control throughout specified flight map with minimum pilot workload
- Fast thrust response

  1.0 second from 62% to 95% forward thrust

  1.5 seconds from takeoff to maximum reverse thrust
- Specified noise and pollution goals

The general structure of the control system is shown in Figure 2. The digital electronic control is the heart of the system and controls the manipulated variables in response to commands representing those which would be received from an aircraft propulsion system computer. The system includes a hydromechanical control which incorporates an electro-hydraulic servovalve through which the digital control maintains primary control of the fuel flow. The fuel-operated servomechanisms in the hydromechanical control serve primarily as backup fuel-controlling elements and acceleration/deceleration limits although they are the primary controlling elements for the core compressor stators.

An F101 fuel pump is used for supplying engine fuel, for operating servomechanisms in the hydromechanical control, and for providing a source of high pressure fuel for operation of the actuators which position the core compressor stator vanes. A variable-displacement, constant-pressure hydraulic pump supplies fluid for operation of the actuators which position the fan nozzle and the hydraulic motor which drives the variable-pitch actuation mechanisms.

The experimental system includes both automatic and manual operating modes. The automatic mode provides integrated control of engine variables to permit exploration of steady-state and transient characteristics of the engine. The manual mode and several partial-automatic/partial-manual modes provide experimental flexibility to allow independent manipulation of controlled variables so that engine characteristics can be completely mapped.

The definition of the automatic control mode was made primarily on the basis of a tolerance analysis. This analysis used a computer program which evaluated many potential modes. The modes were evaluated relative to the accuracy with which they maintain key engine variables when subjected to typical control and engine manufacturing tolerances, sensing tolerances, and

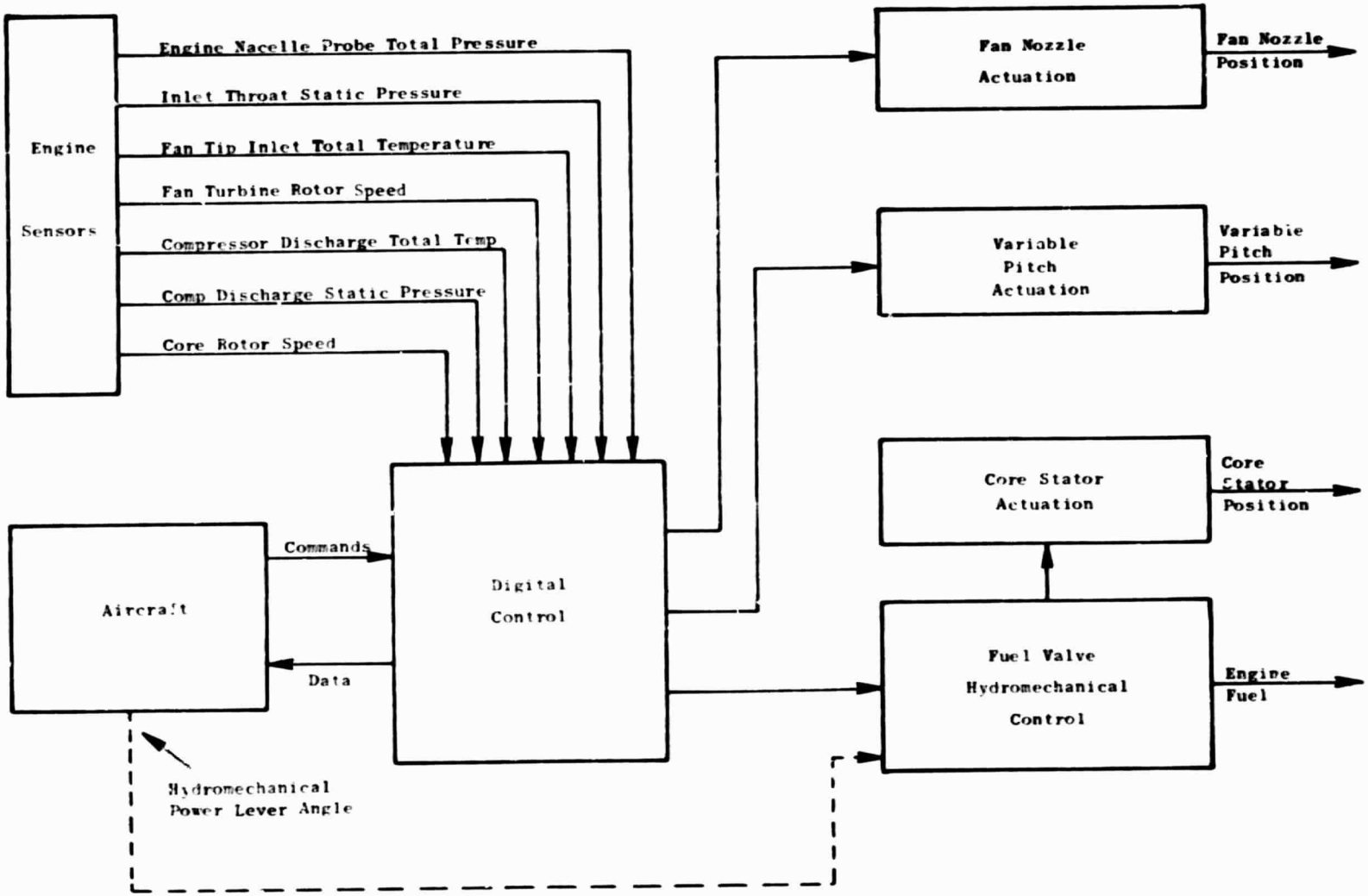

Figure 2. QCSEE UTW Control System Schematic.

hardware deterioration. Scheduling practicality, stability, response, and failure considerations were also factors in choosing the control mode. The automatic mode chosen from the above studies is one in which fuel flow is manipulated to control engine pressure ratio (PS3/PT0 which is a variable related closely to thrust), fan pitch is manipulated to control fan speed, and fan nozzle area is manipulated to control inlet duct Mach number (a key inlet noise parameter).

ANALYTICAL MODEL

The analytical model represents the functional relations that exist between the variables of the QCSEE UTW engine and control system. The engine portion of the model is based on the steady-state conservation equations of the cycle deck with the addition of significant dynamics. The model included two different representations of the engine. One is used for hybrid simulation studies concerned with the forward thrust mode, and the second for studies on the reverse thrust mode. The model contains detailed representations of the primary control system components, which are the fan speed control, the inlet duct Mach number control, and the engine pressure ratio and compressor stator controls. The contents of these models are discussed in the following sections.

Forward Thrust Engine Model

General- The engine model is based on the digital cycle deck used to generate the QCSEE preliminary technical requirements. Significant dynamics represented are rotor dynamics, heat soak, and combustion delay. The transient effects of heat soak, combustion delay, and compressor stator error are based upon past experience with the F101 core engine. Distortion and reingestion effects are not included in the model. The component models use overall component maps with the exception of the variable-pitch fan. Mixing of gas flows has been lumped at the engine stations where a temperature calculation is necessary in order to conserve memory and equipment. Figure 3 illustrates the information flow between components in the forward thrust engine model and should help the reader in understanding the description for individual components discussed in the following paragraphs.

Inlet - The inlet model receives flight altitude, Mach number and temperature increment from standard day ambient temperature as determined by the desired flight condition. Fan front face total flow is received from the fan when the inlet is in the installed mode. Outputs are free stream pressure and temperature, inlet throat static and total pressures, and fan front face total temperature and pressure. The inlet is assumed ideal with a specific heat ratio of 1.4. No distortion or reingestion effects are considered. The only dynamics are to provide inlet simulation stability in the installed mode which produces a total pressure drop between inlet throat and fan front face.

Fan - The fan model receives front face total temperature and pressure from the inlet, physical speed from the LP rotor, pitch angle from the control, compressor inlet flow from the compressor, and bypass jet nozzle flow from the fan nozzle. Outputs are fan hub and tip discharge total temperatures and pressures, and hub and tip horsepowers. The variable-pitch fan map is based on the cycle deck representation which uses corrected inputs to perform standard day calculations that are uncorrected to obtain the proper results.

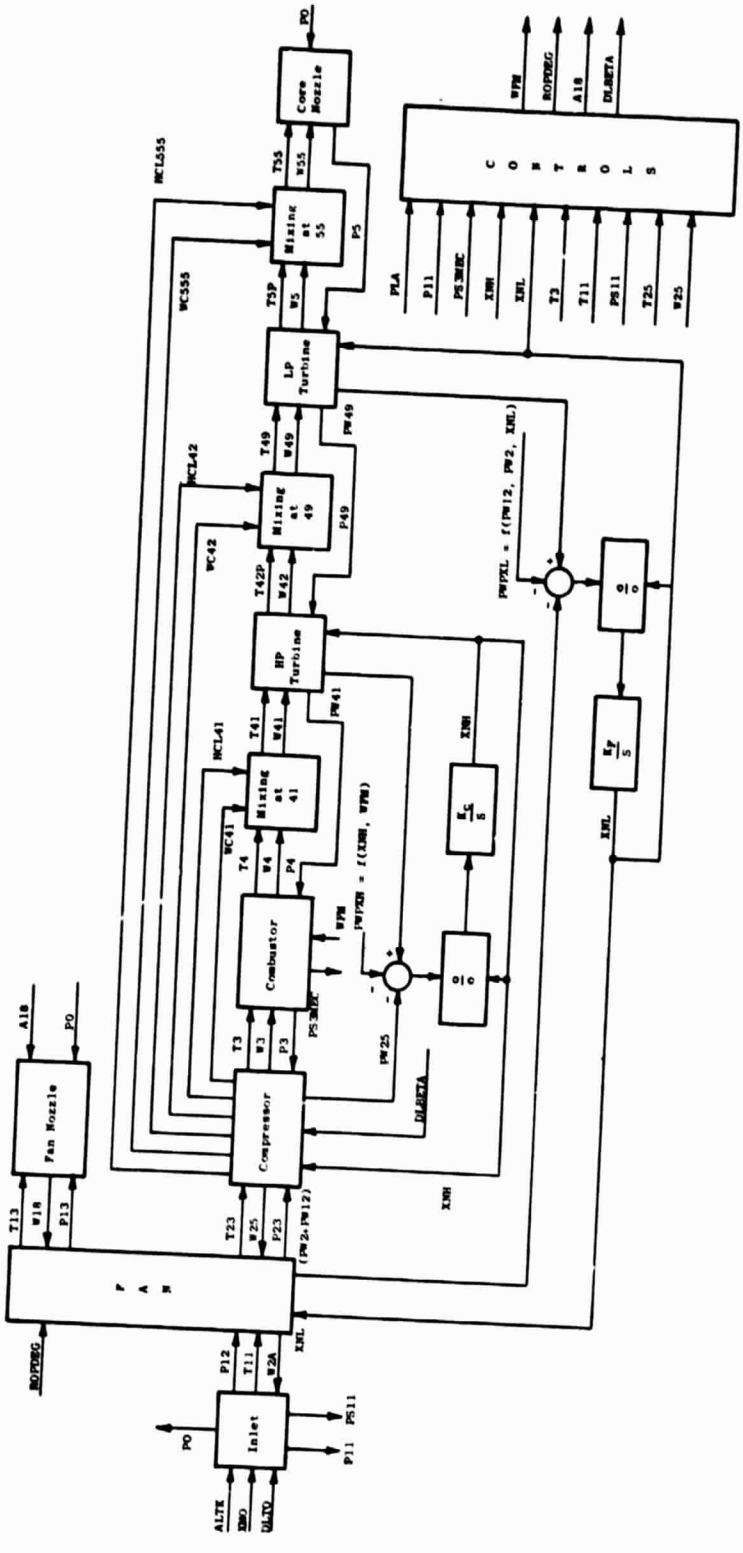

Figure 3. Forward Thrust Simulation Information Flow Diagram.

Reynolds number effects are assumed to be insignificant. The only dynamics in the simulation of this model come from an internal iteration on the fan map work function.

Fan Nozzle - The fan nozzle model receives fan tip discharge total temperature and pressure from the fan, free stream pressure from the inlet, and bypass jet nozzle throat actual area from the control. The representation is steady state since an investigation of the duct volume indicates time constants of less than 8.0 msec on nozzle flow. The total pressure drop from fan tip discharge to bypass jet nozzle throat was linearized as a function of the square of downstream flow function.

Compressor - The compressor model receives fan hub discharge total temperature and pressure from the fan, compressor discharge total pressure from the combustor, physical speed from the HP rotor, and off-stator error from the control. Produced are compressor inlet and discharge airflows, compressor discharge total temperature, compressor horsepower, and cooling flows and enthalpies. Reynolds number effects are assumed negligible and omitted. Compressor inlet total pressure drop is linearized with respect to inlet flow function between ground idle and takeoff power levels. The off-stator error (DLBETA) is used to modify compressor airflow based on experience with previous representations of the F101 core compressor. The only dynamics are due to heat soak which produces an effective lag in compressor discharge total temperature.

Combustor - The combustor model receives compressor discharge airflow and total temperature from the compressor, high pressure turbine inlet total pressure from the HP turbine, and fuel flow from the control. Produced by the simulation are combustor discharge gas flow, compressor discharge total and static pressure, and HP turbine first-stage nozzle inlet total temperature. The total pressure drop across the combustor is linearized with respect to compressor discharge flow function, as is the drop from total to static pressure at the compressor discharge. Both linearizations are based on values at ground idle and takeoff power conditions. The only dynamics are due to a combustion delay between the fuel flow produced by the control and the fuel burned in the engine which is based on experience with the F101 combustor.

Mixing - Mixing of primary gas flow and cooling flow occurs at several points in the model and is basically the same at each. Inputs are the primary gas flow and its total temperature and the cooling flow and its enthalpy. Steady-state conservation of energy is then used to solve the resulting total temperature. Outputs are gas flow and total temperature after mixing. There is no effect on total pressure.

Mixing prior to the high pressure turbine differs from the other mixing models due to the dynamics of a heat soak calculation which produces a lagged total temperature output. These dynamics are based on previous experience with similar configurations. The other mixing models have no dynamics; small filters are used to stabilize the simulation of these mixing models.

High Pressure Turbine - The high pressure turbine model receives rotor inlet gas flow and total temperature from a mixer, low pressure turbine inlet total pressure from the LP turbine, and physical speed from the HP rotor. Produced are HP turbine inlet total pressure, discharge gas flow, discharge total temperature before mixing, and horsepower. To conserve memory, the overall component maps of the cycle deck were refit to provide the desired accuracy using a fewer number of points. Volume dynamics are not included because their natural frequencies are significantly higher than the frequency range to be represented by the model. The only dynamic effect is a 20 millisecond lag on HP turbine inlet gas flow which is necessary for simulation stability.

Low Pressure Turbine - The low pressure turbine model receives rotor inlet gas flow and total temperature from a mixer, discharge total pressure from the core nozzle, and physical speed from the LP rotor. Produced are LP turbine inlet total pressure, discharge gas flow, discharge total temperature before mixing, and horsepower. To conserve memory, the overall component maps of the cycle deck were refit to provide the desired accuracy using a fewer number of points. Volume dynamics are not included because their natural frequencies are significantly higher than the frequency range to be represented by the model. The only dynamic effect is a 25 millisecond lag on LP turbine inlet total pressure which is necesaary for simulation stability.

Core Nozzle - The core nozzle model receives low pressure turbine frame discharge gas flow and total temperature from a mixer, and free stream pressure from the inlet. The representation is steady state, i.e., no volume dynamics. The total pressure drop from primary jet nozzle throat to low pressure turbine discharge was linearized with respect to the square of the downstream flow function using the values at the ground idle and takeoff power conditions.

Rotor Dynamics - Rotor speeds are computed by using the conservation of angular momentum. The fan (LP) rotor receives fan tip and hub horsepowers from the fan, low pressure turbine horsepower from the low pressure turbine, and a horsepower loss term. The horsepower loss term is an empirically determined function based on cycle deck data. All moments of inertia have been reflected to the fan side of the gearbox. Using this inertia, a dynamic value for fan physical speed is calculated.

For the core (HP) rotor, a dynamic HP compressor physical speed is calculated using the core inertia and horsepowers from the compressor, HP turbine, HP rotor loss calculation and desired customer power takeoff. The HP rotor horsepower loss calculation is based on empirical fit of cycle deck data.

Reverse Thrust Engine Model

The model of the UTW engine for reverse thrust includes the same core engine components as used in the forward thrust engine model; the reverse inlet, fan, and fan nozzle are different. Due to digital memory limitations of the hybrid computer used, it was not possible to implement the cycle

deck representations for the reverse inlet, fan, and fan nozzle. For this reason, the reverse thrust model is not as accurate as might be desired in either the forward or reverse mode. However, the slight loss of steady-state accuracy is judged to be of minor importance, since the transition region between forward and reverse is not defined in the cycle deck. As shown in Figure 4, the model is constructed with two different paths or modes depending on the direction of fan front face total flow (W2A). The forward mode occurs when W2A is greater than zero. The reverse mode occurs when W2A is less than or equal to zero. Additional logic to provide a smooth transition between the modes is another necessary portion of the model.

In the forward mode, the inlet of the reverse thrust model is the same as used in the forward thrust model. In the reverse mode, the inlet functions as a nozzle by calculating a back pressure for the fan. The inlet/nozzle uses the free stream pressure from the standard inlet, fan pitch angle from the control, and fan front face flow and total temperature from the fan to calculate fan front face pressure. Also calculated is reverse thrust due to the fan.

Three different fan maps are used in the reverse thrust model depending on whether the fan is in the forward, reverse through stall, or reverse through flat pitch mode. The forward mode fan map uses a flow map acquired from NASA, and both reverse flow maps are based on the NASA technique. Modifiers to extend the fan flow maps through the transition region are based on GE and NASA test data from similar fans.

In the forward mode, the fan receives fan front face total temperature and pressure from the inlet, pitch angle from the control, physical speed from the fan rotor, compressor inlet airflow from the compressor, and fan tip discharge total pressure from the fan nozzle. Efficiency is curve fit as a function of pressure ratio and corrected fan speed. Produced are fan tip and hub total temperatures, fan front face flow, bypass jet nozzle flow, hub discharge total pressure, and tip and hub horsepower.

In the reverse mode, the fan receives front face total pressure from the inlet, tip discharge total temperature and pressure from the fan nozzle, compressor inlet airflow from the compressor, pitch angle from the control, and physical speed from the LP rotor. Efficiency is assumed to be constant. Produced are fan front face flow and total temperature, bypass jet nozzle flow, and tip and hub horsepowers. None of the fan representations include dynamic effects.

In the forward mode, the nozzle of the reverse thrust model receives fan tip discharge total temperature and bypass jet nozzle flow from the fan, bypass jet nozzle throat actual area from the control, and free stream pressure from the inlet. Produced is fan tip discharge total pressure. In the reverse mode, the nozzle receives free stream temperature and pressure from the inlet,, and bypass jet nozzle flow from the fan. Produced are fan tip and hub discharge total temperatures and pressures. No volume dynamics are used.

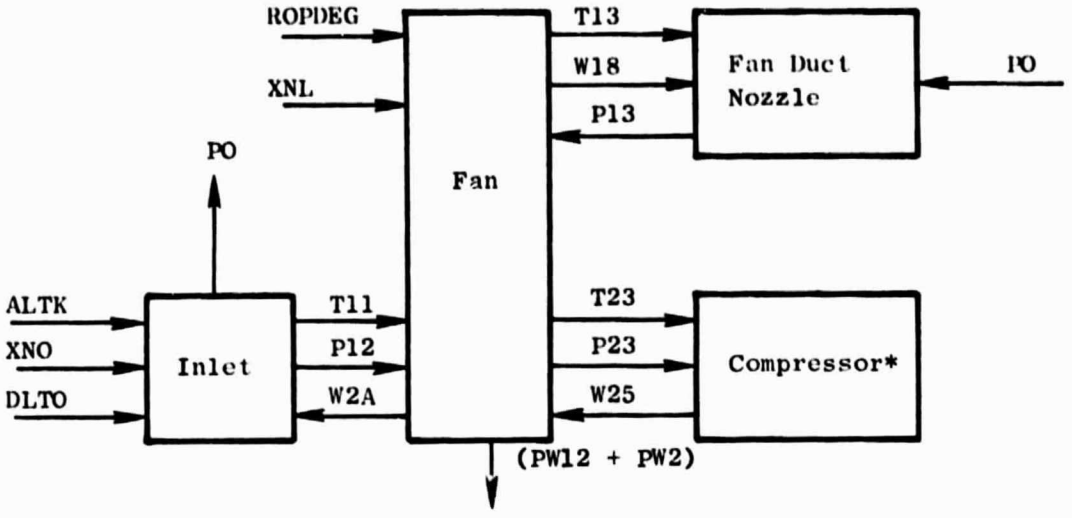

Forward Mode (W2A > 0)

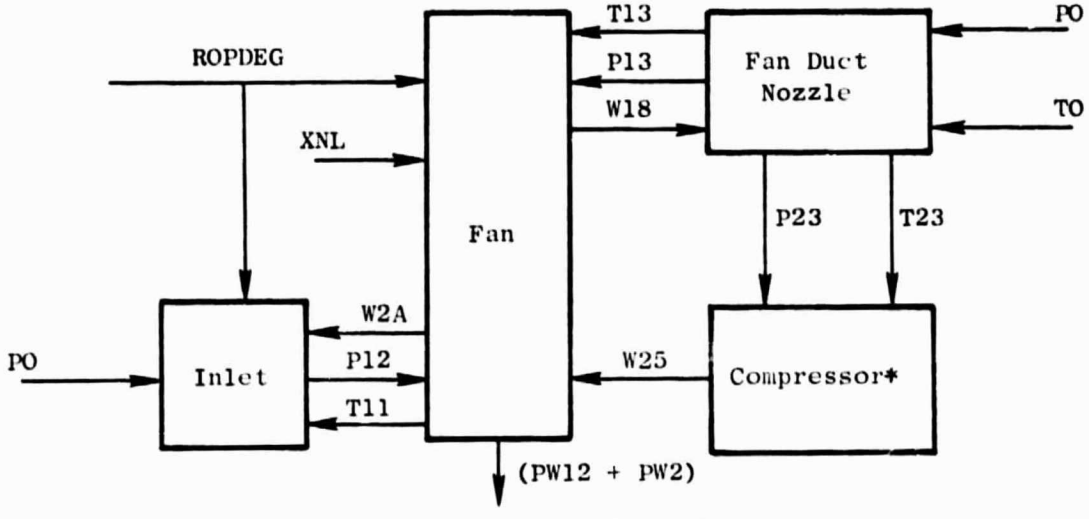

Reverse Mode (W2A ≤ 0)

* Model of core compressor and succeeding core engine components is the same as used in the forward thrust simulation.

Figure 4. Reverse Thrust Simulation Information Flow Diagram

Fan Speed Control

The schematic of the fan speed control model is shown in Figure 5. The model includes representations for the digital electronic and the hydromechanical portions of this control. The digital electronic portion contains the fan speed, the fan pitch floor, and the fan pitch roof controllers; for a forward thrust command, the output from one of these controllers is selected to control the hydraulic motor and thus manipulate fan pitch. For a reverse thrust command, control of the hydraulic motor is switched to the reverse pitch controller. The hydromechanical portion of the fan speed control model includes a servovalve, hydraulic motor, and a gear drive assembly. The following paragraphs discuss the combined operation of the digital electronic controllers and the hydromechanical actuation system. Next, details included in the models for the digital electronic and hydromechanical portions are described.

Control Operation - The primary control mode for high power, forward thrust conditions is the manipulation of fan pitch to control fan speed. The inputs to the fan speed controller are (1) the difference between the scheduled and sensed fan speed, and (2) the sensed position of the hydraulic motor which positions the fan blade pitch. When the sensed pitch angle is within the prescribed roof and floor limits, the output of the fan speed controller is selected and determines the torque motor current output (I_B) from the digital control. This current positions an electro-hydromechanical servovalve which is ported to the hydraulic motor. The magnitude and polarity of the current (I_B) determines the magnitude and direction of hydraulic flow to the motor - and thus the rate and direction of motor rotation. The motor shaft is geared to the fan blades and thus positions their pitch angle.

The output of the motor position sensor feeds back to the fan speed controller, which computes the rate of change of sensed motor position. This rate signal is fed through a first order lag before it is subtracted from a signal which is proportional to fan speed error. For small perturbations, the transfer function from fan speed error to fan pitch angle is approximated at low frequencies by:

$$\frac{\Delta\text{Fan Pitch}}{\Delta\text{Fan Speed Error}} \approx \frac{K(0.3\,S+1)}{S}$$

The lead time constant in this transfer function is due to, and thus equal to, the time constant of the above mentioned first order lag in the feedback to the fan speed controller. In summary, the fan speed - pitch control is an integrating type control with lead compensation. The lead time constant is sized to compensate for the engine lag from fan pitch angle to fan speed and, thus, provide adequate stability margin for accurate, fast response fan speed control.

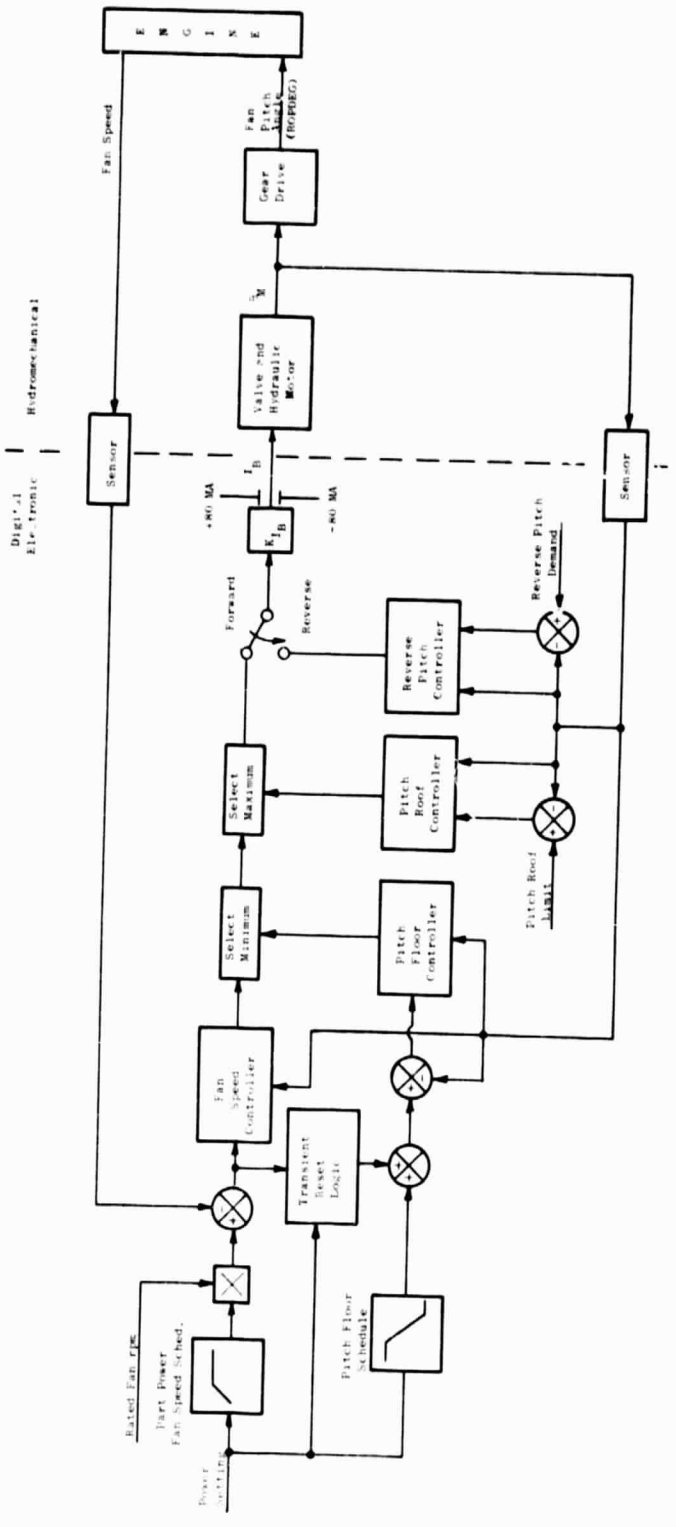

Figure 5. Fan Speed Control Model.

The fan pitch floor and roof controllers limit the pitch angle to maximum and minimum values in the forward thrust mode. Both of these controllers use the lagged rate feedback technique discussed above and produce the following transfer function characteristics at low frequencies:

$$\frac{\Delta \text{Fan Pitch}}{\Delta \text{Pitch Position Error}} \sim \frac{K(0.3\ S+1)}{S(0.1\ S+1)}$$

Thus each is an integrating-type position control, for accuracy considerations.

The floor schedule, which is a function of power setting, feeds the floor controller. If the fan speed controller requests a pitch position more closed (positive) than the floor schedule, the pitch floor controller output is selected and controls the motor position. During throttle bursts from approach to takeoff power conditions, the transient reset logic biases the floor schedule four degrees in the opened (negative) direction until the fan accelerates to within 3 percent of the final speed. This reset action is a contributing factor in achieving the required acceleration time to 95 percent thrust.

The purpose of the roof limit controller is to protect against fan stall during transients in the forward thrust mode. This controller is selected to control the hydraulic motor when the fan speed controller requests a pitch angle further open than the roof limit.

For a reverse thrust command, control of the hydraulic motor is switched to the reverse thrust controller. The dynamic design of this position control is the same as the floor and roof controls. Transient time from takeoff to reverse pitch position is 0.80 to 0.95 seconds.

Digital Electronic Portion of Speed Control - The simulation has been used to develop the design and specifications for the digital electronic portion of the fan speed control. Appendix A contains the block diagrams and the specifications for gains, time constants, limits, and schedules which define the digital electronic portion of this control for the first build of the UTW experimental engine. The model used in simulation studies represents those details in Appendix A which have been essential to develop/evaluate the steady-state stability and transient response of the UTW experimental engine and overall control system. The model includes the Appendix A specifications for gains, time constants, limits, fan pitch floor and roof schedules, transient reset logic, and switching logic between automatic forward and reverse thrust. Because of computer facility limitations when the UTW simulation was being developed, the takeoff speed schedule (function of PTO and T12) and the logic for detecting a failure in one of the position feedback sensors are not included in the simulation; the judgment is that these items are not essential in predicting stability and transient response at experimental engine test conditions. Also it should be noted that the part power fan speed schedule in the simulation is set at a constant equal to 3067 rpm, which is the fan speed at the takeoff, sea level static, standard

day condition. This schedule has not been developed for low power setting conditions due to limitations in the QCSEE cycle deck definition for the fan; final development of this schedule should be accomplished after fan performance tests on the QCSEE experimental engine.

The model includes 0.01 second lag time constants for the torque motor driver amplifier, speed sensor, and hydraulic motor position sensor. The effect of the digital control computer time delay is approximated by an analog type representation which is based on current estimates for total cycle time of the control computer and on sample data effects of digital to analog conversion (Reference 2). The representation for digital control computer time delay is discussed in the report section on techniques used in the "Hybrid Simulation."

Fan Pitch Hydromechanical Actuation System -- Two fan pitch hydromechanical actuation systems are being developed as a part of the UTW experimental engine program. A hydraulic motor/harmonic drive/cam system is being developed by the Hamilton Standard Division of United Technologies Corporation (HS) under subcontract to the General Electric Company. A hydraulic motor/ball spline actuation system is being developed by GE. A description of the hardware for these two actuation systems is contained in the UTW Engine Digital Control System Design Report (Reference 1).

Both detailed and simplified models of these two actuation systems have been constructed. The detail models of the HS and GE actuation systems have been used primarily in simulation studies on performance as affected by the hydromechanical component characteristics and limits; for example, gearbox friction, motor friction, allowable peak motor speed, etc. These detail models have been based on information supplied by HS and GE component design engineers. A description of these models and the simulation study results are presented in the control system design report (Reference 1).

Because of computer facility limitations, simplified models for the HS and GE actuation system designs have been constructed for use in simulation studies associated with overall engine-control system steady-state and transient response. The representation for the no-back is simplified in these models; hydraulic pump dynamics are not included. The frequency response (1 to 5 Hz range) for both simplified models has been compared with the frequency response from the respective detail model; reasonable agreement has been demonstrated in each case.

The simplified model for the GE actuation system design was used in early simulation studies on engine-control system hunting at the takeoff power setting; results of this hunting investigation are discussed in the control system design report (Reference 1). Subsequently, NASA and GE selected the HS design to be the primary actuation system for the first build of the UTW experimental engine. Engine-control system dynamic response with the HS design is discussed in the results section of this simulation report.

The simplified model for the GE actuation system design is described by the block diagram in Figure 6. This model includes the servovalve dynamics and also the effect of motor pressure drop (ΔP_M) on servovalve flow (Q_{BV}) and motor leakage flow (Q_{LM}). Hydraulic motor speed (N_M) is represented as a linear function of the difference between Q_{BV} and Q_{LM}. (Note: Motor and gear assembly inertias are not included in this model because the frequency range of concern is five Hertz or less; the inertias do not have a significant effect in this frequency range.) The fan blade aero load is approximated by a linear function of blade position (ROPDEG); this approximation is sized for the ROPDEG range at the takeoff power condition. The operation of the no-back is simulated by the logic in Figure 6, which switches as a function of motor speed (N_M) being less than - 8rpm. When operating at forward thrust blade angle positions, this logic provides a reasonable representation of whether fan blade loads are transmitted through the no-back upstream to the motor.

The simplified model for the HS actuation system design is described by the block diagram in Figure 7. This model includes the dynamics associated with the servovalve and the valve pressure drop. The difference between servovalve flow (Q_{BV}) and motor displacement flow (Q_M) is used to calculate motor pressure drop (ΔP_M), based on the bulk modulus effect in the servovalve lines to the hydraulic motor. The equation used in the simulation is:

$$\Delta P_M = \left[\frac{\partial P_M/\partial Q_E}{\tau_M S+1}\right]\left[Q_{BV} - Q_M\right]$$

The dynamic representations for the hydraulic motor and the downstream gearbox/harmonic drive/cam assembly are coupled by the flex shaft spring rate; lumped inertias are used in each representation. Friction and fan blade aero loading are included. The operation of the no-back is approximated by the logic in Figure 7, which switches as a function of downstream gearbox input shaft speed (N_C) being less than - 20 rpm and also the direction of the total load torque (T_L). The load torque produces a twisting moment to close the fan blades when $T_L \geq 0$ and to open when $T_L < 0$. In the forward thrust mode, $T_L \geq 0$; whereas, $T_L < 0$ during reverse thrust operation. The switching logic for $T_L < 0$ was not included in the actual simulation; and the simulation predicts a transient time to reverse no more than 0.03 second less than had the logic been included.

Inlet Duct Mach Number Control

The schematic of the inlet duct Mach number control is shown in Figure 8. The model includes representations for the digital electronic and hydromechanical portions of this control. The digital electronic portion contains the

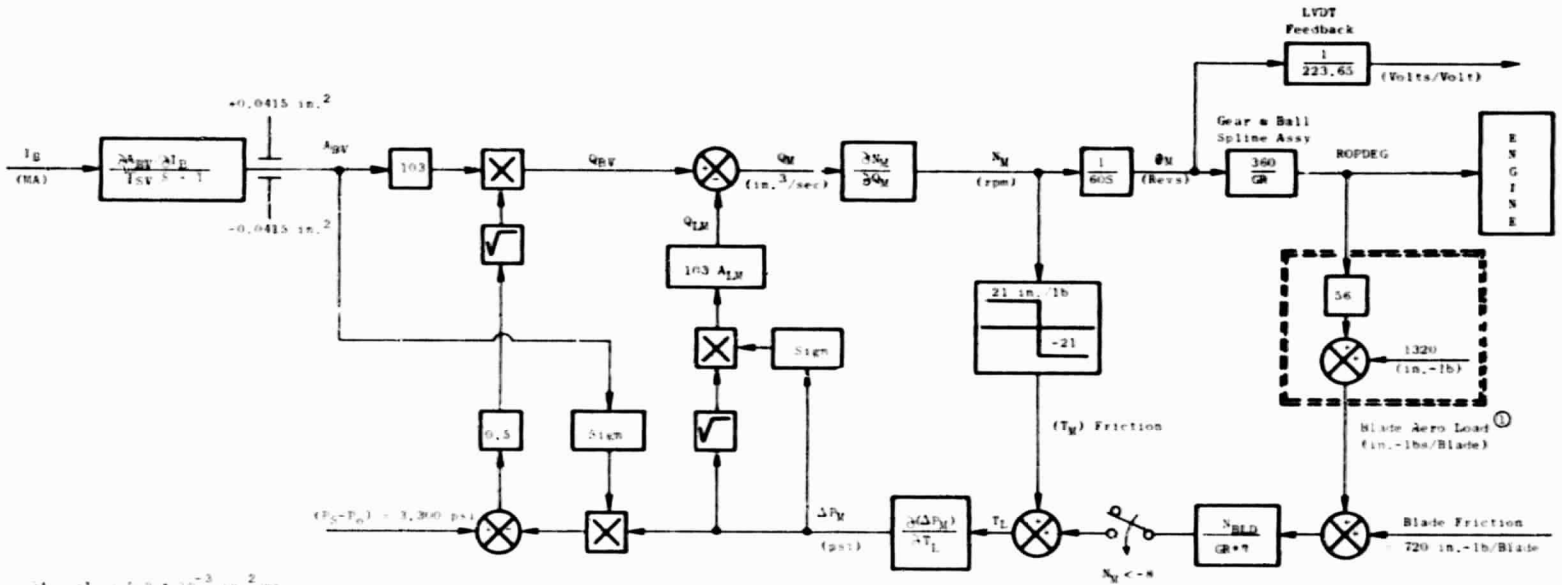

$A_{BV} = I_B = 5.2 * 10^{-3}$ in.² ma
$\tau_{SV} = 9.1 * 10^{-2}$ sec
$A_{LM} = 3.234 * 10^{-4}$ in.²
$\frac{\partial N_M}{\partial Q_M} = 136.42$ rpm/in.³ sec
$\frac{\partial \Delta P_M}{\partial T_L} = 14.286$ psi/in.-lb
$\tau = 0.66025$
GR = 666 revs rev ②
N_{BLD} = 18 Blades

Notes

① Linear Approximation for Blade Aero Load at Takeoff Power Setting.

② Initial Design Value of Gear Ratio = 666 Used in Simulation Studies, Final Design Value Selected After Studies is GR = 474.64

Figure 6. Fan Pitch Hydromechanical Actuation System (GE Design) Simplified Model for Hunting Investigation at Takeoff Power Setting.

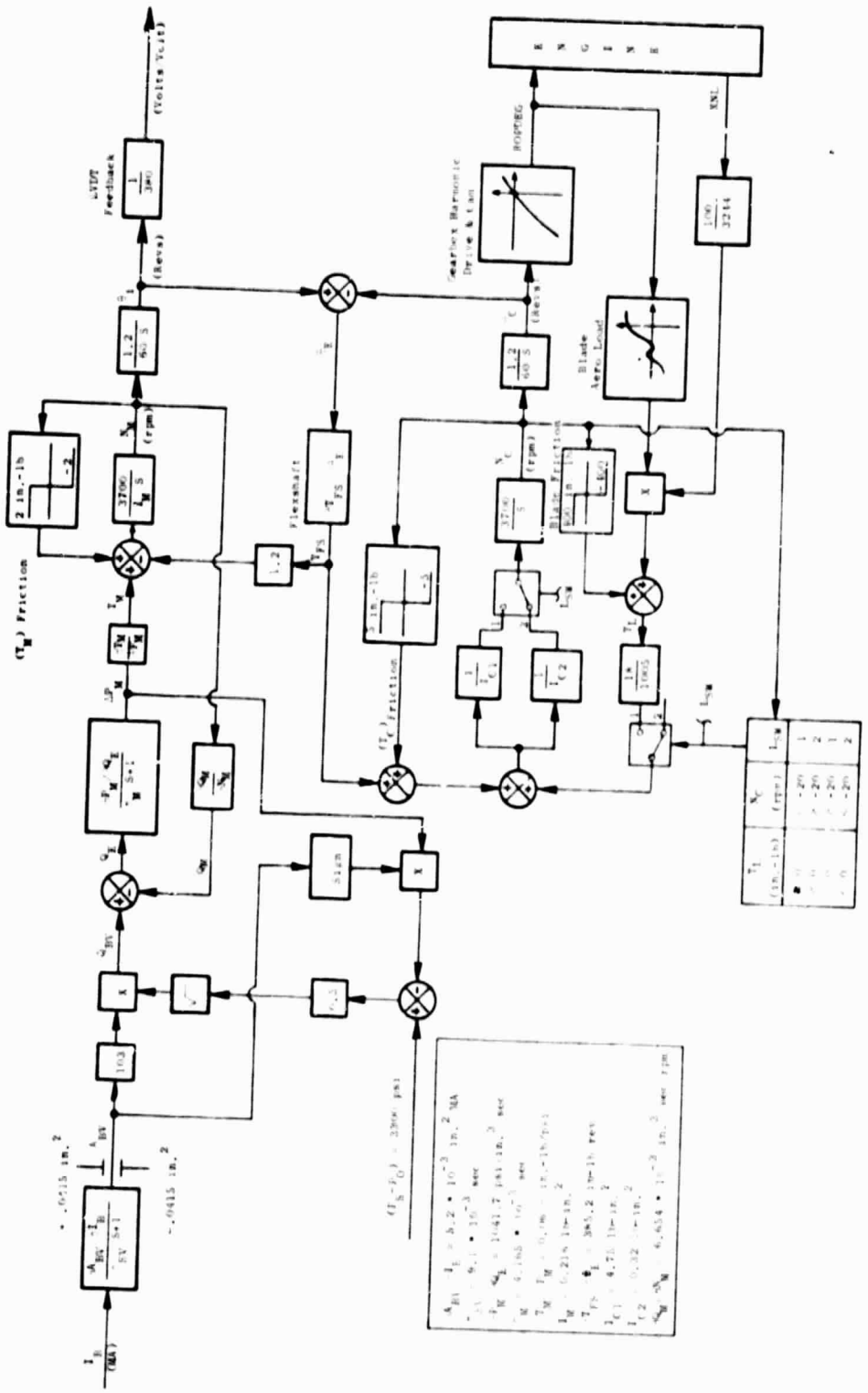

Figure 7. Fan Pitch Hydromechanical Actuation System (HS Design) Simplified Model for Engine-Control System Transient Response Studies.

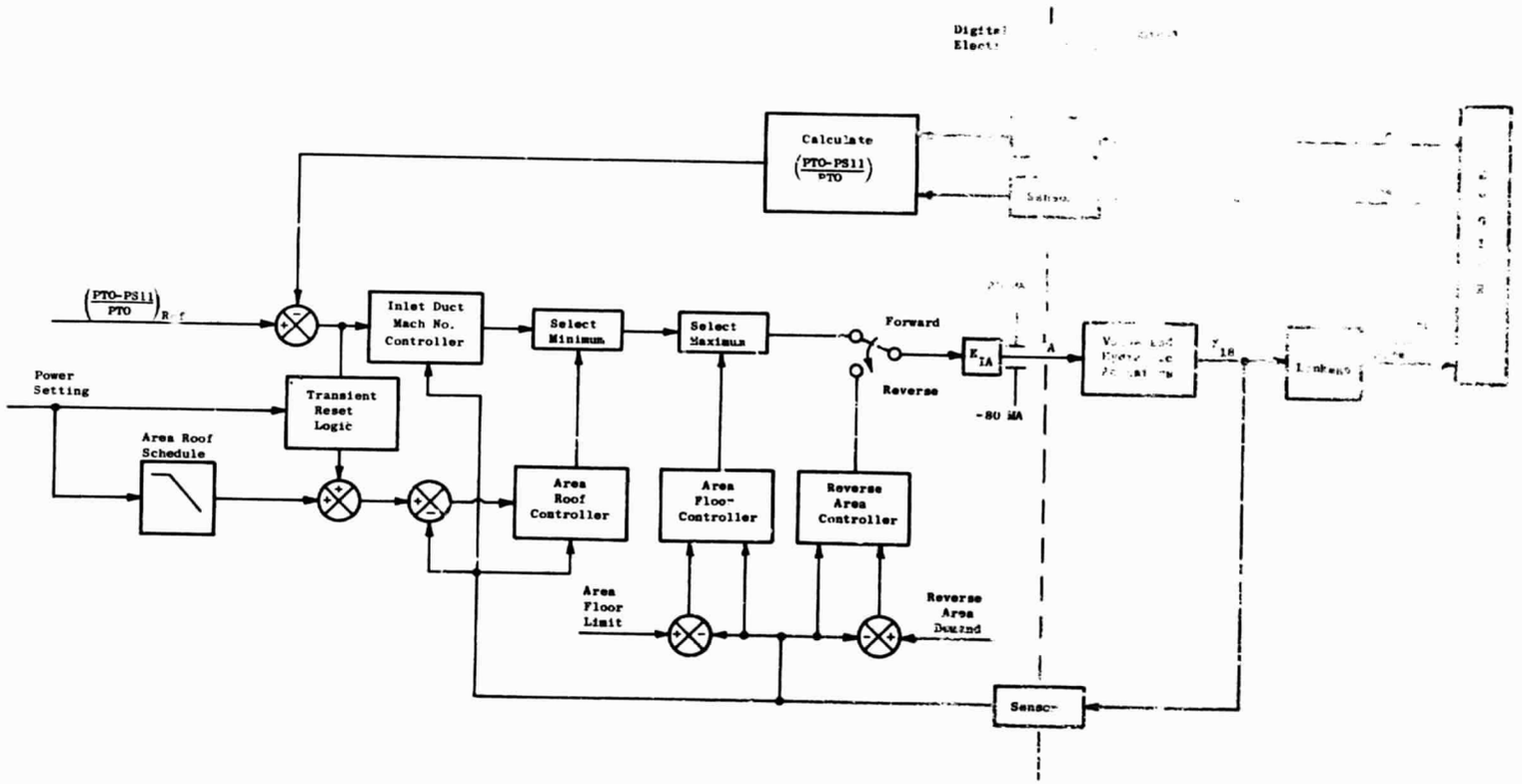

Figure 8. Inlet Duct Mach Number Control Model.

inlet duct Mach number controller, the area roof controller, and the area floor controller; for a forward thrust command, the output from one of these controllers is selected to control the position of the hydraulic actuators and thus manipulate fan exhaust nozzle area. For a reverse thrust command, control of the actuators' position is switched to the reverse area controller. The hydromechanical portion of the inlet duct Mach number control model includes a servovalve, hydraulic actuators, and the linkage relation between actuator position and nozzle area. The following paragraphs discuss the combined operation of the digital electronic controllers and the hydromechanical actuation system. Next, details included in the models for the digital electronic and hydromechanical portions are described.

Control Operation - The primary control mode for high power, forward thrust conditions is manipulating the nozzle area to control the inlet duct Mach number. The inputs to the inlet duct Mach number controller are (1) the difference between the constant reference and sensed values for (PTO-PS11)/PTO, and (2) the sensed position (X18) of the nozzle actuators. (PTO-PS11)/PTO is a function of average Mach number at the throat of the inlet; PS11 is the static pressure at the throat; PTO is from a total pressure probe mounted on the engine nacelle and is proportional to the inlet total pressure. The above pressure ratio reference is a constant equivalent to a 0.79 Mach number. Maintaining the inlet Mach number is needed to meet engine noise goals. When the sensed nozzle actuator position is within the prescribed roof and floor limits, the output of the inlet Mach number controller is selected and determines the torque motor current output (I_A) from the digital control. This current positions a servovalve which is ported to hydraulic actuators. The magnitude and polarity of the current (I_A) determines the magnitude and direction of hydraulic flow to the actuators and, thus, the rate and direction of actuator motion. The actuators are linked to and, therefore, determine the exhaust nozzle area.

The output of the actuator position sensor feeds back to the inlet Mach number controller, which computes the rate of change of sensed actuator position. This signal is fed through a first order lag before it is subtracted from a signal which is proportional to inlet $\Delta P/P$ error. For small perturbations, the transfer function from (PTO-PS11)/PTO error to nozzle area is approximated at low frequencies by:

$$\frac{\Delta \text{ Area}}{\Delta \left[(PTO-PS11)/PTO\right]_{Error}} \approx \frac{K(0.139\ S+1)}{S}$$

The lead-time constant in this transfer function is due to, and thus equal to, the time constant of the above mentioned lag in the feedback to the inlet Mach number controller. Thus, the inlet Mach number-nozzle area control is

an integrating type control with lead compensation and has been designed to provide adequate stability margin for accurate control of inlet Mach number.

The model includes the nozzle area roof controller, which limits maximum opening of the nozzle. This controller has been designed to produce the following transfer function characteristics at low frequencies:

$$\frac{\Delta \text{ Area}}{\Delta \text{ Area Position Error}} \simeq \frac{K}{S}$$

Therefore, this roof control is an integrating type position control for accuracy consideration.

The roof schedule is a function of power setting. If the inlet Mach number controller requests an area more open than the roof schedule, the roof controller output is selected and controls the position of the nozzle actuators. The roof schedule (a function of power setting) has been designed to work in conjunction with the fan speed-pitch control. As power setting is reduced from the takeoff position and the fan speed control closes the pitch angle to maintain the fan reasonably close to the takeoff speed, the roof schedule limits the nozzle opening in order to limit inlet Mach number at 0.79. This protects against high inlet pressure losses which are predicted in the range above 0.83 Mach number and also helps to protect against thrust decay on rapid thrust transients to takeoff. The roof schedule allows area to open until 80 percent power setting. At lower power settings a constant maximum area is scheduled; this prevents flow separation at the exhaust nozzle. Thus, at power settings below 80 percent, inlet Mach number drops below the 0.79 reference value.

During throttle bursts from approach to takeoff power conditions, the transient reset logic biases the roof schedule 1290 cm^2 (200 $in.^2$) closed until (PT0-PS11)/PT0 increases to within 0.05 PS1A/PS1A of the final (PT0-PS11)/PT0 at takeoff power. This reset action contributes to the rapid initial rise in thrust and also reduces overshoots of the 0.79 Mach number limit during the transient to takeoff power.

The nozzle area floor limit controller limits the minimum opening of the nozzle. This floor limit control has the same dynamic design as the roof limit control.

On a reverse thrust command, control of the nozzle actuators is switched to the reverse area controller. With exception of the schedules, the dynamic design of this position control is the same as the roof and floor controllers. The rate feedback limit [DALIM = 3.8 cm/sec (1.5 in./sec)] is sized to produce 95% of the change from takeoff to reverse area in less than one second, with no subsequent overshoot of reverse area. This is best explained by a transient in the report section on "Simulation Results." As shown in Figure 19, the actuation time from 16,452 to 26,452 cm^2 (2550 to 4100 $in.^2$) of exhaust nozzle area (i.e., approximately 95% of the change from takeoff to reverse area) is 0.85 seconds; this is followed by a gradual increase to the final

reverse area. A larger rate feedback limit would produce more anticipation of reaching the final reverse area and, thus, increase the time for 95% of the area change. Reducing the rate feedback limit would produce less anticipation and eventually lead to transients which overshoot the final reverse area.

Digital Electronic Portion of Inlet Duct Mach Number Control - The simulation has been used to develop the design and specifications for the digital electronic portion of the inlet duct Mach number control. Appendix B contains the block diagrams and the specifications for gains, time constants, limits, and schedules which currently define the digital electronic portion of this control for the first build of the experimental engine. The model used in simulation studies represents those details in Appendix B which have been essential to develop/evaluate the steady-state stability and transient response of the UTW experimental engine and overall control system. The model includes the Appendix B specifications for gains, time constants, limits, nozzle area roof schedule, transient reset logic, and switching logic between automatic forward and reverse thrust. When the UTW simulation was being developed, the nozzle area floor limit controller was not included in the hybrid simulation. This floor controller limits minimum opening of the nozzle, and selection of this controller is not expected during steady state or transient operation at experimental engine test conditions (Note: Selection normally can occur at high altitude, high Mach number flight condition). Furthermore, the dynamic design of the floor controller is the same as the roof controller. Therefore, omission of this controller is judged reasonable when considering available computer equipment should be used to represent control functions more important to establish the UTW experimental engine control design.

The model for the inlet duct Mach number controller includes 0.01 second lag time constants for the torque motor driver amplifier and the sensor lags. The effect of the digital control computer time delay is approximated by an analog type representation similar to that used in the fan speed control - the details of which are discussed in the report section on techniques used in the "Hybrid Simulation."

Nozzle Area Hydromechanical Actuation System - The model of this actuation system is described by the block diagram in Figure 9. As shown, the model includes dynamics associated with the servovalve, the valve pressure drop, head and rod actuator areas, friction, and the nozzle actuator load. Fan bypass exhaust nozzle area (A18) is a linear function of actuator stroke (X18).

The servovalve is assumed to have no overlap. Thus when current changes sign, the supply and return pressures are switched immediately to feed opposite sides of the actuator pistons.

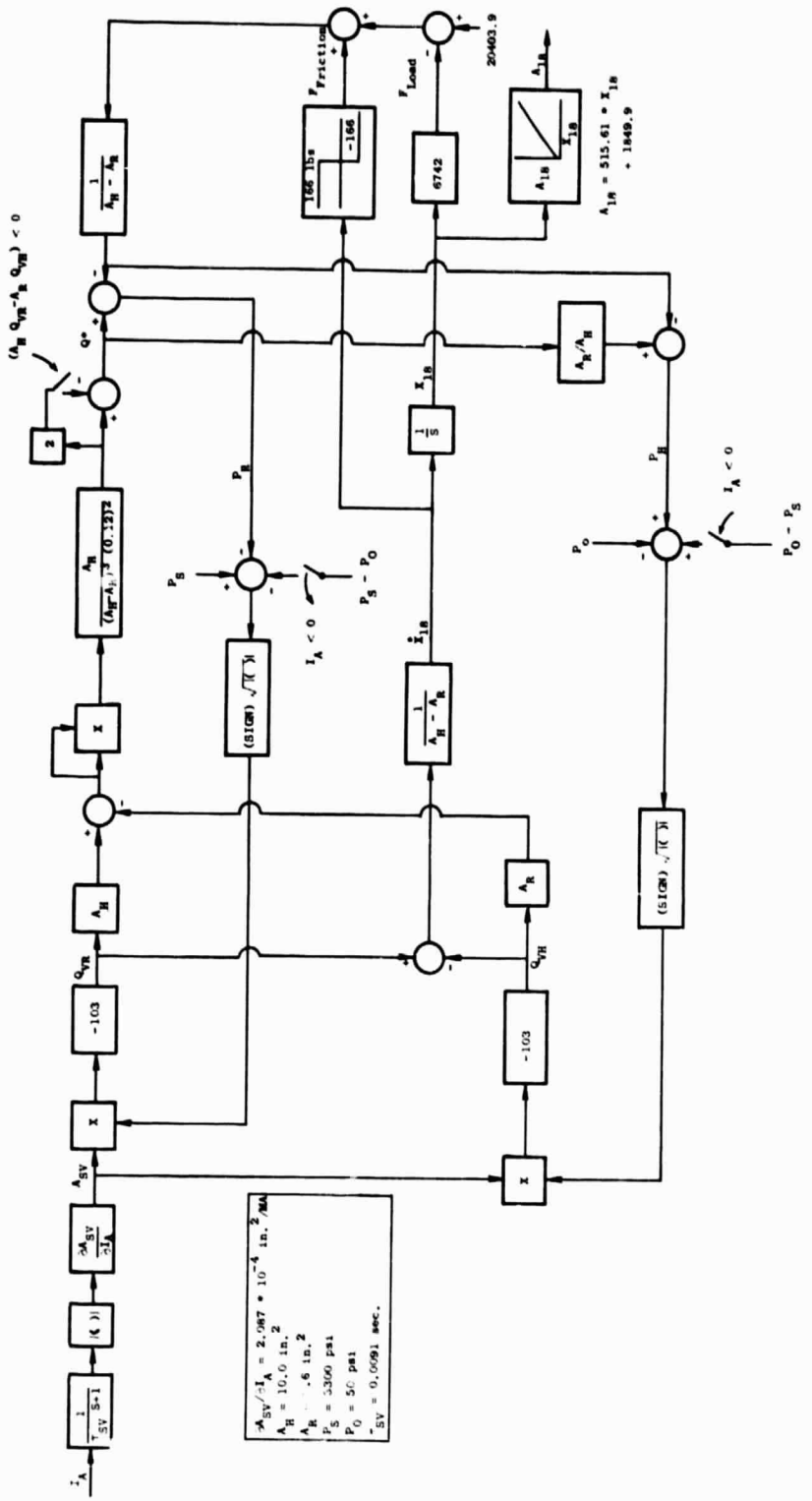

Figure 9. Fan Exhaust Nozzle Hydromechanical Actuation System Model.

ORIGINAL PAGE IS
OF POOR QUALITY

Engine Pressure Ratio and Compressor Stator Controls

The schematic of the engine pressure ratio and compressor stator controls is shown in Figure 10. The model includes representations for the digital electronic and the hydromechanical portions of the engine pressure ratio control and also a representation of the hydromechanical compressor stator control. As indicated by Figure 10, several control modes are accommodated by the engine pressure ratio control. During forward thrust operation, the primary control mode is the manipulation of fuel flow to control the engine pressure ratio (referred to as EPR, which is the ratio PS3/PT0). EPR is a variable related closely to engine thrust. The control mode is changed to either the fan speed, core turbine inlet temperature, core idle speed, maximum core speed, hydromechanical maximum core speed, WF/PS3 accel schedule, or the WF/PS3 decel schedule, whenever the engine tries to operate beyond the scheduled limit of any one of these variables.

For reverse thrust, the primary control mode is manipulation of fuel flow to control fan speed. Changing from a primary control mode of EPR-fuel flow in forward thrust to one of fan speed-fuel flow in reverse thrust is determined by digital control logic, whose state is a function of the reverse mode command, the reverse interlock adjustments, and the sensed position of the fan pitch hydraulic motor. The above mentioned core speed, turbine temperature, and accel/decel schedule controllers are selected during reverse thrust, whenever the engine tries to operate beyond the scheduled limit of any one of these variables. The digital switching logic opens the signal path from the output of the EPR controller to the control mode selector logic and thus to the fuel servovalve during reverse thrust operation. Therefore, the EPR-fuel flow control mode is not used in reverse thrust.

The following paragraphs discuss the operation and dynamics of the EPR control. Details included in the models for the digital electronic and hydromechanical portions of this control and also the compressor stator control are described next.

EPR Control Operation - For forward thrust in the approach through takeoff power setting range, fuel flow is manipulated to control EPR (i.e., PS3/PT0). Inputs to the EPR controller are the scheduled and the sensed PS3/PT0, and their difference is compared with the lagged rate of change of sensed metering valve position. When the engine operates within the core speed, core turbine inlet temperature, and accel/decel schedule limits, the difference between the PS3/PT0 error and the sensed valve rate then determines the torque motor current output (I_w) from the digital control. This current positions an electro-hydromechanical servovalve which is ported to the metering valve power piston. The magnitude and polarity of the current (I_w) thus determines the rate and direction of metering valve power piston position. The metering valve area is proportional to the square of the power piston position (XMV); a pressure regulator maintains a constant pressure drop across the metering valve; and, thus, the metered fuel flow to the engine is proportional to the square of the power piston position.

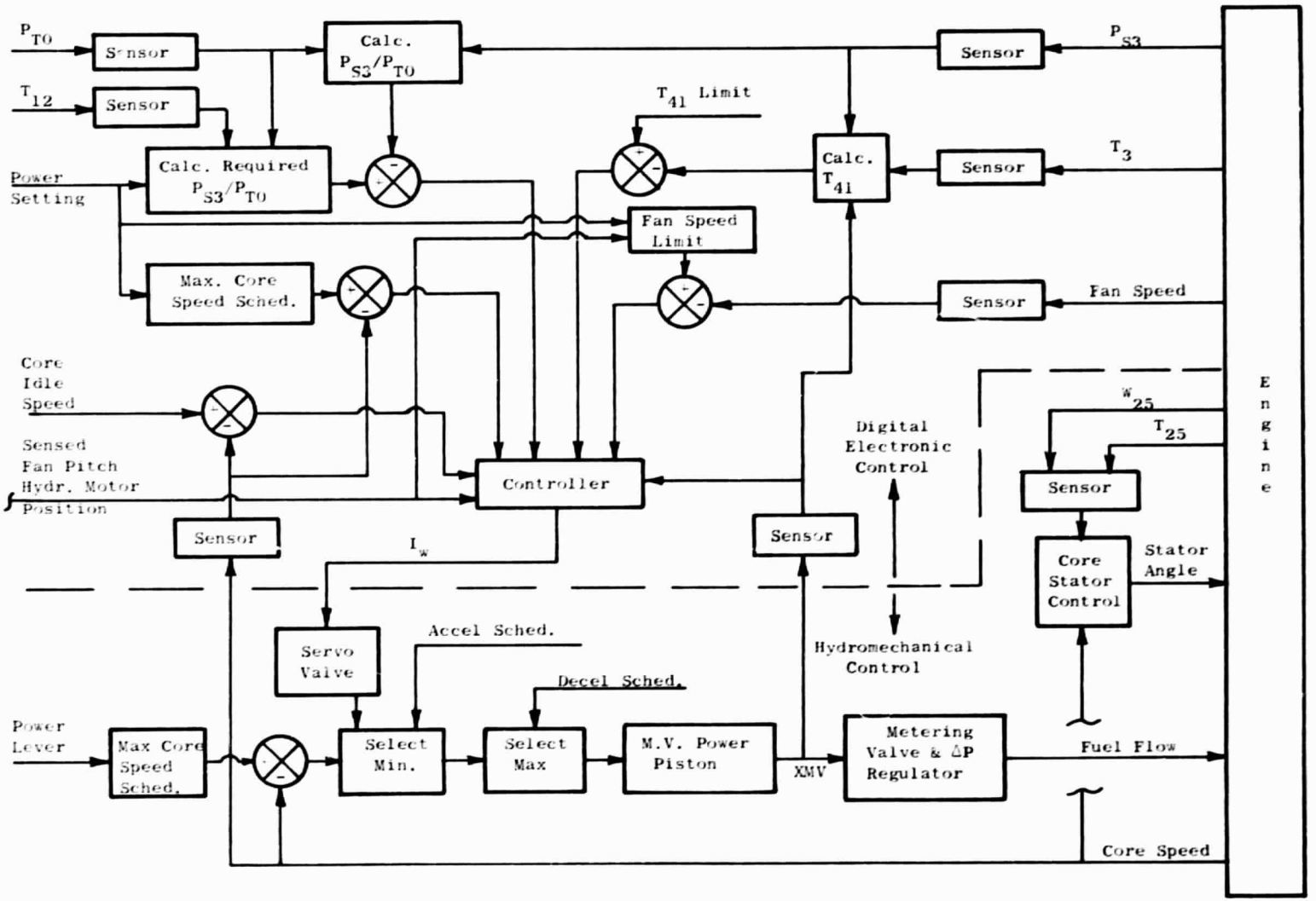

Figure 10. Core Engine Pressure Ratio and Compressor Stator Control Model.

For small perturbations, the transfer function from PS3/PTO error to fuel flow is approximated at low frequencies by:

$$\frac{\Delta \text{ Fuel Flow}}{\Delta \text{ PS3/PTO Error}} \simeq \frac{K(0.25\ S+1)}{S(0.1\ S+1)}$$

The gain (K) varies with respect to the square law shape of the metering valve area. The lead time constant in this transfer function is due to, and thus equal to, the time constant of the above mentioned lag on the rate of change of sensed metering valve position. In summary, the PS3/PTO - fuel flow control is an integrating type control with lead-lag compensation and is designed to provide accurate control of PS3/PTO.

The dynamic designs of the limit controls for core speed, fan speed, and turbine inlet temperature are similar to the PS3/PTO control design, in that each is an integrating type control. They differ in the respect that these limit controls employ lead compensation and not lead-lag compensation. To compensate for engine and sensor lags, lead time constants are 0.5 seconds for the maximum core speed control, the idle core speed control, and the fan speed control; a 0.1 second lead time constant is used in the core turbine inlet temperature control.

During engine accelerations, fuel flow is limited by the WF/PS3 accel fuel schedule, which is a function of both the core speed and compressor inlet temperature. The time constant of the inlet temperature sensor is a function of the inlet airflow to the compressor.

During transients to reverse thrust, the control logic operates in the following manner:

- When the reverse push button is activated, the control mode is switched from PS3/PTO - fuel control mode to the core speed - fuel control mode. The core speed demand is set at a flight idle position, which causes the fuel flow and, thus, core speed to decrease.

- When fan pitch angle passes a predetermined interlock position, the control mode is switched from the flight idle core speed - fuel control mode to the fan speed - fuel control mode.

For transients from reverse back to forward thrust, the control mode is switched from the fan speed to the flight idle core speed - fuel control mode, and finally back to the PS3/PTO - fuel control mode when fan pitch angle passes the predetermined interlock release position for reverse to forward thrust transitions.

Digital Electronic Portion of Engine Pressure Ratio Control - The simulation has been used to develop the design and specifications for the digital electronic portion of the EPR control. Appendix C contains the block diagrams and specifications for gains, time constants, and schedules which currently

define the digital electronic portion of this control for the first build of the UTW experimental engine. The model used in simulation studies represents those details in Appendix C which have been essential to develop/evaluate the steady state stability and transient response of the UTW experimental engine and overall control system. The model includes the Appendix C specifications for gains, time constants, limits, power setting schedule, T_3 sensor dynamics, switching logic between automatic forward and reverse thrust, and the reverse interlock adjustments. The EPR takeoff schedule, the remote WF control input, and the logic for detecting a fan speed (N1T) feedback sensor failure are not included in the simulation; the judgment is that these items are not essential in predicting stability and transient response at experimental engine test conditions.

The model includes 0.01 second time constants to represent the dynamic lags of the fan and core speed sensors, the metering valve position sensor, and the torque motor driver amplifier. The sensor dynamics for compressor discharge static pressure (PS3) is represented by a 0.02 second lag time constant. The T_3 sensor lag is a function of compressor discharge airflow, i.e., $T_{T3} = f(W_3)$. The effect of the digital control computer time delay is approximated by an analog type representation similar to that used in the fan speed-variable-pitch control, which is discussed in the report section on techniques used in the "Hybrid Simulation."

Hydromechanical Fuel Control Model - The model of the hydromechanical fuel control is described by the block diagram in Figure 11. This model includes the hydromechanical core speed backup control, the accel and decel schedules, the torque motor servovalve (fed by I_w from the digital control), and the logic for selecting one of these to control the metering valve power piston position (XMV).

For small perturbations, the transfer function of the hydromechanical core speed backup control is approximated at low frequencies by:

$$\frac{\Delta \text{ Fuel Flow}}{\Delta \text{ Core Speed Error}} \approx \frac{K(0.5\,S+1)}{S}$$

The gain (K) varies with respect to both the level of core speed and the square law shape of the metering valve area. This backup control is an integrating type control with a 0.5 second lead to compensate for the engine lag.

The temperature (T25) and pressure (PS3) sensor lags are contained in the model. The lag time constant (T_{FDT}) for the T25 sensor is a function of compressor inlet airflow (W25). The lag time constant for the PS3 sensor is 0.02 seconds.

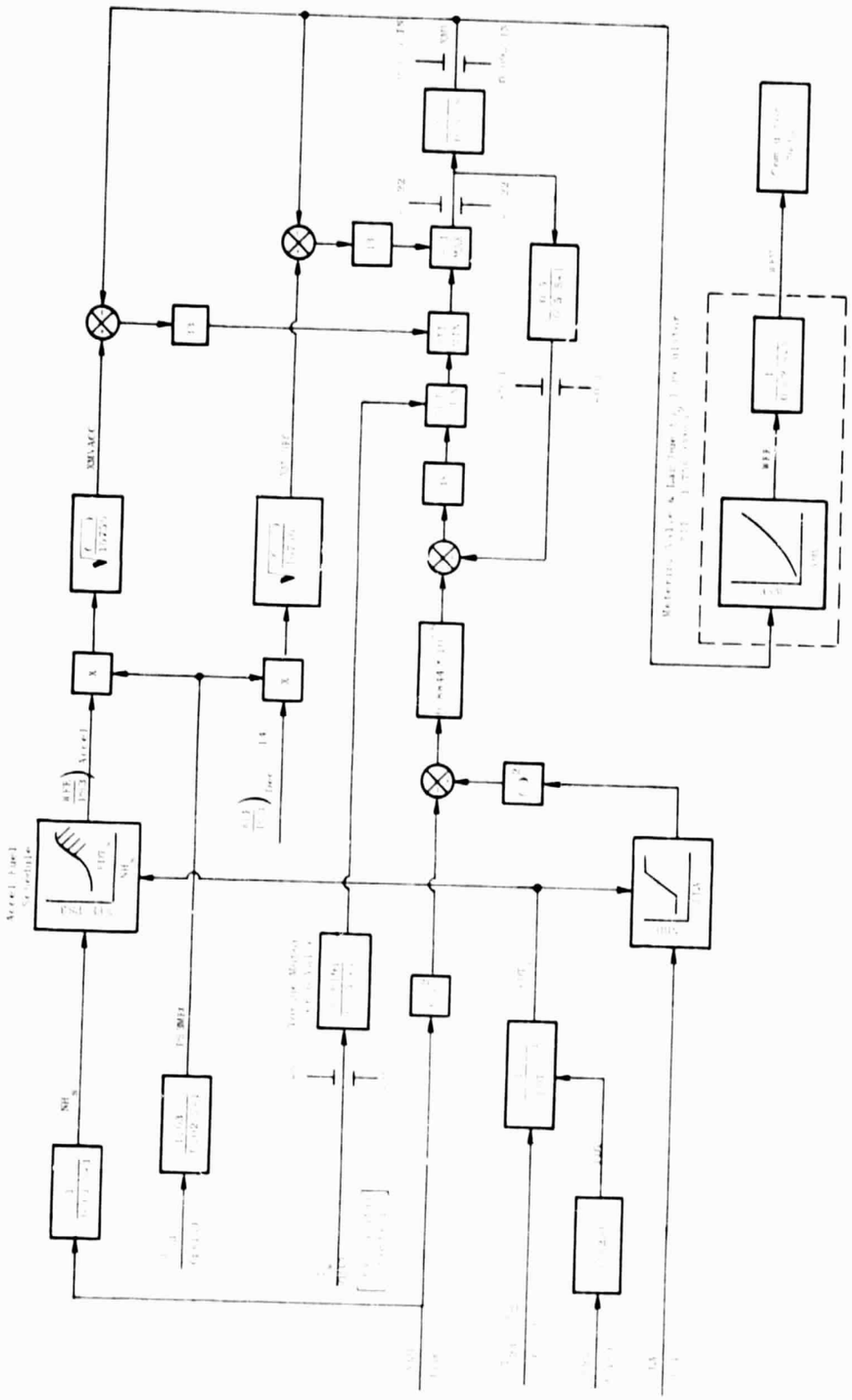

Figure 11. Hydromechanical Fuel Control Model.

The hydromechanical power lever angle and the maximum core speed schedule of NHD = f(PLA) have not been included in the model. A constant NHD of 14,460 (i.e., 100% core speed) has been used in the model and simulation studies to date, based on the assumption that the power lever is set for the high speed flat.

F101 test data indicate that the manifold and combustion time delay is approximately 0.025 seconds. This time delay has been approximated by a 0.025 second first order lag.

Core Compressor Stator Control Model - The core compressor stator vanes are positioned by a hydromechanical control. As shown in Figure 12, a cam schedules the stator position as a function of sensed core speed (NHS) and sensed compressor inlet temperature (FDT_S). The error between the scheduled and mechanical feedback from the stator actuator pistons determines the flow to these pistons. The response of this position control is represented by a first order lag, whose time constant (TCBETH) is in the 0.03 to 0.05 second range. TCBETH is a linear function of fuel flow and approximates the dynamic effect of fuel pump discharge pressure, which is the power source for operating the stator actuators.

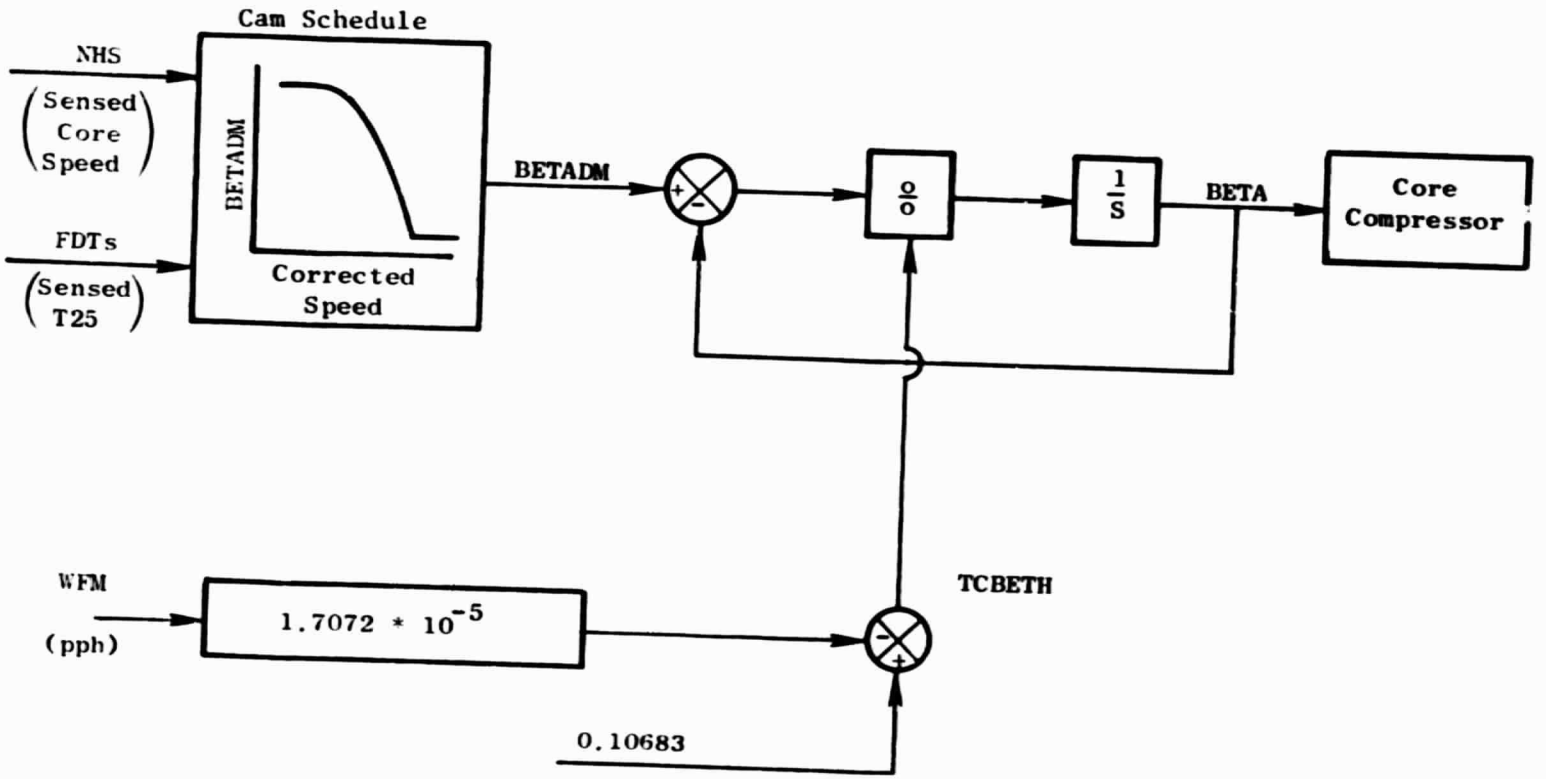

Figure 12. Core Compressor Stator Control Model.

HYBRID SIMULATION

The hybrid simulations of the QCSEE UTW forward and reverse thrust models were constructed at the General Electric AEG Dynamic Analysis Simulation Center. The simulations were implemented on an EAI 690 Hybrid Computing System which consisted of two EAI 680 Analog Computers with a total of 224 amplifiers, an EAI 693 Hybrid Interface Unit with 64 channels for A/D and D/A conversion, and an EAI 640 Digital Computer with a 16,000 word core memory. Peripheral equipment includes two EAI 8875 8-channel strip chart recorders, an EAI 600 high speed line printer, an EAI 500 card reader, and X-Y recorders.

Techniques

The digital computer was used primarily for function generation and nonlinear operations. It was also used to provide steady-state output of significant engine variables from the forward thrust simulation on the high speed line printer. The analog computers were used primarily for simulation of dynamics and engine pressures and gas flows. Transient data was output from the digital computer to the strip chart and X-Y recorders. The split of the total load between the analog and digital computer portions of the hybrid (see Table I) was based on previous experience with similar engine models.

Table I. EAI 690 Hybrid Computation Split.

EAI 640 Digital	EAI 680 Analog
Function generation and calculations for:	Calculations for:
Inlet	Inlet input
Fan	Fan iteration
Fan nozzle	
Compressor	Compressor heat soak
Combustor	Compressor discharge pressure Combustion delay
Mixing at 41	Turbine heatsoak
HP Turbine	HPT inlet pressure and flow
Mixing at 49	Temperature and flow at 49
LP Turbine	LPT inlet pressure and flow
Mixing at 55	Temperature and flow at 55
Core Nozzle	
Thrust	
Main Engine Control	Control Dynamics Rotor Dynamics

The digital program for simulating the UTW forward thrust engine and control model required approximately 15,500 words of core memory. The resulting digital sampling interval (with steady analog inputs) was approximately 60 milliseconds. As a consequence, the simulation was operated at a time base which is 20 times slower than real time.

The digital program for simulating the reverse thrust model required about 2900 words less memory than the forward thrust model, but most of this reduction was due to eliminating the portion of the digital program which provides the steady-state printout of engine variables. The simulation of the reverse thrust model was operated at the same 20 to 1 time base.

The simulation of the digital electronic control computer portions of the fan speed, the inlet duct Mach number, and the engine pressure ratio controls is primarily contained on the analog portion of the hybrid computer. As a consequence, the simulation does not account for round-off errors associated with the 12-bit words in the digital control computer. It has been assumed that the software program for the digital control computer will be scaled/designed to prevent deteriorating effects of round-off errors on control performance.

The simulation of the three above mentioned controls includes an approximation for the effect of the digital control computer time delay on each. The current estimate for the total cycle time of the control computer is 0.010 seconds (this has been estimated by the computer design group prior to completion of the software program). An analog type representation is used to simulate this cycle time; it includes an estimate for the sample data effects of digital to analog conversion (Reference 2), which is 0.005 seconds. Therefore, the analog of the digital control computer time delay is represented by total delay of 0.015 seconds, which has been approximated by a first order lag whose time constant is 0.015 seconds. This first order lag representation provides a reasonable approximation for phase shift in the range of the control loop crossover frequencies (important for stability considerations). This lag does provide some effect of time delay during large transients, but not precise. A 0.015 second lag is included in the simulation of each the fan speed, the inlet duct Mach number, and the engine pressure ratio controls; these lags are located just prior to the analog amplifiers which simulate their respective torque motor driver amplifiers.

Simulation Verification

The simulation of the forward thrust model was compared with the technical requirements cycle deck at four operating points which were felt to be of primary importance for current and future control studies. These points were takeoff, 65% of takeoff, and 15% of takeoff net thrust at the sea level static, standard day flight condition and also 16,587 N (3729 lb) net thrust at a flight condition of 9144 m (30,000 ft), 0.8 Mach number, and +18 degrees Rankine above standard day ambient temperature. The comparison data were

Table II. Steady-State Verification Data for UTW Forward Thrust Simulation.

	Takeoff, Sea Level Static, Standard Day			65% of Takeoff, Sea Level Static, Standard Day		
	Cycle Deck	Simulation	Percent Error	Cycle Deck	Simulation	Percent Error
CASE	1[illegible]			127		
ALT	[illegible]	0	—	0	0	—
DTAMB	0	0	—	0	0	—
FN	17434	17250	-1.05	11323	11225	- .86
XM11	.7769	.7761	- .10	.6280	.6275	- .08
ROPDEG	- .98	- .98	0	3.41	3.41	0
XNL	3066	3057	- .29	3066	3065	- .03
W2A	877.8	875.6	- .25	795.4	794.0	- .18
SM12	14.42	14.87	3.12	26.99	27.39	1.48
A18	2547	2547	0	3300	3300	0
XNH	13106	13120	.11	12713	12692	- .16
W25	67.15	67.14	- .01	58.89	58.7	- .32
T25	552.1	552.0	- .02	544.9	544.6	- .06
SM25	19.49	19.18	-1.59	24.43	24.20	- .94
T3	1231	1228	- .24	1170	1166	- .34
P3	207.7	207.4	- .14	174.7	174.0	- .40
PS3	196.7	196.6	- .05	165.2	164.8	- .24
WFE	5649	5649	0	4361	4361	0
W8	68.72	68.70	- .03	60.11	59.86	- .42
T8	1643	1638	- .30	1542	1546	.26

Table II. Steady-State Verification Data for UTW Forward Thrust Simulation (Concluded).

	15% of Takeoff, Sea Level Static, Standard Day			16,587 N (3729 lb) Net Thrust, 9144 m (30,000 ft), 0.8 Mach No., +18° Above Std. Day Ambient Temperature		
	Cycle Deck	Simulation	Percent Error	Cycle Deck	Simulation	Percent Error
CASE	122	0	—	407		
ALT	0	0	—	30000	30000	—
XM	0	0	—	.8	.8	—
DTAMB	0	0	—	18	18	—
FN	2615	2510	-4.02	3729	3720	.03
XM11	.2256	.2232	-1.06	.8029	.8130	1.26
ROPDEG	- .98	- .98	0	1.60	1.60	0
XNL	1228	1240	.98	3335	3388	1.59
W2A	348.0	344.0	-1.15	415.8	416.2	.10
SM12	4.25	4.27	.47	10.0	10.33	3.30
A18	2547	2547	0	1894	1894	0
XNH	10085	10024	- .60	12861	12852	- .07
W25	25.88	25.34	-2.09	33.47	33.32	- .45
T25	523.5	523.6	.02	526.5	527.1	.11
SM25	25.85	24.70	-4.45	17.37	17.01	-2.07
T3	857.3	853.4	- .45	1190	1185	- .42
P3	61.45	60.3	-1.87	102.8	102.5	- .29
PS3	57.57	56.65	-1.60	97.50	97.35	- .15
WFE	1017	1017	0	2813	2813	0
W8	26.16	25.58	-2.22	34.25	34.10	- .44
T8	1199	1208	.75	1530	1524	- .39

generated by setting simulation fuel flow, pitch angle, and fan exhaust nozzle area at the cycle deck values. The cycle deck data, simulation data, and percent error are shown in Table II.

The simulation data in Table II shows good agreement with the cycle deck at the takeoff thrust, the 65% of takeoff thrust, and the 16,587 N (3279 lb) net thrust operating points. All percent errors are less than 1.6% except for fan stall margin (SM12) and core stall margin (SM25). Although the percent errors for SM12 range as high as 3.3%, the actual difference in terms of stall margin is 0.45% or less. For the above operating points, percent errors for SM25 range from -0.94% to -2.07%; however, the largest core stall margin difference is -0.39%. Agreement deteriorates at the 15% of takeoff thrust operating point, where a 4.02% error is indicated for net thrust (FN). This deterioration can be attributed to several factors, which include round-off errors, truncation errors, and map inaccuracies due to linear interpolation.

A similar comparison is made for the reverse thrust simulation. Since control schedules had been developed which were different from the preliminary technical requirement cycle data, the forward thrust simulation was used to provide baseline data takeoff and 62% of takeoff net thrust at the sea level static condition. Technical requirements cycle deck data were used for full reverse through stall and full reverse through flat pitch. Simulation data for the forward thrust mode were generated using the control, while reverse thrust simulation data were generated by fixing fuel flow and fan pitch angle. The comparison data are presented in Tables III and IV. Good agreement is shown in the forward thrust mode and reverse through stall with less than 1.5% error. The reverse through flat pitch data indicate a fan problem with a 12.67% error in net thrust.

Since the simulation was developed prior to any testing of the UTW engine and the control system hardware, it was not possible to verify transient operation of the simulation. However, it was considered important to investigate the effect of the simulation time base on transients. Simulation transients were run at a time base 100 times slower than real time; there was no observable difference between these transients and those obtained with the 20 to 1 time base. The conclusion was that the hybrid computer digital computation time, the analog/digital multiplexer skewing, and iteration dynamics had negligible effect on transient results when using the 20 to 1 time base in the simulation.

Table III. Steady-State Verification Data For UTW Reverse Thrust Simulation.

(In Forward Thrust Mode)

	Takeoff, Sea Level Static, Standard Day			62% of Takeoff, Sea Level Static, Standard Day		
	Baseline	Simulation	Percent Error	Baseline	Simulation	Percent Error
ALT	0	0	—	0	0	—
XM	0	0	—	0	0	—
DTAMB	0	0	—	0	0	—
FN	17420	17490	.40	10875	11005	1.20
XM11	.7888	.7893	.06	.6108	.6158	.82
ROPDEG	-1.36	-1.66	(Δ = .3)	1.96	1.96	0
XNL	3060	3062	.06	2790	2808	.64
W2A	881.6	881.6	0	780.8	784.8	.51
A18	2561	2555	-.23	3258	3258	0
XNH	13176	13154	-.17	12432	12418	-.11
W25	67.40	67.52	.17	55.80	55.90	.18
T25	552.4	552.3	-.02	540.8	540.6	-.04
SM25	18.62	18.90	1.50	27.25	27.38	.48
T3	1234	1231	-.24	1131	1130	-.09
P3	209.2	209.2	0	161.3	161.4	.06
PS3	198.2	198.2	0	152.4	152.4	0
WFE	5748	5725	-.40	3817	3808	-.23
W8	68.98	69.12	.20	56.86	56.92	.10
T8	1654	1648	-.36	1490	1484	-.40

Table IV. Steady-State Verification Data for UTW Reverse Thrust Simulation.

(In Reverse Thrust Mode)

	Max. Rev. (Thru Stall) Sea Level Static, +31° Above Std. Day Ambient Temperature			Max. Rev. (Thru Flat) Sea Level Static, +31° Above Std. Day Ambient Temperature		
	Cycle Deck	Simulation	Percent Error	Cycle Deck	Simulation	Percent Error
ALT	0	0	—	0	0	—
XM	0	0	—	0	0	—
DTAMB	31	31	—	31	31	—
FN	-6406	-6490	1.31	-5263	-5930	12.67
ROPDEG	-95	-95	0	+83	+83	0
XNL	2979	2985	.20	3408	3432	.70
W2A	-468.0	-468.4	.08	-380.2	-397.6	4.58
XNH	12732	12720	-.09	12601	12564	-.29
W25	49.75	49.62	-.26	48.49	48.84	.72
T25	549.7	549.4	-.05	549.7	549.3	-.07
SM25	24.43	24.35	-.33	25.23	25.40	.67
T3	1176	1172	-.34	1162	1156	-.52
P3	148.3	147.9	-.27	143.8	144.4	.42
PS3	140.3	140.0	-.21	136.0	136.8	.59
WFE	3744	3744	0	3609	3609	0
W8	50.79	50.64	-.30	49.50	49.82	.65
T8	1609	1614	.31	1604	1600	-.25

SIMULATION RESULTS

Forward Thrust Transient Response

One of the QCSEE program objectives is to develop the technology which will yield the engine thrust response characteristics required for powered-lift operations. This objective is quantified into the specific requirement that the propulsion systems shall be designed to meet the dynamic response at altitudes up to 1829 m (6000 ft) as defined in Figure 13. To simplify the discussion of transient response, the overall requirements defined in Figure 13 were interpreted as a response time from 62 to 95 percent net thrust in one second.

The forward transient thrust characteristics of the UTW experimental engine were studied at the sea level static (SLS), standard day condition. The overall results of these studies are shown in Figure 14, which depicts time to 95 percent net thrust as a function of initial power setting. This figure shows that the time from 62 to 95 percent net thrust for a nominal control design is 0.85 seconds. Simulation results indicate that response times will decrease slightly as altitude is increased up to 1829 m (6000 ft). The conclusion from these results is that the experimental engine will meet the thrust response requirement.

Simulated Go-Around Maneuver - For this study, the approach thrust condition was defined as 62 percent net thrust. At this thrust condition, the control output variables are scheduled as follows:

- Fuel flow is manipulated to maintain the scheduled engine pressure ratio
- Fan exhaust nozzle area is opened to reduce thrust; the area roof controller limits and controls the nozzle at the scheduled roof area for 62 percent power setting.
- Fan pitch angle is closed to maintain a high fan speed; the fan pitch floor controller limits and controls the pitch at the scheduled floor angle of + 2 degrees (closed) for 62 percent power setting. (Note: For the simulation studies, the fan pitch floor schedule limits the angle to the + 2 degree closed position due to fan model limitations. This + 2 degree limit at 62 percent net thrust prevents the simulation from operating in an ill-defined region of the fan map. During experimental engine test at 62 percent net thrust, it expected that the floor schedule will be adjusted to permit further closure of fan pitch; this will provide the capability to manipulate the fan pitch and thus control and maintain the fan speed at the takeoff value of 3065 rpm.)

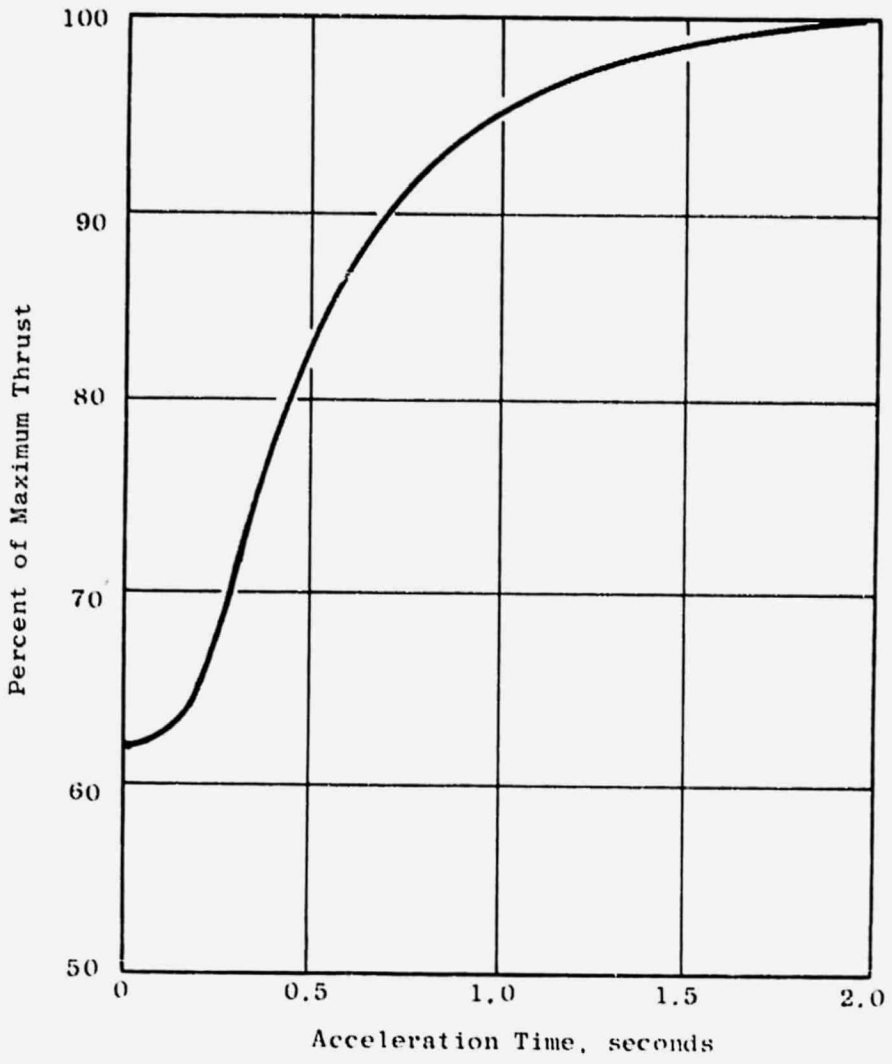

Figure 13. Engine Dynamic Thrust Response Requirement.

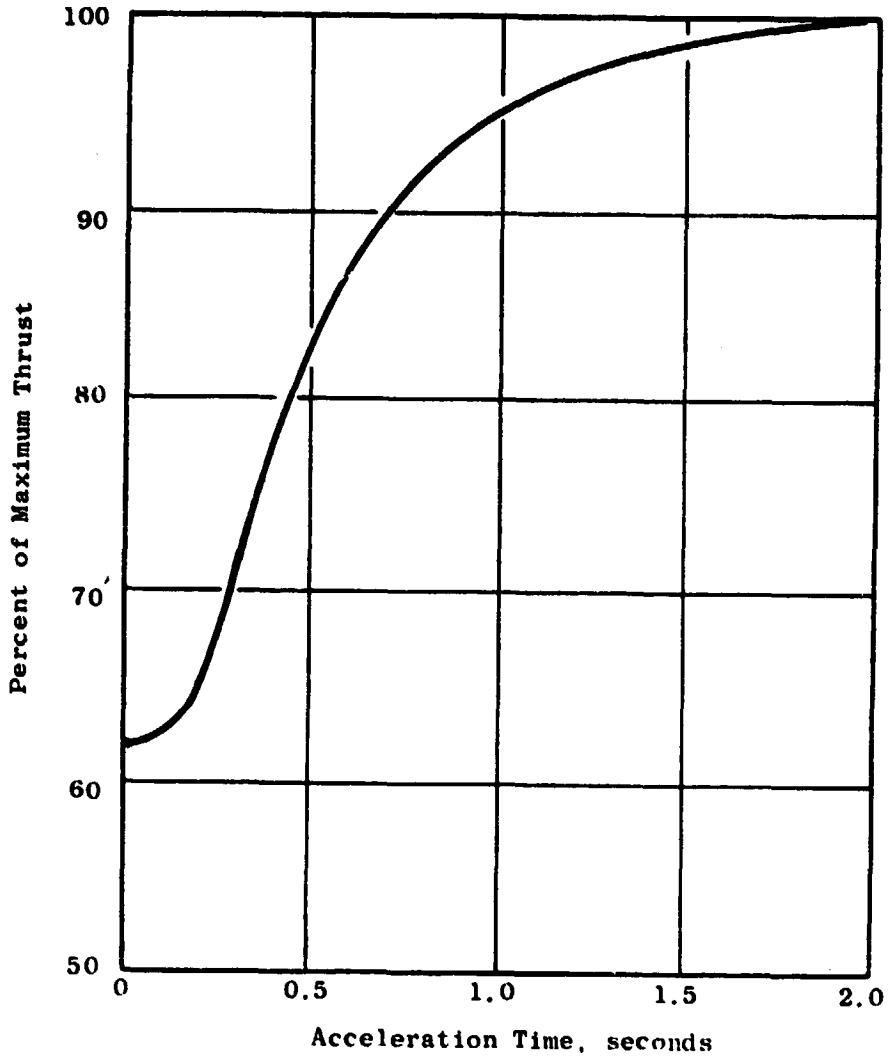

Figure 13. Engine Dynamic Thrust Response Requirement.

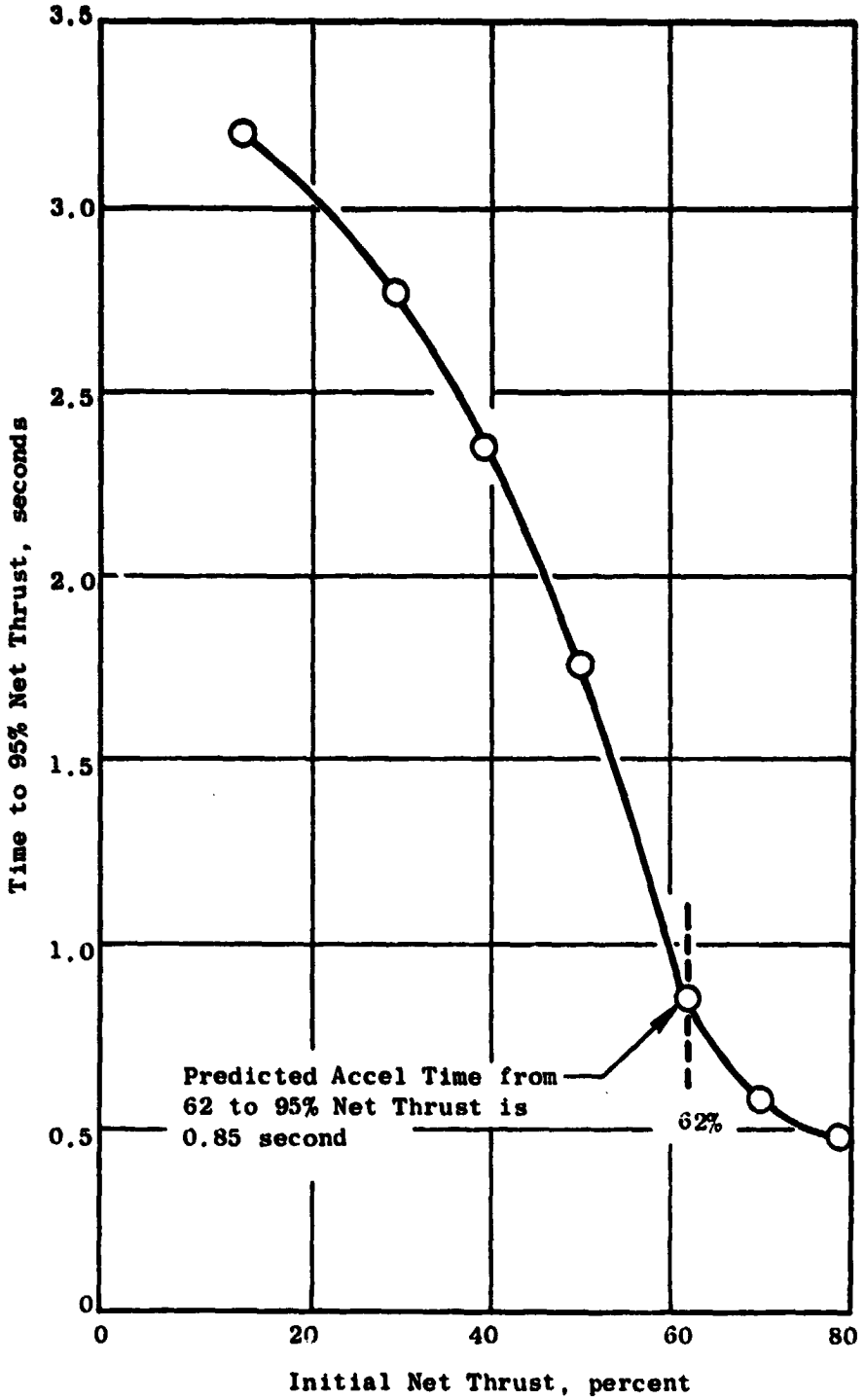

Figure 14. Nominal Transient Response for Bursts to 100% Net Thrust at Sea Level Static, Standard Day, Zero Bleed.

The left hand portion of Figure 15 shows the specific values of selected engine and control variables at the 62 percent net thrust condition. The transient values of these variables after a step increase in power setting are also shown.

The control system is designed to provide the required transient response and to maintain safe engine operation. As shown in Figure 15,

- The transient thrust response time from power setting change to achievement of 95 percent thrust is 0.85 seconds.

- The fuel flow is increased, but limited by the acceleration fuel schedule to prevent compressor stall and excessive turbine over-temperature. Minimum compressor stall margin is 15.5 percent and turbine temperature peaks 140 degrees above the final temperature.

- The fan exhaust nozzle is rapidly moved to a position slightly less than takeoff area. This action provides a rapid increase in thrust (62 to 78 percent in 0.3 seconds) and limits the inlet Mach number overshoot to 0.02 above the final steady state value of 0.78.

- The fan pitch is rapidly opened to close proximity of the final takeoff position by the transient reset function in the control. This action is also a contributing factor in producing the above rapid thrust increase during the first 0.3 seconds. At approximately one second after the step increase in power setting, the transient reset function is removed, and fan pitch is manipulated to control the fan at the takeoff speed. The fan pitch closes slightly and then opens while settling to the final, steady-state fan speed.

Acceleration Study - The specified tolerance for the WF/PS3 acceleration fuel schedule in the hydromechanical control affects the core engine acceleration time, which, in turn, affects the time to achieve 95 percent net thrust during a throttle burst from 62 to 100 percent net thrust. In this engine operating range, the specified tolerance for the acceleration fuel schedule is ±4 percent from nominal. The effect of this ±4 percent tolerance on transient response was investigated on the simulation. The results in Figure 16 show the response time trend as a function of the accel fuel schedule tolerance. In this figure, the time scale multiplier indicates the time to accelerate from 62 to 95 percent thrust as compared to the baseline case of zero accel fuel schedule tolerance. In particular, this figure shows that the nominal response time from 62 to 95 percent net thrust should be multiplied by approximately 1.3 when the accel schedule operates at the -4 percent tolerance limit and by approximately 0.85 for the +4 percent tolerance limit. As indicated in a previous paragraph, the baseline thrust response time from 62 to 95 percent net thrust is 0.85 seconds. Therefore, the predicted range on this thrust response time due to accel schedule tolerances is 0.72 to 1.10 seconds. The 1.10 seconds is not a concern item for the experimental engine test since the specific gravity adjustment in the hydromechanical fuel control can be used to compensate for a negative tolerance on the accel fuel schedule.

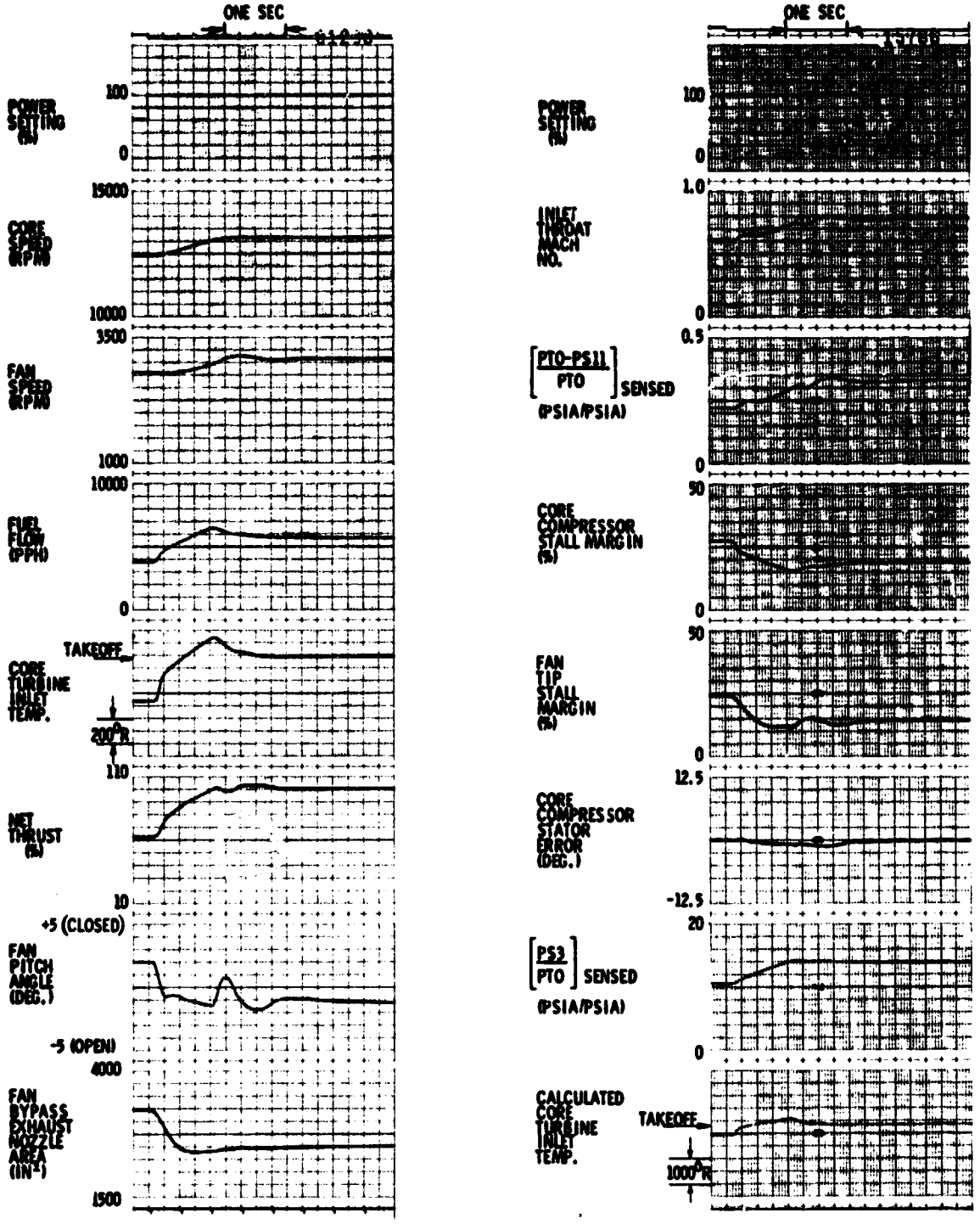

Figure 15. Transient Response for Throttle Burst from 62 to 100% Thrust at Sea Level Static, Standard Day, Zero Bleed.

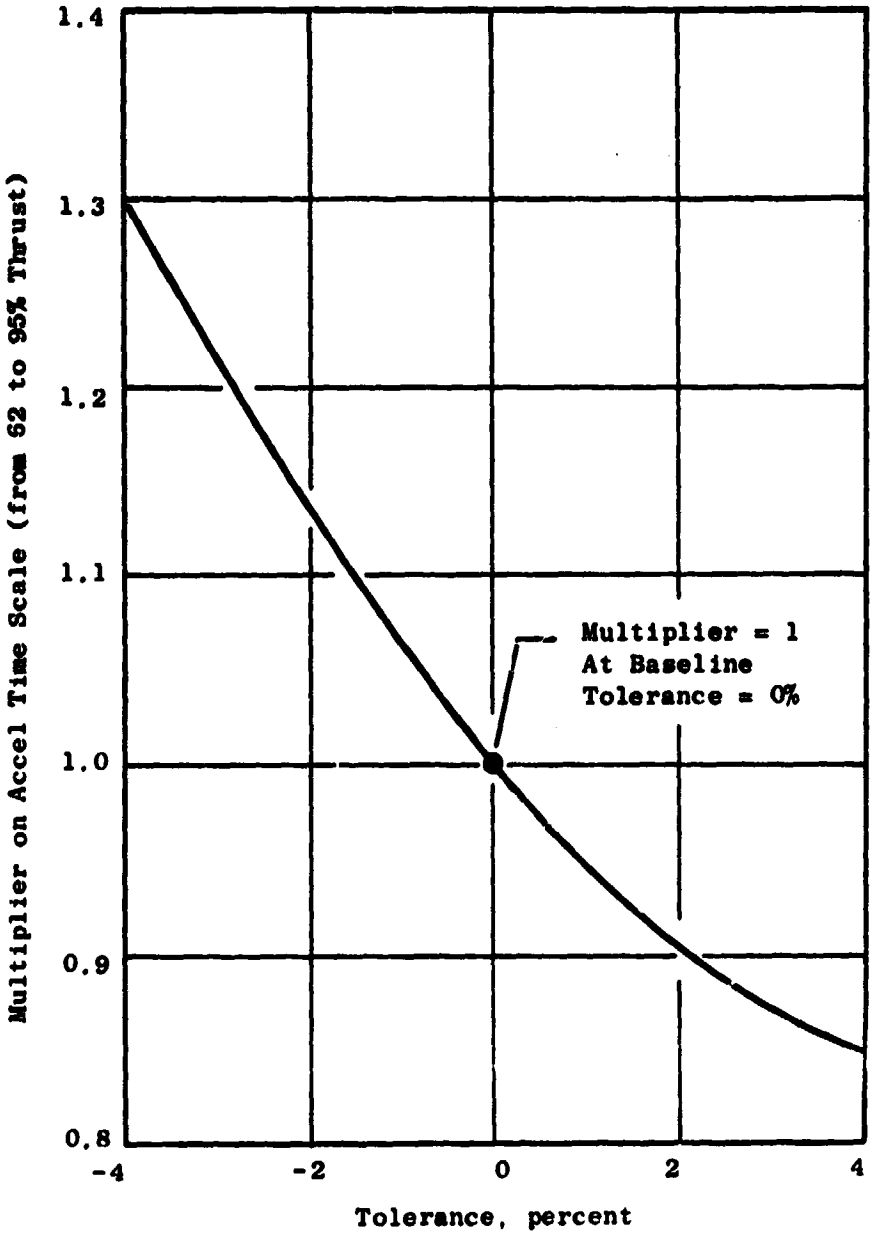

Figure 16. Effect of WF/PS3 Acceleration Fuel Scheduling Tolerance on Accel Time from 62 to 95% Net Thrust.

Deceleration Study - The control system is designed to provide fast deceleration capability and to maintain safe engine operation. A throttle chop from 100 to 62 percent net thrust is shown in Figure 17. The left hand portion of this figure shows the specific values of selected engine and control variables at the 100 percent net thrust condition. The start of the deceleration to 62 percent net thrust is indicated by the step decrease in power setting. As shown in Figure 17:

- The fuel flow is decreased, but limited by the deceleration fuel schedule to prevent combustor blow out.
- Thrust decreases as the core and fan rotors begin their deceleration.
- The fan pitch is moved rapidly to close proximity of the scheduled floor limit (i.e., two degrees closed) at the 62 percent power setting. This action is a contributing factor in producing the 100 to 80 percent thrust reduction during the first 0.5 seconds.
- The fan exhaust nozzle is opened to its scheduled roof limit at the 62 percent power setting. The core and fan rotors undershoot their final value as the nozzle is opening.
- The transient time to 62 percent thrust is about 0.9 seconds.
- During this deceleration transient, a rather uniform increase in fan stall margin is maintained until the system settles to the final thrust.

Reverse Thrust Transient Response

One of the QCSEE program objectives is to develop the technology which will yield fast thrust reversal capability for the powered-lift system. A key factor in achieving this objective is the design and evaluation of the control system logic. This control logic must operate to position the variable geometry while maintaining safe engine operation during the transition to reverse. The purpose of this study on reverse transient response was to evaluate the proposed control logic.

The specific transient requirement is that thrust reversals from maximum installed net forward thrust to maximum reverse thrust shall be achieved in less than 1.5 seconds. This requirement has been interpreted to mean that reverse thrust shall settle to greater than 95 percent of the final value in less than 1.5 seconds after receipt of the reverse command. Figure 18 depicts this interpretation.

In the UTW experimental engine, the variable-pitch fan will be used to reverse direction of the fan duct airflow and thus provide reverse thrust. Two directions for changing fan pitch angle are to be demonstrated; one is

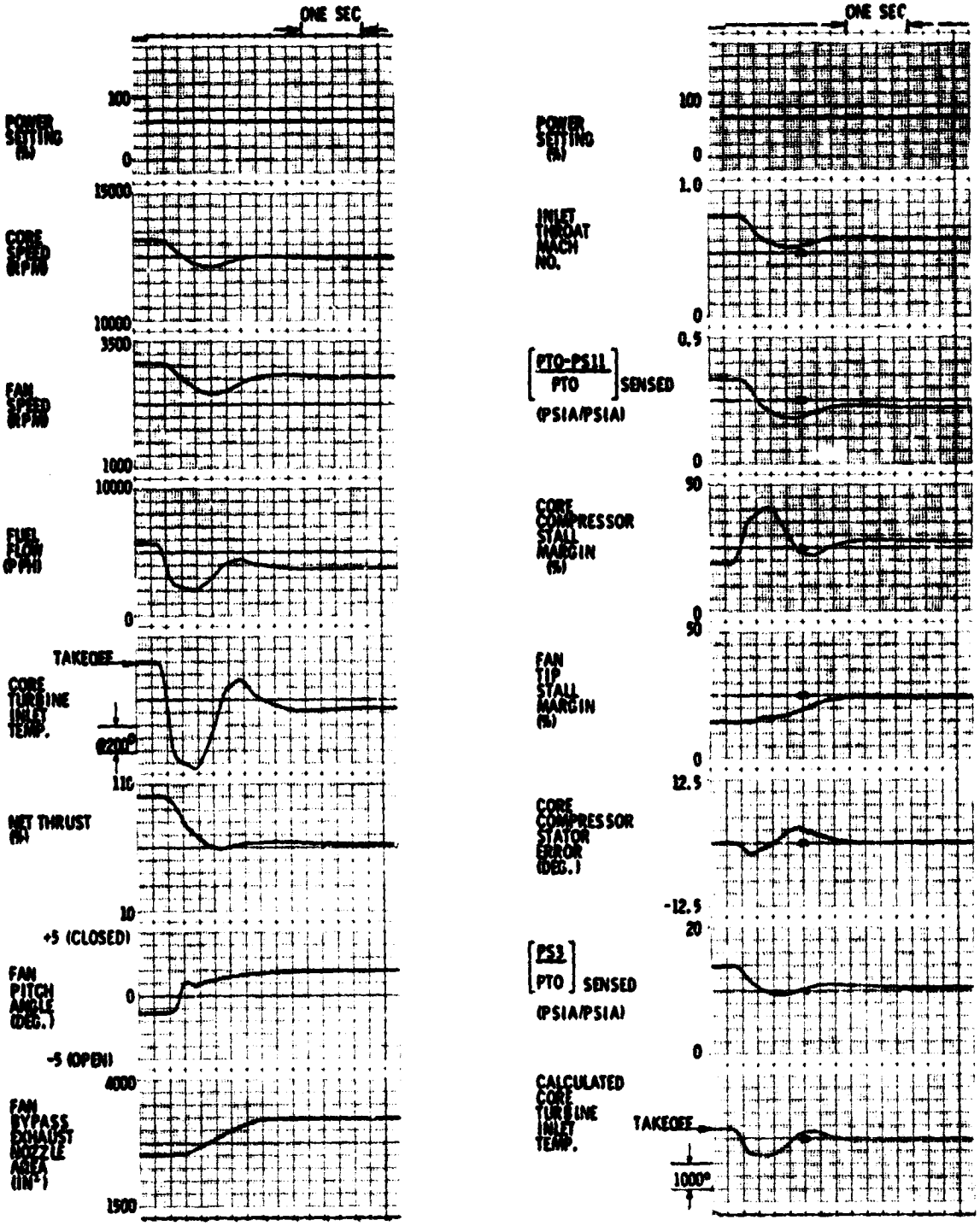

Figure 17. Transient Response for Throttle Chop from 100 to 62% Net Thrust at Sea Level Static, Standard Day, Zero Bleed.

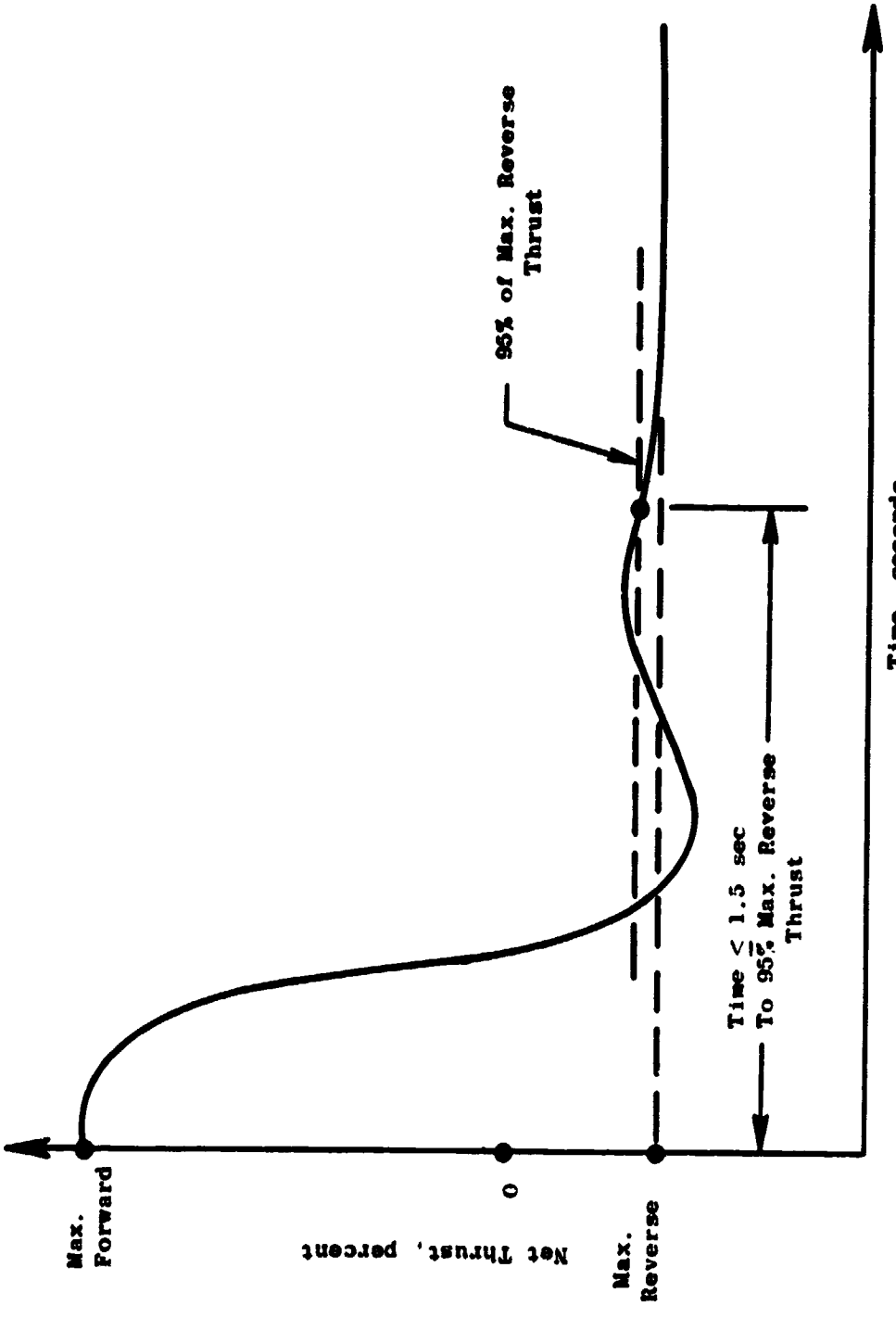

Figure 18. Interpretation of Time Requirement for Transients from Maximum Installed Net Forward Thrust to Maximum Reverse Thrust.

the forward to reverse pitch angle changes through stall (i.e., feather); the second is angle changes through flat pitch. During transitions between the forward and reverse thrust fan pitch angle positions, the fan shaft power absorption decreases and, thus, causes a tendency for the fan to accelerate. Quantitative information on fan horsepower during transition does not exist at this point in the UTW experimental engine development program and will not be known until the fan is tested on the engine. It is expected, however, that transitions through flat pitch will have less fan shaft power absorption and, thus, more tendency to overspeed when compared to reverse transients through stall.

Because of the unknown fan shaft power absorption level, the simulation has been used to investigate a range of minimum fan horsepowers during the transients to reverse. The objective has been to determine the range of control adjustments needed to prevent excessive fan speeds and yet achieve the required transient time of 1.5 seconds during experimental engine testing. This study on reverse thrust transients was performed at the Sea Level Static (SLS), Standard Day condition.

Reverse Transients Through Stall - A transient from takeoff power to maximum reverse through stall is shown in Figure 19. The initial condition in this figure shows the specific values of selected engine and control variables at the takeoff power condition. The transient to reverse is initiated by the reverse command. Upon receipt of this signal the control system operates as follows:

- Power control of the engine is switched from the pressure ratio - fuel control mode to a core speed - fuel control mode. The core speed demand is set at a flight idle position, which causes the fuel to decrease.
- The fan pitch angle is opened to a predetermined reverse position.
- The fan nozzle is opened to a predetermined reverse position.
- When fan pitch angle passes a predetermined interlock position, the power control of the engine is switched from the flight idle core speed - fuel flow control mode to the fan speed - fuel flow control mode.

As shown in Figure 19, the nozzle area and fan pitch are moved rapidly from the takeoff to the reverse position. Fuel flow is reduced and produces a corresponding reduction in turbine inlet temperature and core speed. Fan speed decreases and then increases due to the expected reduction in fan horsepower during transition through stall. For the transient in Figure 19, the pitch angle - fuel flow interlock position is set at -80 degrees. (Note: Reverse transients through stall were performed for interlock positions over the range from -20 through -80 degrees; also, the digital control hardware includes an engineering panel adjustment input so that final interlock positions can be established during experimental engine test.) When pitch

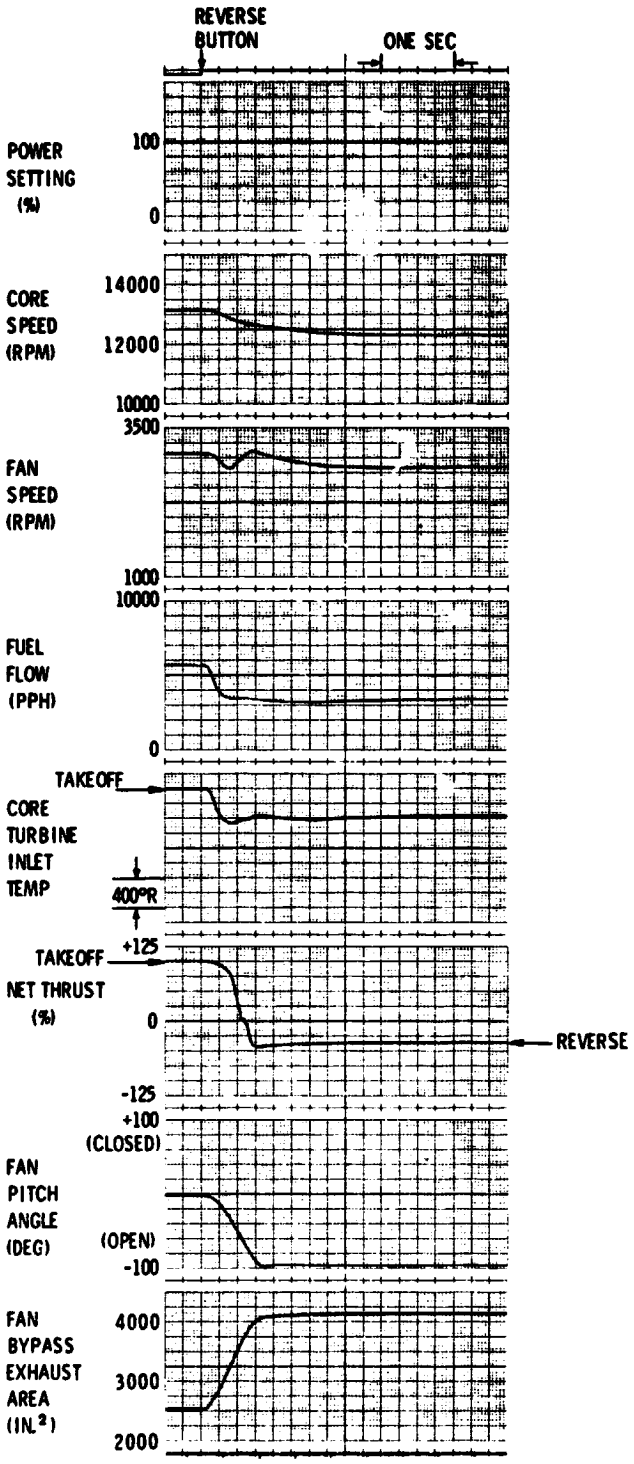

Figure 19. Transient from Takeoff to Maximum Reverse Through Stall at Sea Level Static, Standard Day.

angle passes through the 80 degree interlock point, the power control is switched to the fan speed - fuel flow control mode. Since fan speed is above the final value, fuel flow continues to decrease and eliminates the fan speed error to achieve the final steady-state speed. Reverse thrust is achieved in approximately 0.7 seconds after initiation of the reverse command.

Time from forward to reverse thrust is affected by many variables. Some of these are:

- Core speed idle speed setting - too low of a setting will cause excessive reversal times and too high of a setting will cause the fan to accelerate.
- Minimum fan horsepower absorption in stall - the absolute level and its variations are not predictable. Horsepower absorption will affect times to reverse since it will affect the transient fan speed characteristics, which must be controlled to provide engine protection. Figure 20 shows the range of minimum fan horsepower considered in this simulation study.
- The pitch angle - fuel flow interlock point - early releases should reduce time to reverse but may cause a tendency for the fan to overspeed.
- Fan pitch rate of change
- Fan exhaust nozzle rate of change
- Dynamics associated with airflow reversal in the fan and its duct
- Fan stall recovery point of the fan during the reverse transient.

The first three of the above mentioned variables were jointly investigated on the simulation. The purpose was to determine the variation in engine transient characteristics with several levels of minimum fan horsepower absorption, core idle speed settings, and pitch angle interlock points. For the conditions investigated, the results indicate that the core idle speed adjustment should be set between 11,700 to 12,500 rpm. With this core idle speed adjustment range and the capability to adjust the pitch angle interlock release point, the simulation predicts that the experimental engine will achieve reverse thrust in less than 1.5 seconds without excessive fan speeds.

The last four items mentioned above were not investigated on the engine simulation. Sufficient data were not available to model and investigate the fan stall recovery point and the dynamics associated with airflow reversal. The fan exhaust nozzle rate of change was not investigated because the system is designed for rapid nozzle opening to reduce forward thrust. However, the control system hardware is designed with an adjustable nozzle rate limit so that this parameter may be investigated during experimental engine testing. The fan pitch angle rate of change was not investigated because it is expected

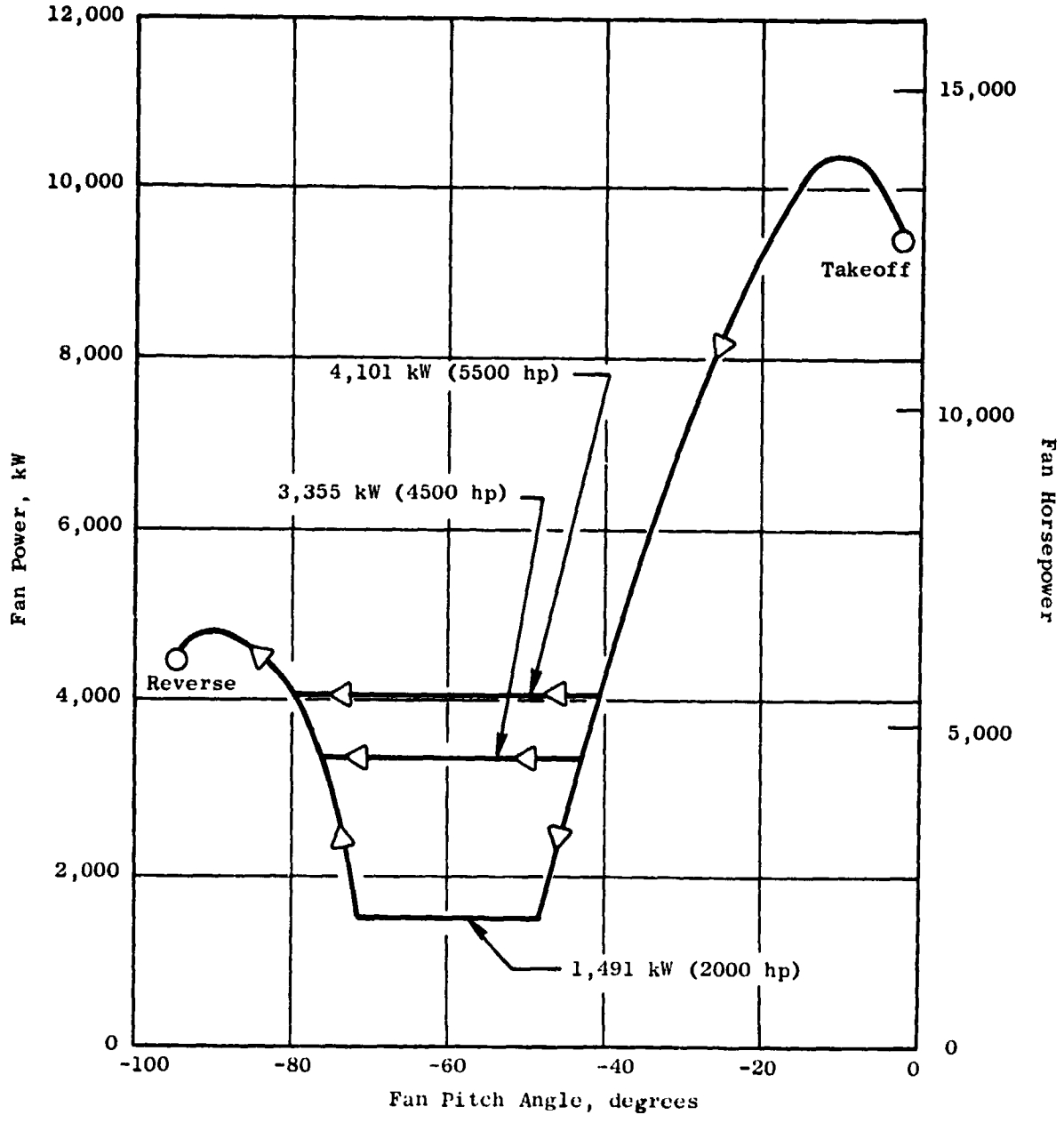

Figure 20. Fan Horsepower Transient Versus Fan Pitch Angle During Transition from Takeoff to Maximum Reverse Thrust Through Stall.

that a rapid rate of blade angle change is required to reduce the fan stresses. However, the control system hardware is designed with an adjustable fan pitch rate limit so that this parameter may be investigated during experimental engine testing.

Reverse Transients Through Flat Pitch - A transient from takeoff power to reverse through flat pitch is shown in Figure 21. The left hand portion of this figure shows the specific values of selected engine and control variables at the takeoff power condition. The transient to reverse is initiated by the reverse command. Upon receipt of this signal, the control logic causes the fuel flow to decrease, the fan nozzle to open to its reverse position, and the fan pitch to close to its reverse position. For this transient, power control of the engine is switched from the pressure ratio - fuel flow mode, to the core speed - fuel control mode, and finally to the fan speed - fuel flow control mode, in the same manner as described in the report section on reverse transients through stall.

As shown in Figure 21, the nozzle area and fan pitch are rapidly moved from the takeoff to their reverse positions. Fuel flow is reduced and produces a corresponding reduction in turbine inlet temperature and core speed. Fan speed increases due to the low level assumed for fan shaft horsepower absorption [minimum = 1.5 Mw (2000 horsepower)]. For the transient in Figure 21, the pitch angle - fuel flow interlock position is set at + 70 degrees. (Note: Reverse transients through flat pitch were performed for interlock positions over the range from + 30 to + 70 degrees; also, the digital control hardware includes an engineering panel adjustment input so that final interlock position can be established during experimental engine test.) At the 70 degree interlock point, the decel schedule continues to control fuel flow because the fan speed is above the final value. As the fan decelerates, fuel flow increases in order to control the fan at the final speed level.

The takeoff to reverse transient in Figure 21 predicts that fan speed will exceed the maximum reverse thrust speed limit of 3408 rpm (i.e., fan turbine speed = 8400 rpm) when the fan shaft power absorption reduces to the 1.5 Mw (2000 hp) minimum during the transition. Simulation results in Table V show that reductions in the core idle speed adjustment does not reduce the peak fan speed below 3500 rpm, and therefore, speed still exceeds the maximum limit. A potential design change to reduce the above peak fan speed is to delay closing the fan pitch to its reverse position. This involves adding more logic to the control design for the experimental engine and thereby having different logic for reverse transients through stall pitch and through flat pitch. The decision has been to continue with the original control logic design until quantitative information on fan shaft power absorption has been determined from the fan evaluation portion of the engine test program. This decision was based on the following considerations:

- Delay in closing fan pitch to reverse position could cause unacceptable transient times to reverse thrust.
- Reverse thrust transients through stall pitch had been selected as the primary mode.

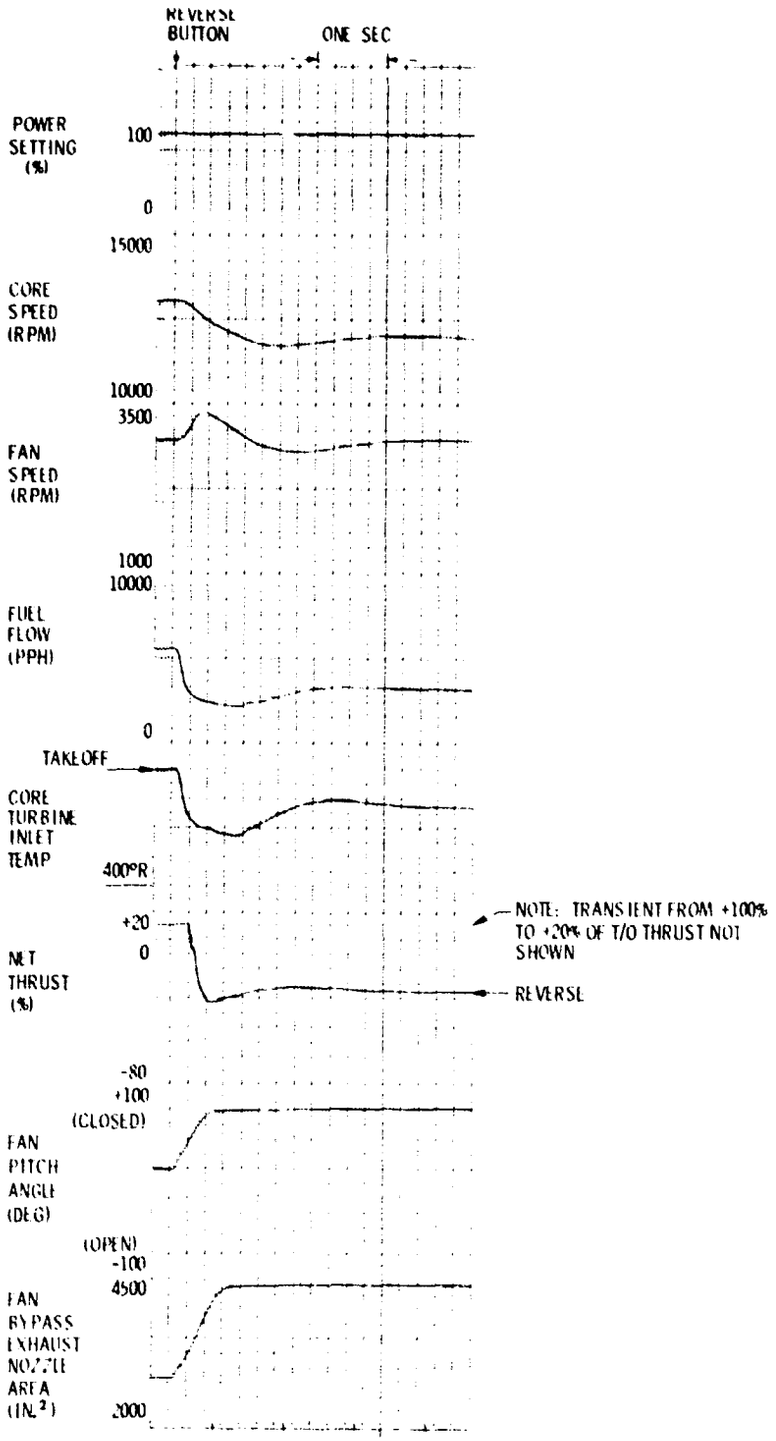

Figure 21. Transient from Takeoff to Reverse Through Flat Pitch at Sea Level Static, Standard Day.

Table V. Effect of System Variables on Peak Fan Speed During Forward to Reverse Thrust Transients Through Flat Pitch.

Forward Thrust Power Setting (%)	Forward To Reverse Interlock Position (Deg)	Minimum Fan Shaft Power Absorption		Core Idle Speed Adjustment (rpm)	Peak Fan Speed During Transition To Reverse (rpm)
		MW	(Horsepower)		
100	70	1.5	2000	11400	>3500
100	70	1.5	2000	11000	>3500
100	70	1.5	2000	10800	>3500
60	70	1.5	2000	11400	3110
60	70	1.5	2000	11000	3100
60	30	1.5	2000	11000	3120
50	70	1.5	2000	11400	2825
50	70	1.5	2000	11000	2740
100	70	3.4	4500	11000	3440
65	70	3.4	4500	11000	3070
60	70	3.4	4500	11000	2890

- As shown by simulation results in Figure 22, the original control design can be used for reverse transients which start from power settings in the approach thrust range (i.e., 60 percent power setting).

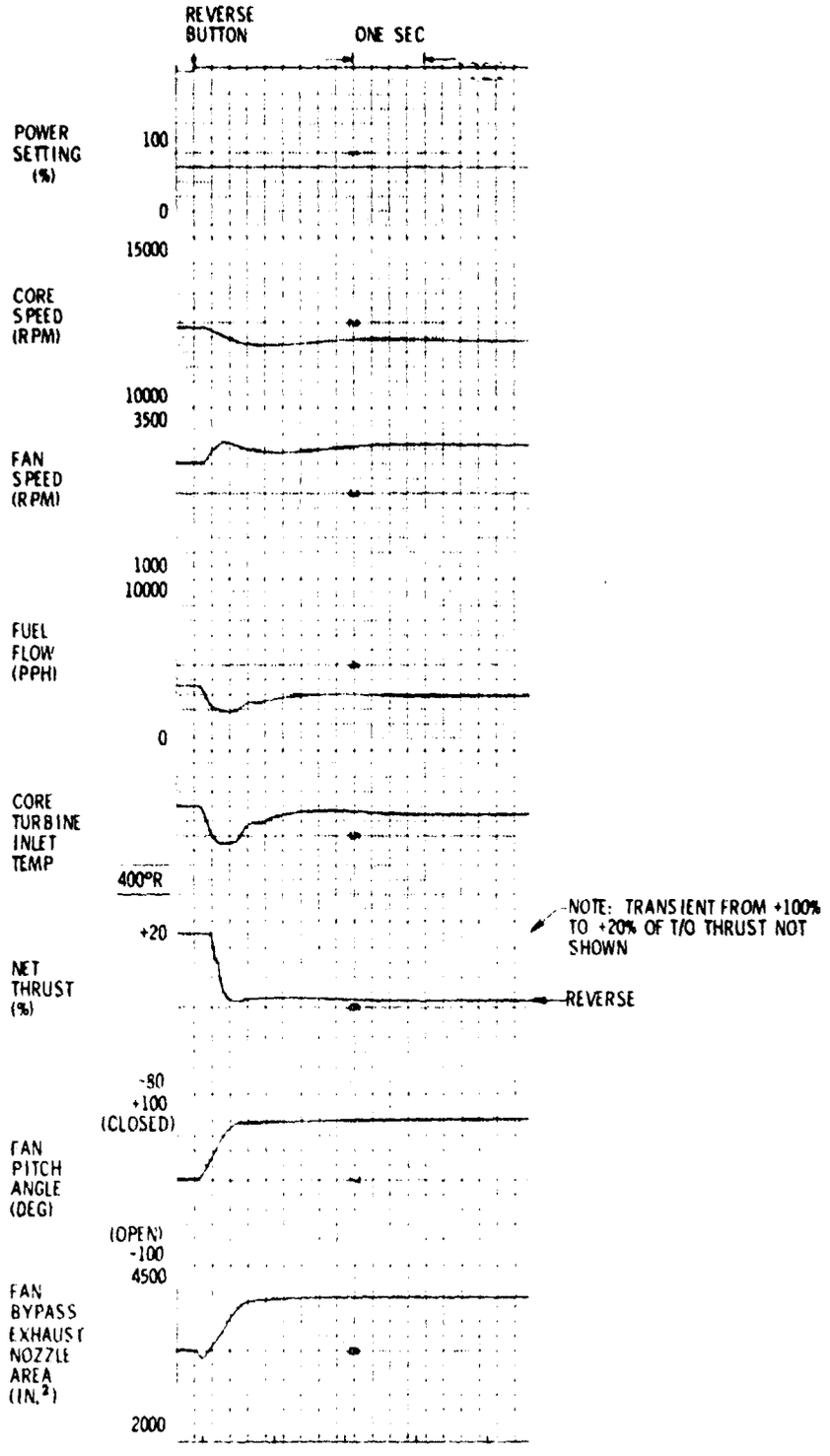

Figure 22. Transient from 60° Power Setting to Reverse through Flat Pitch at Sea Level Static, Standard Day.

SUMMARY OF RESULTS

Hybrid simulations of the UTW experimental engine have been constructed and used to develop the control system dynamic design. The engine simulation for forward thrust was based on the digital cycle deck used to generate the QCSEE preliminary technical requirements. Simulation results for throttle bursts from 62% to 100% net thrust predict that the experimental engine will meet the dynamic thrust response requirement of 62% to 95% net thrust in one second. Results for transient stall margins, temperature, and inlet Mach number indicate that safe engine operation will be maintained during this engine transient. Transient results also predict fast, safe deceleration capability during throttle chops.

A range of minimum fan shaft power absorption has been considered in the engine simulation for reverse thrust since experimental data are not yet available. Absolute levels and variations of minimum power absorption affect peak fan speed during the transition from forward to reverse. Currently, the minimum power levels are not predictable; however, it is expected that power absorption during fan blade transitions through flat pitch will be less than the power absorption for transitions through stall.

For the conditions investigated during takeoff to maximum reverse thrust through stall, simulation results predict that the experimental engine will achieve reverse thrust in less than 1.5 seconds without excessive fan speeds.

For the fan loading investigated for the takeoff to maximum reverse transient through flat pitch, the predicted fan speed will peak over the maximum reverse speed limit. A design change to the control logic would be needed to reduce peak fan speed for this transient. Results indicate that the current control design will prevent excessive fan speeds if transients to reverse start from forward power settings of 60% or lower. The decision has been made to continue with the current control logic design until substantial quantitative information on fan shaft power absorption has been determined in the fan evaluation portion of the experimental engine test program.

APPENDIX A

UTW FAN SPEED DIGITAL ELECTRONIC CONTROL BLOCK DIAGRAMS AND SPECIFICATIONS

(For Experimental Engine)

Included in this appendix are the detailed block diagrams and the specifications for schedules, gains, time constants, and limits which currently define the digital electronic portion of the fan speed control for the first build of the UTW experimental engine (Figures 23 through 29 and Tables VI through VIII).

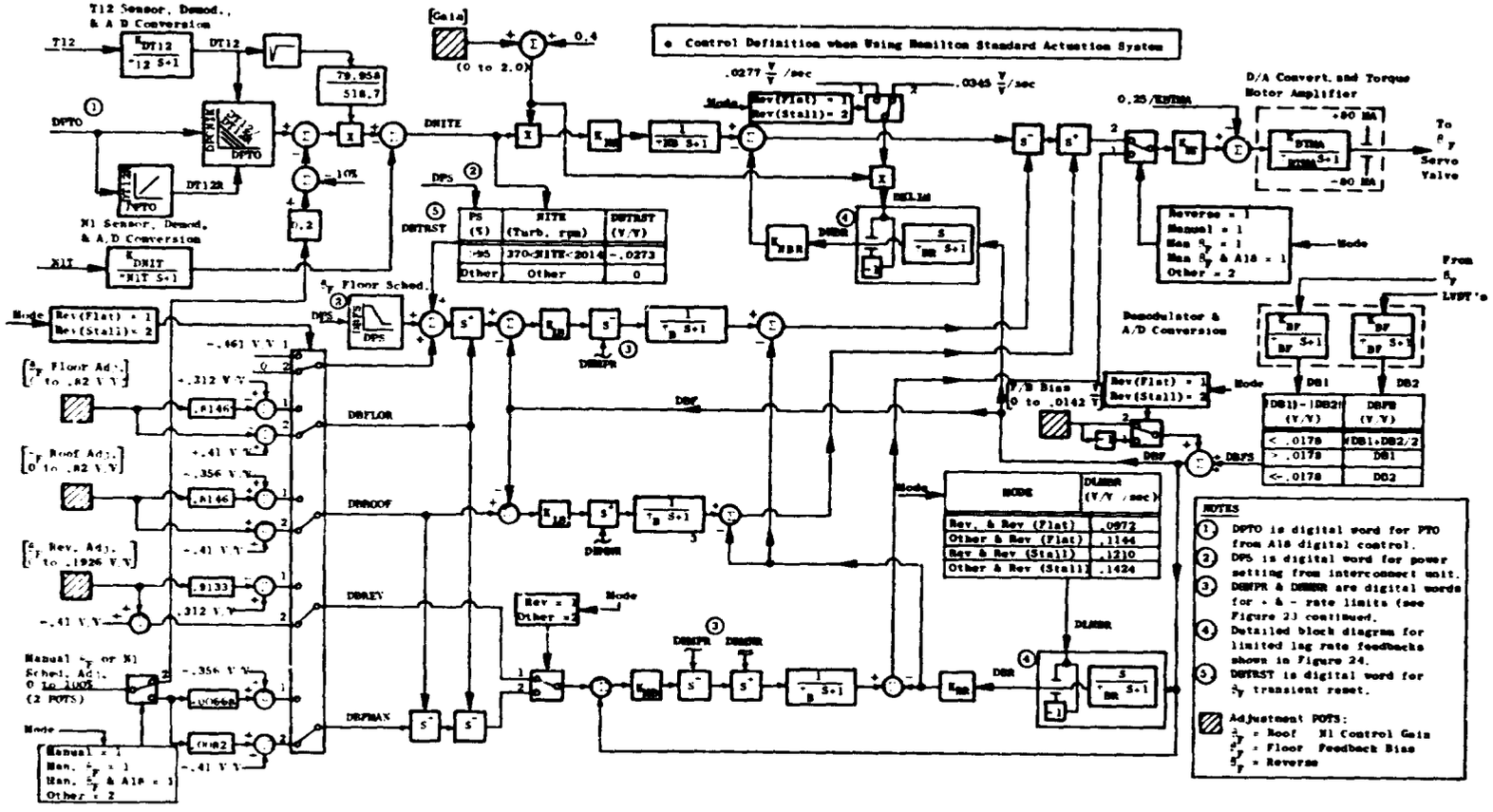

Figure 23. Digital Electronic Fan Speed Control Block Diagram.

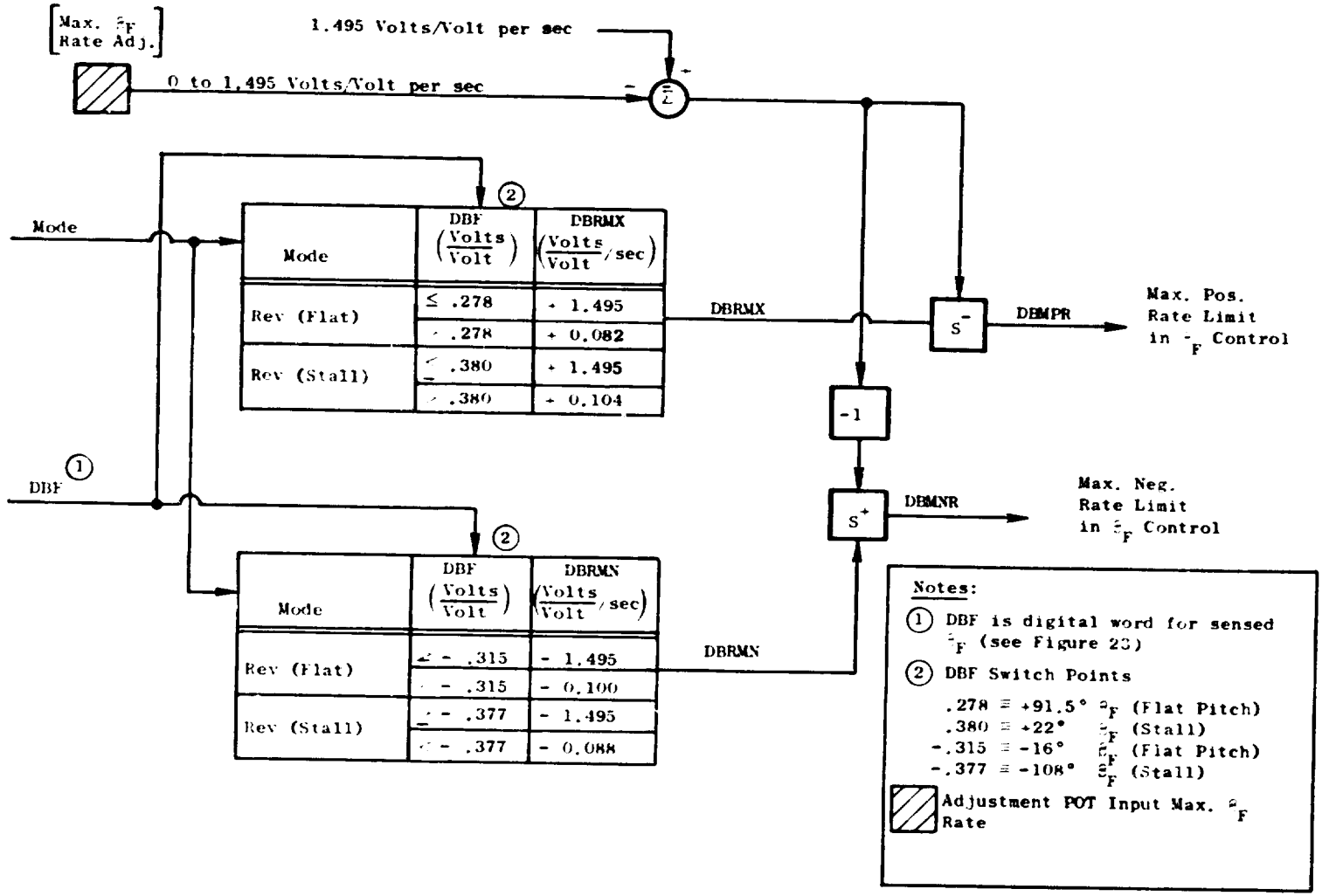

Figure 23. Digital Electronic Fan Speed Control Block Diagram (Concluded).

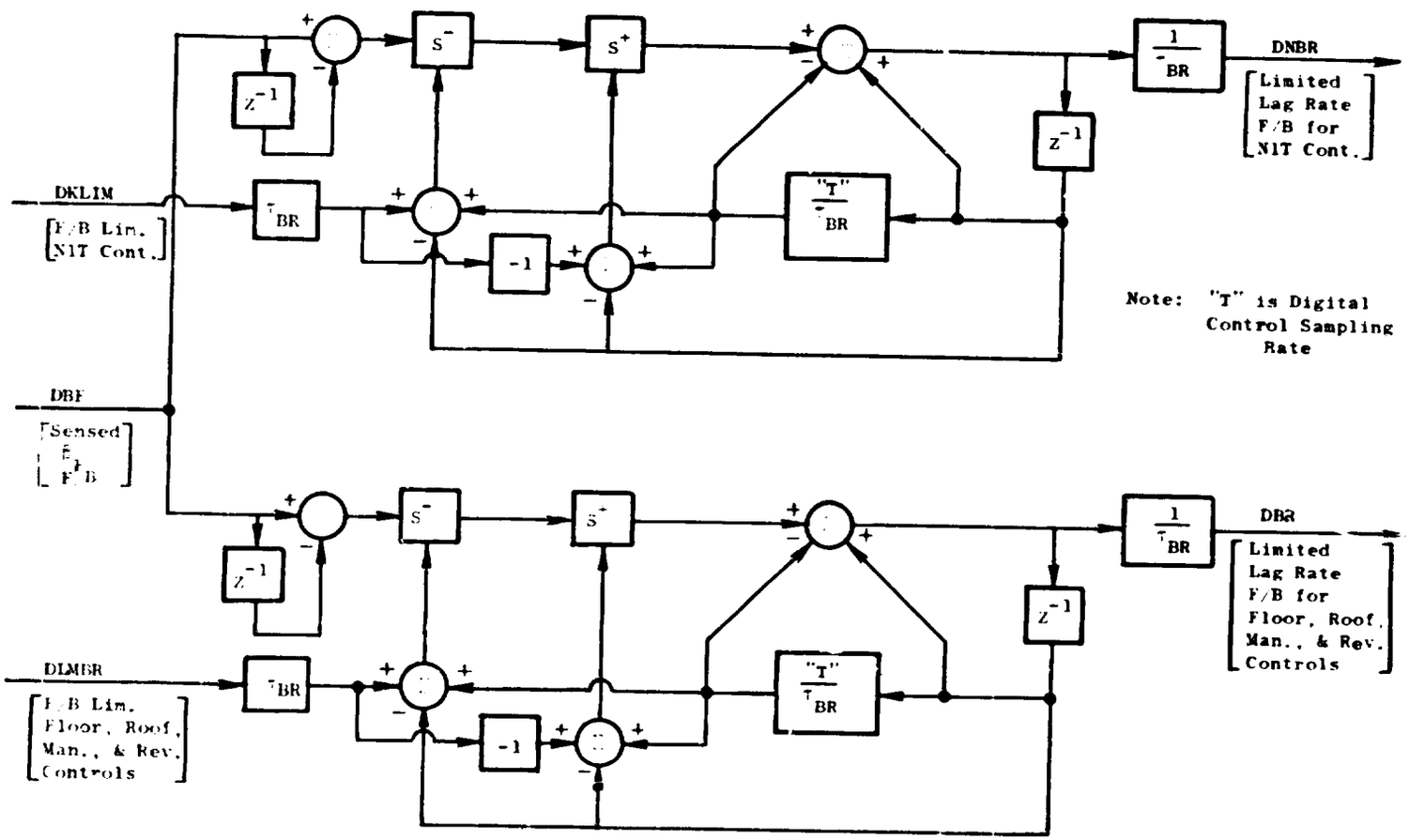

Figure 24. Detail Block Diagrams for Lag Rate Feedbacks with Rate Limits in QCSEE UTW Digital Electronic Fan Speed Control.

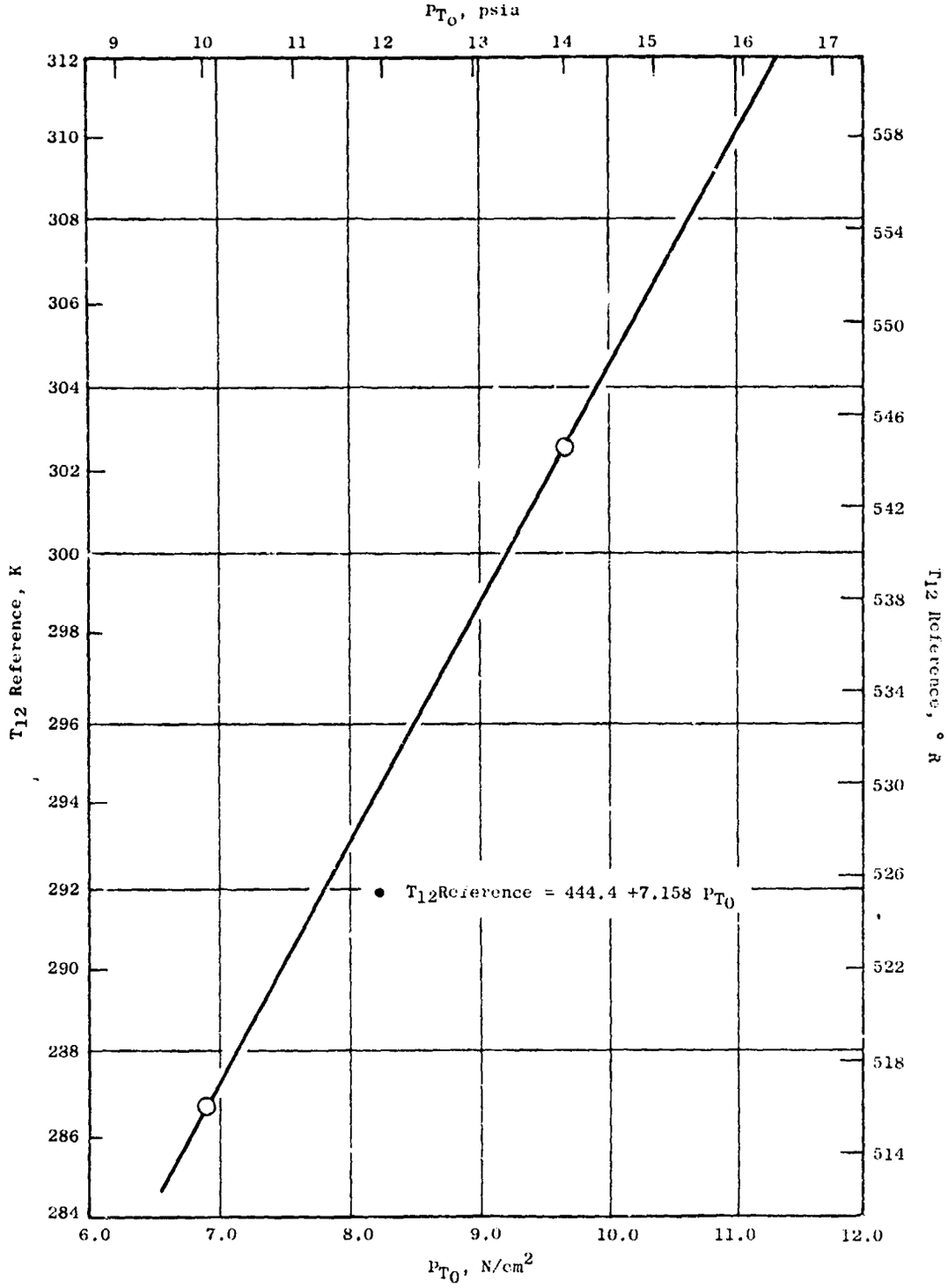

Figure 25. Digital Electronic Control Schedule for T_{12} Reference Versus PTO, Experimental Engine.

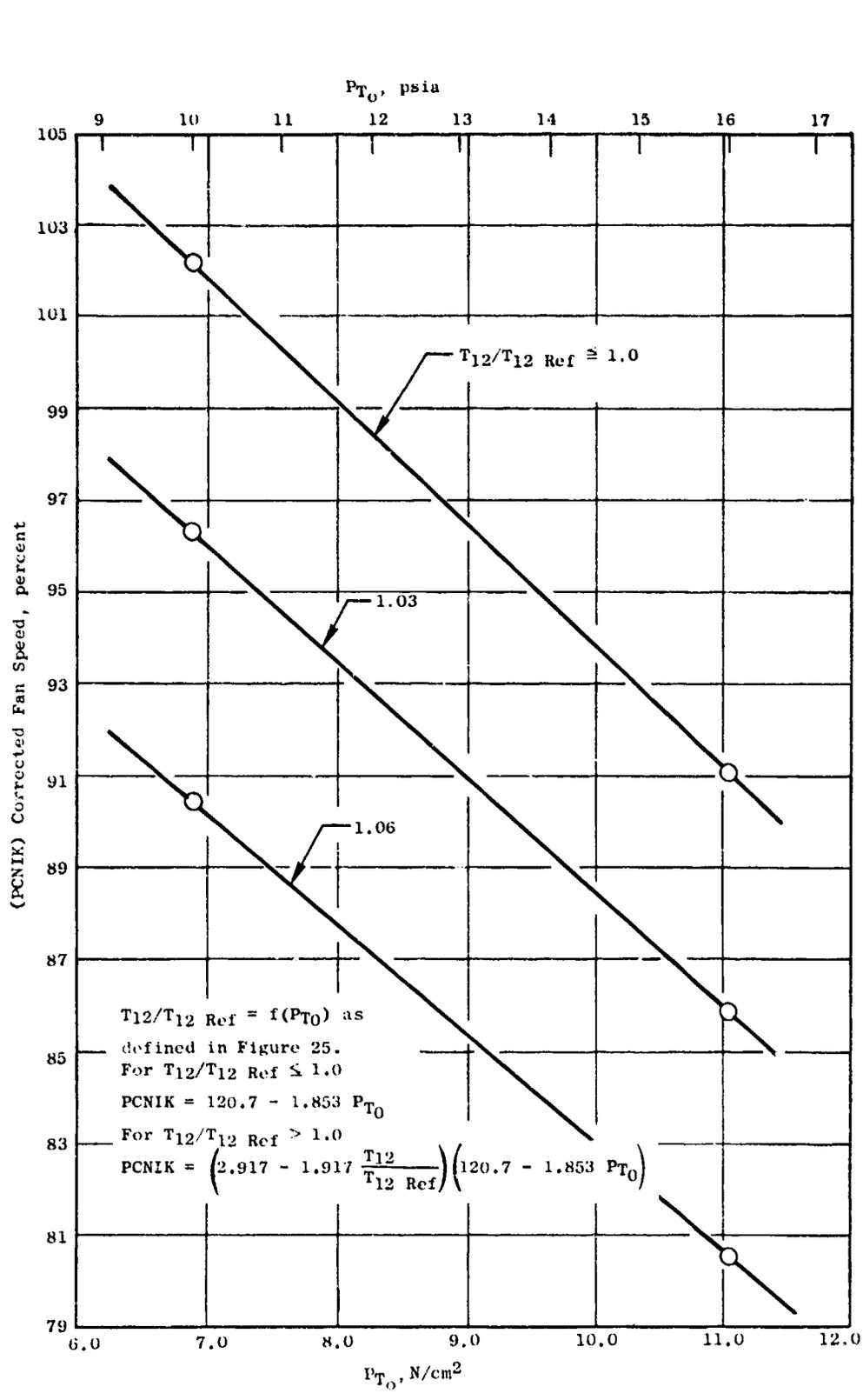

Figure 26. Digital Electronic Fan Speed Control Takeoff Power Schedule, Experimental Engine.

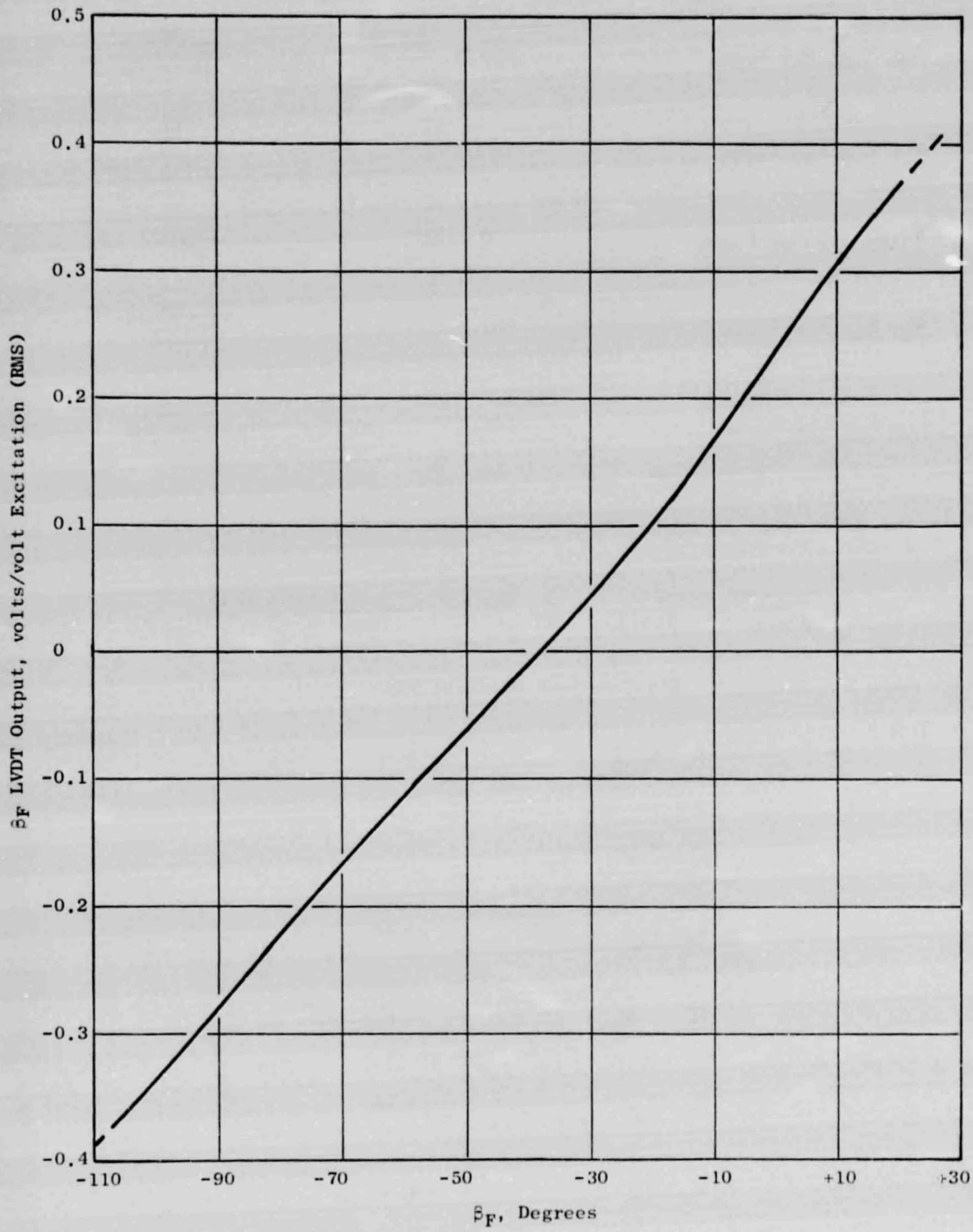

Figure 29. Hamilton Standard β_F LVDT Characteristics for Reverse Through Stall.

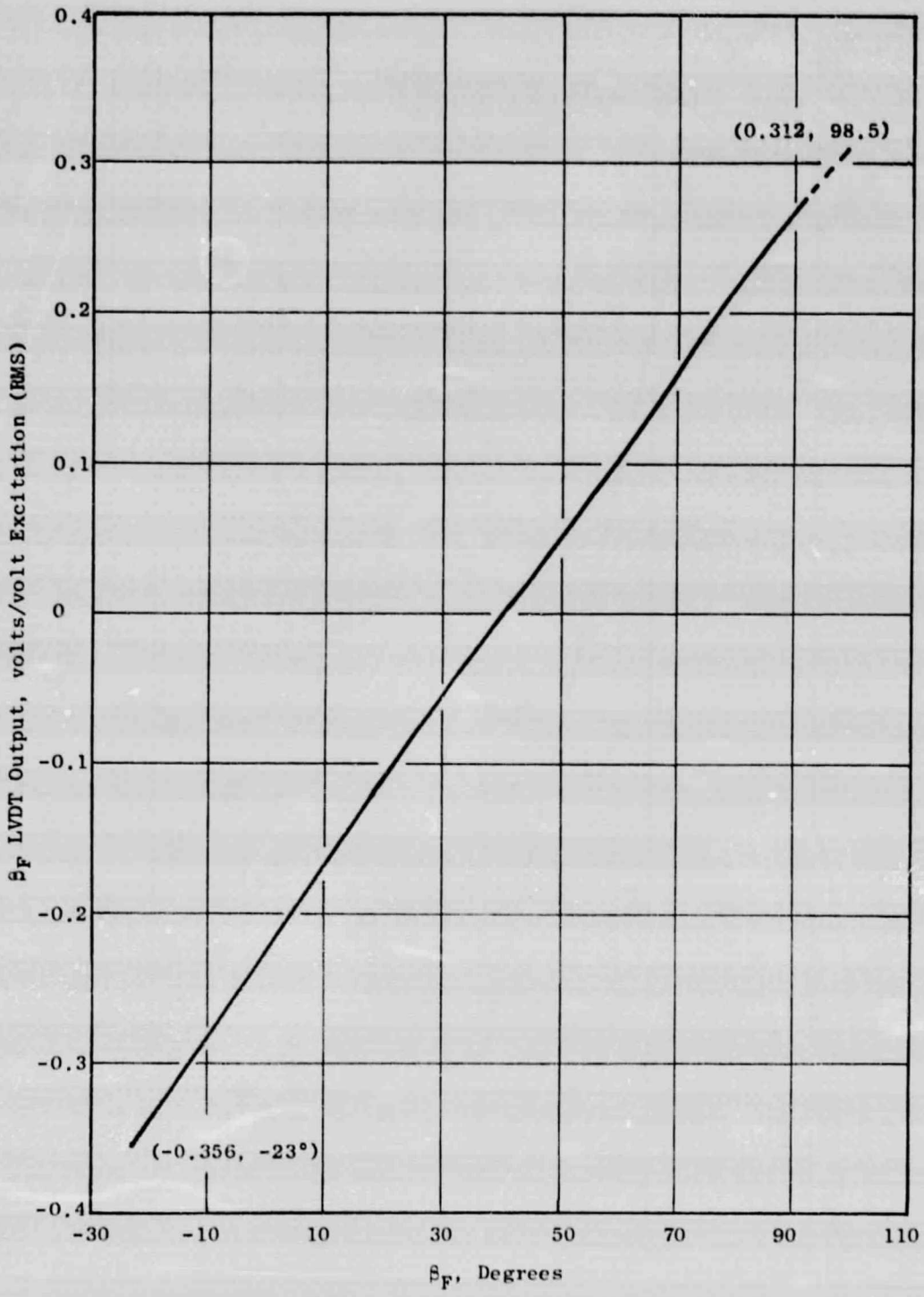

Figure 28. Hamilton Standard β_F LVDT Characteristics for Reverse Through Flat Pitch.

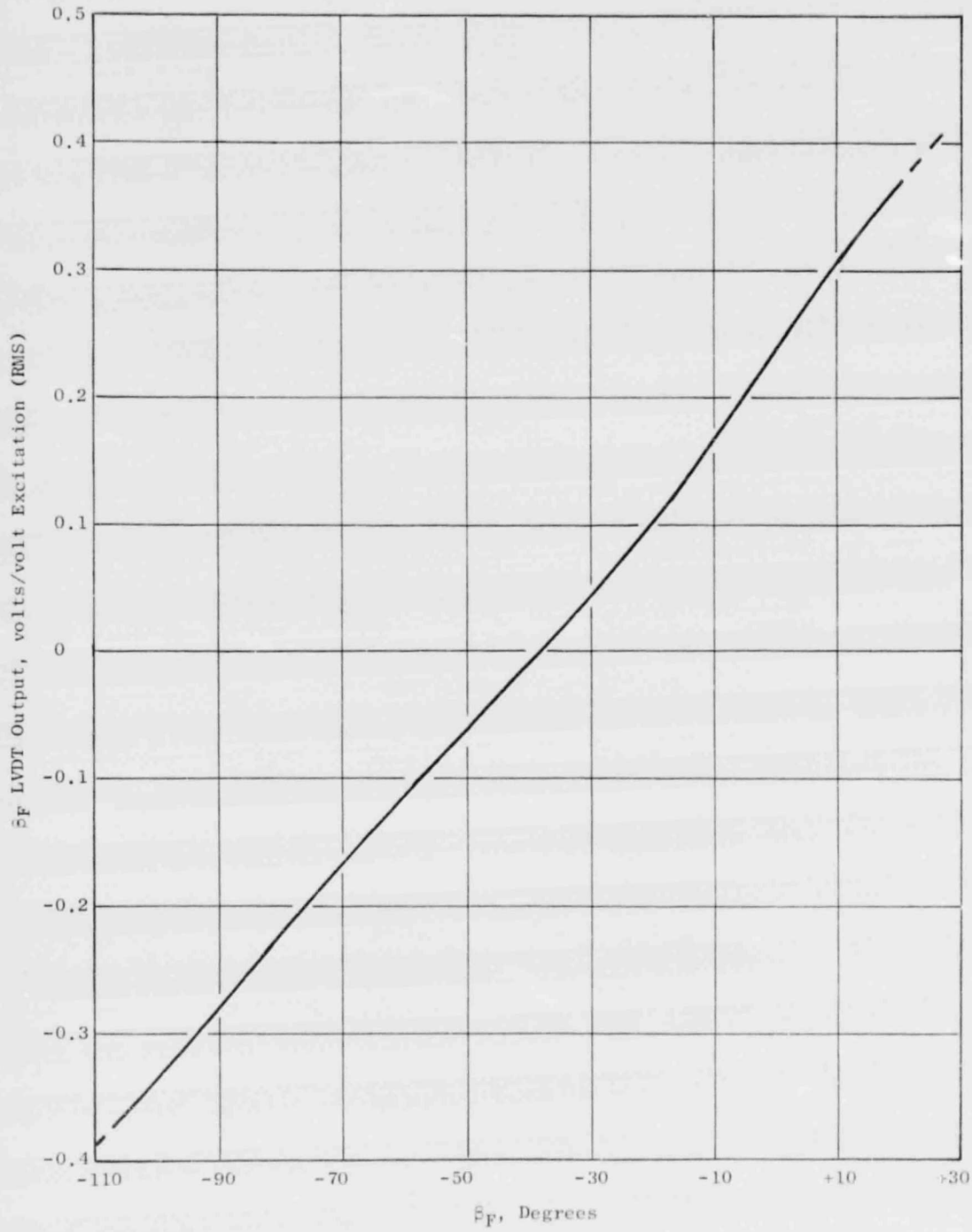

Figure 29. Hamilton Standard β_F LVDT Characteristics for Reverse Through Stall.

Table VI. Digital Electronic Fan Speed Control Gains, Hamilton Standard Actuation System.

$K_{BF}\ K_{NBR}\ K_{BT}\ K_{BTMA}$	268.6	$\frac{MA}{\frac{Volts}{Volt}/sec}$
$K_{BF}\ K_{BR}\ K_{BT}\ K_{BTMA}$	268.6	$\frac{MA}{\frac{Volts}{Volt}/sec}$
$K_{DNIT}\ K_{NB}\ K_{BT}\ K_{BTMA}$	0.02325	$\frac{MA}{rpm}$
$K_{BF}\ K_{LB}\ K_{BT}\ K_{BTMA}$	683.1	$\frac{MA}{\frac{Volts}{Volt}}$
$K_{BF}\ K_{MB}\ K_{BT}\ K_{BTMA}$	341.6	$\frac{MA}{\frac{Volts}{Volt}}$

- The above digital gains are defined based on the following LVDT feedback configuration:

$$\frac{\Delta(\text{LVDT Output})}{\Delta(\text{Worm Gear Input})} = \frac{1}{380}\ \frac{\text{Volts/Volt Excitation (RMS)}}{\text{Rev}}$$

DIGITAL GAIN DISTRIBUTION*

$K_{BT}\ K_{BTMA}$	12.81
$K_{BF}\ K_{NBR}$	20.97
$K_{BF}\ K_{BR}$	20.97
$K_{DN1T}\ K_{NB}$	$1.815 * 10^{-3}$
$K_{BF}\ K_{LB}$	53.33
$K_{BF}\ K_{MB}$	26.66

* The above digital gain distribution is required for the maximum β_F rate limits specified in Figure 23.

Table VII. Digital Electronic Fan Speed Control Time Constants.
(Frequency Range from 0.1 to 10.0 Hz)

Symbol	Description	Value
τ_{BTMA}	D/A Converter and Torque Motor Driver Amplifier Lag	$\leq$ 0.01 sec
τ_{BF}	LVDT, Demodulator, and A/D Converter Lag	$\leq$ 0.01 sec
τ_{T12}	Fan Inlet Temperature Sensor, Demodulator, and A/D Converter Lag	$\leq$ 6.00 sec @ 10 pps/ft^2 Airflow Density
τ_{N1T}	LP Turbine Speed Sensor, Demodulator, and A/D Converter Lag	$\leq$ 0.01 sec
τ_{NB}	Controller Lag in N1T-β_F Control	0.05 sec
τ_{B}	Controller Lag in β_F Floor, β_F Roof, and β_F Manual/Reverse Controls	0.01 sec
τ_{BR}	Rate Feedback Lag in N1T-β_F, β_F Floor, β_F Roof, and β_F Manual/Reverse Controls	0.30 sec

Table VIII. Digital Electronic Fan Speed Control Sensors.

Symbol	Description	Range
DT12	Sensed Fan Inlet Temperature	233 to 344 K (420° to 620° R)*
DN1T	Sensed LP Turbine Speed	0 to 9595 rpm
DBF	Sensed β_F Position	-0.41 to +0.41 $\frac{\text{Volts}}{\text{Volt}}$ Excit. (RMS)

*Sensor shall withstand up to 139 K (250° R) when electrically energized.

APPENDIX B

UTW INLET DUCT MACH NUMBER DIGITAL CONTROL BLOCK DIAGRAMS AND SPECIFICATIONS

(For Experimental Engine)

Included in this appendix are the detailed block diagrams and the specifications for schedules, gains, time constants, and limits which currently define the digital electronic portion of the inlet duct Mach number control for the first build of the UTW experimental engine (Figures 30 through 34 and Tables IX, X, and XI).

Figure 30. Digital Electronic Inlet Duct Mach Number Control Block Diagram.

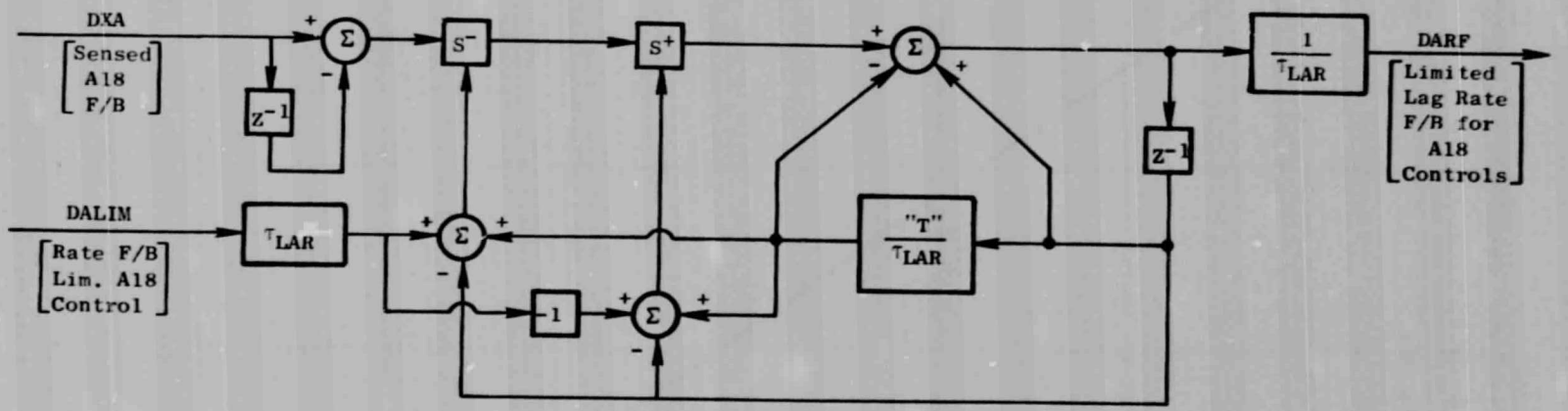

NOTE: "T" is Digital Control Sampling Rate

Figure 31. Detail Block Diagram for Lag Rate Feedback with Rate Limits in Digital Electronic Inlet Duct Mach Number Control.

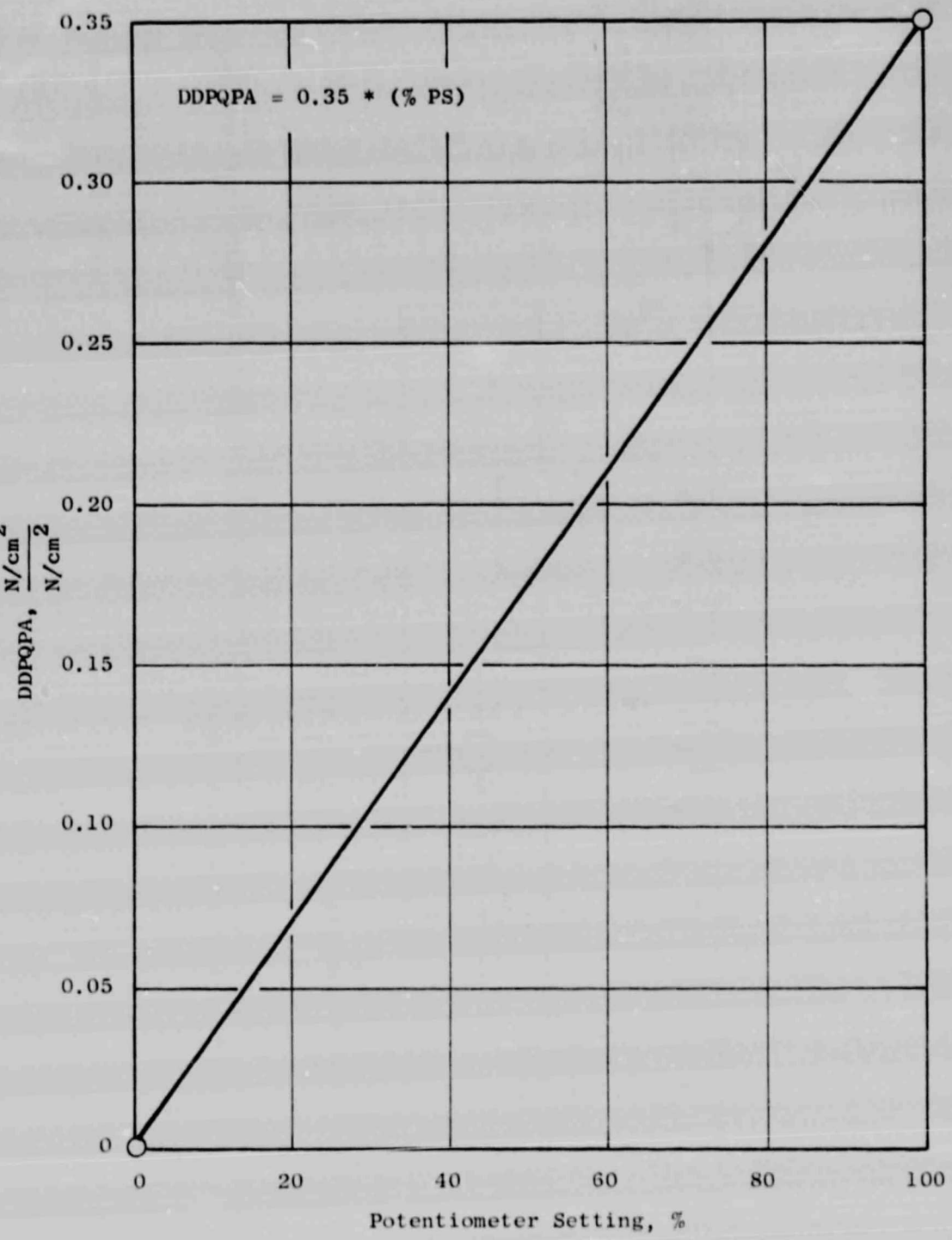

Figure 32. Digital Electronic Inlet Duct Mach Number Control, DDPQPA Component of ΔP/P Reference Vs. Percent of Manual M11 Adjustment Potentiometer.

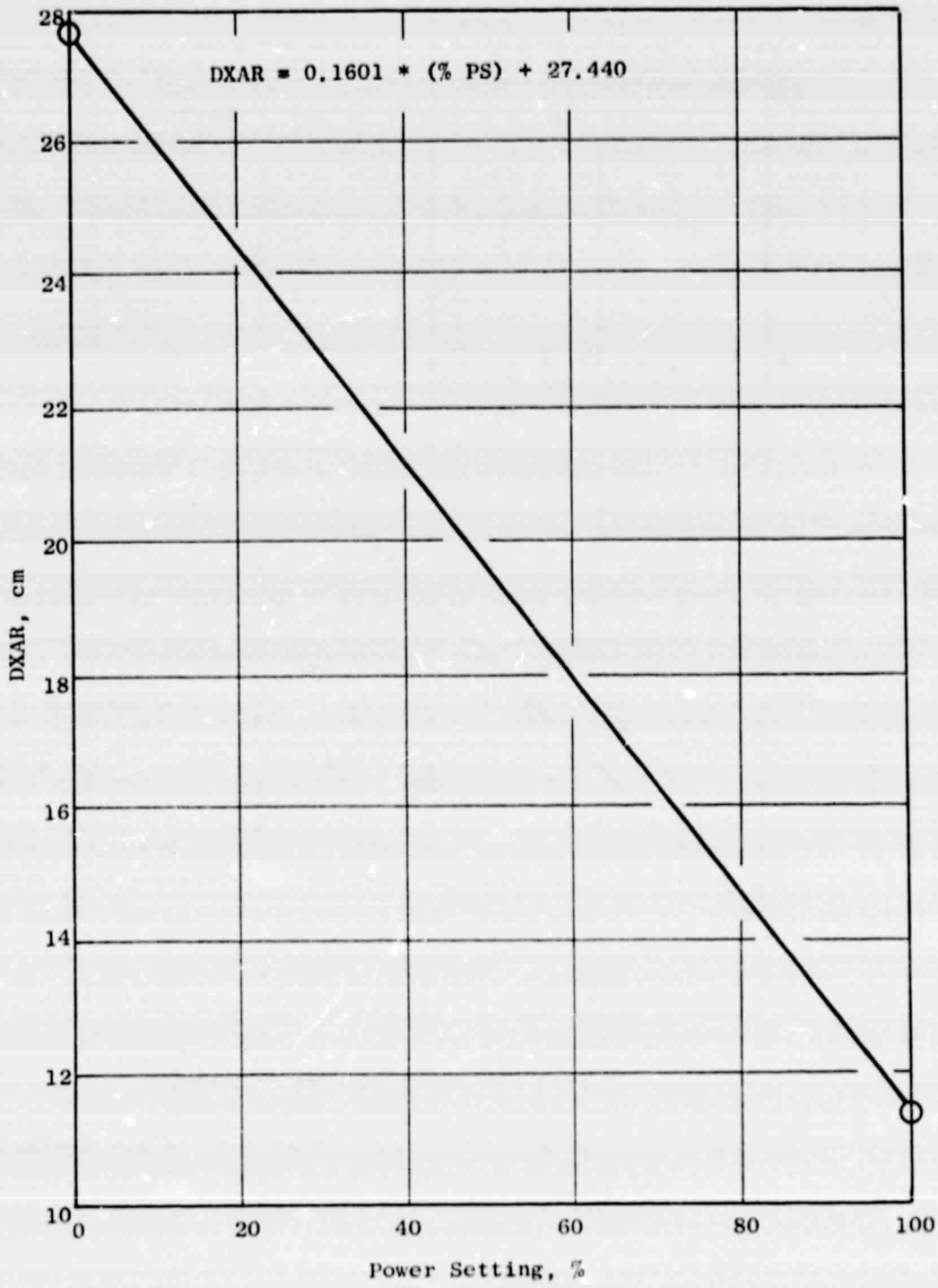

Figure 33. Digital Electronic Inlet Duct Mach Number Control, DXAR Component of X18 Roof Schedule Vs. Power Setting.

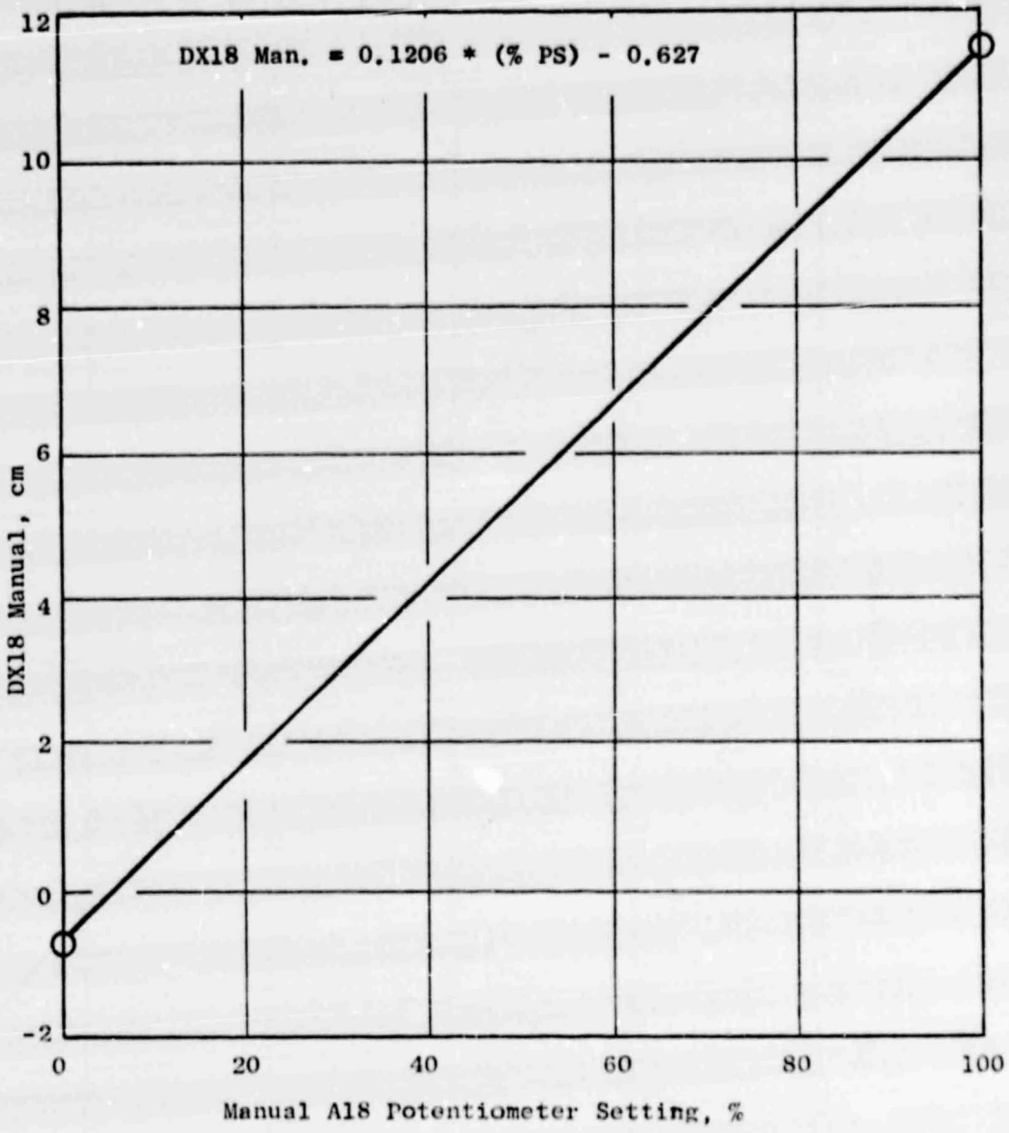

Figure 34. Digital Electronic Inlet Duct Mach Number Control Schedule for Manual X18 Schedule Vs. Manual X18 Adjustment Potentiometer.

Table IX. Digital Electronic Inlet Duct Mach Number Control Gains.

$K_{AF}\ K_{LAR}\ K_{AT}\ K_{ATMA}$	47.07 ma/cm/sec (18.53 ma/in./sec.)
$\frac{K_{DDP}}{K_{PTO}}\ K_{PA}\ K_{AT}\ K_{ATMA}$	178.0 ma/N/cm^2/N/cm^2 (258.1 ma/psi/psi)
$K_{AF}\ K_{LA}\ K_{AT}\ K_{ATMA}$	164.72 ma/cm (64.85 ma/in.)
$K_{AF}\ K_{MA}\ K_{AT}\ K_{ATMA}$	164.72 ma/cm (64.85 ma/in.)

Gain Distribution

$K_{AT}\ K_{ATMA}$	8.056
$K_{AF}\ K_{LAR}$	2.300
$\frac{K_{DDP}}{K_{PTO}}\ KPA$	32.04
$K_{AF}\ K_{LA}$	8.050
$K_{AF}\ K_{MA}$	8.050

Table X. Digital Electronic Inlet Duct Mach Number Control Time Constants.

[Frequency Range From 0.1 to 10.0 Hz]

Symbol	Description	Value, Sec
τ_{LAR}	Rate Feedback Lag in A18 Control	0.139
τ_{LA}	Controller Lag in A18 Roof/Floor Limit Controls	0.139
τ_{MA}	Controller Lag in A18 Manual/Reverser Control	0.139
τ_{ATMA}	D/A Converter and Torque Motor Driver Amplifier Lag	$\leq$0.01
τ_{AF}	LVDT, Demodulator and A/D Converter Lag	$\leq$0.01
τ_{DP}	$[P_{TO}-P_{S11}]$ Sensor, Demodulator, and A/D Converter Lag	$\leq$0.02
τ_{PTO}	P_{TO} Sensor, Demodulator, and A/D Converter Lag	<0.50

Table XI. QCSEE Digital Electronic Inlet Duct Mach Number Control Sensors.

Symbol	Description	Range
DXA	Actuator Stroke Feedback	-0.627 to 12.073 cm (-0.247 to 4.753 in.)
DDP	$[P_{TO}-P_{S11}]$ Sensed	0 to 8.3 N/cm^2 (0 to 12 psi)
DPTO	P_{TO} Sensed	1.4 to 13.1 N/cm^2 (2 to 19 psia)
$\frac{DDP}{DPTO}$	$[(P_{TO}-P_{S11})/P_{TO}]$ Sensed	0 to 0.3252 $\frac{N/cm^2}{N/cm^2}$ (0 to 0.4717 psia/psia)

APPENDIX C

UTW ENGINE PRESSURE RATIO DIGITAL CONTROL BLOCK DIAGRAMS AND SPECIFICATIONS

(For Experimental Engine)

Included in this appendix are the detailed block diagrams and the specifications for schedules, gains, time constants, and limits which currently define the digital electronic portion of the engine pressure ratio control for the first build of the UTW experimental engine (Figures 35 through 40 and Tables XII through XV).

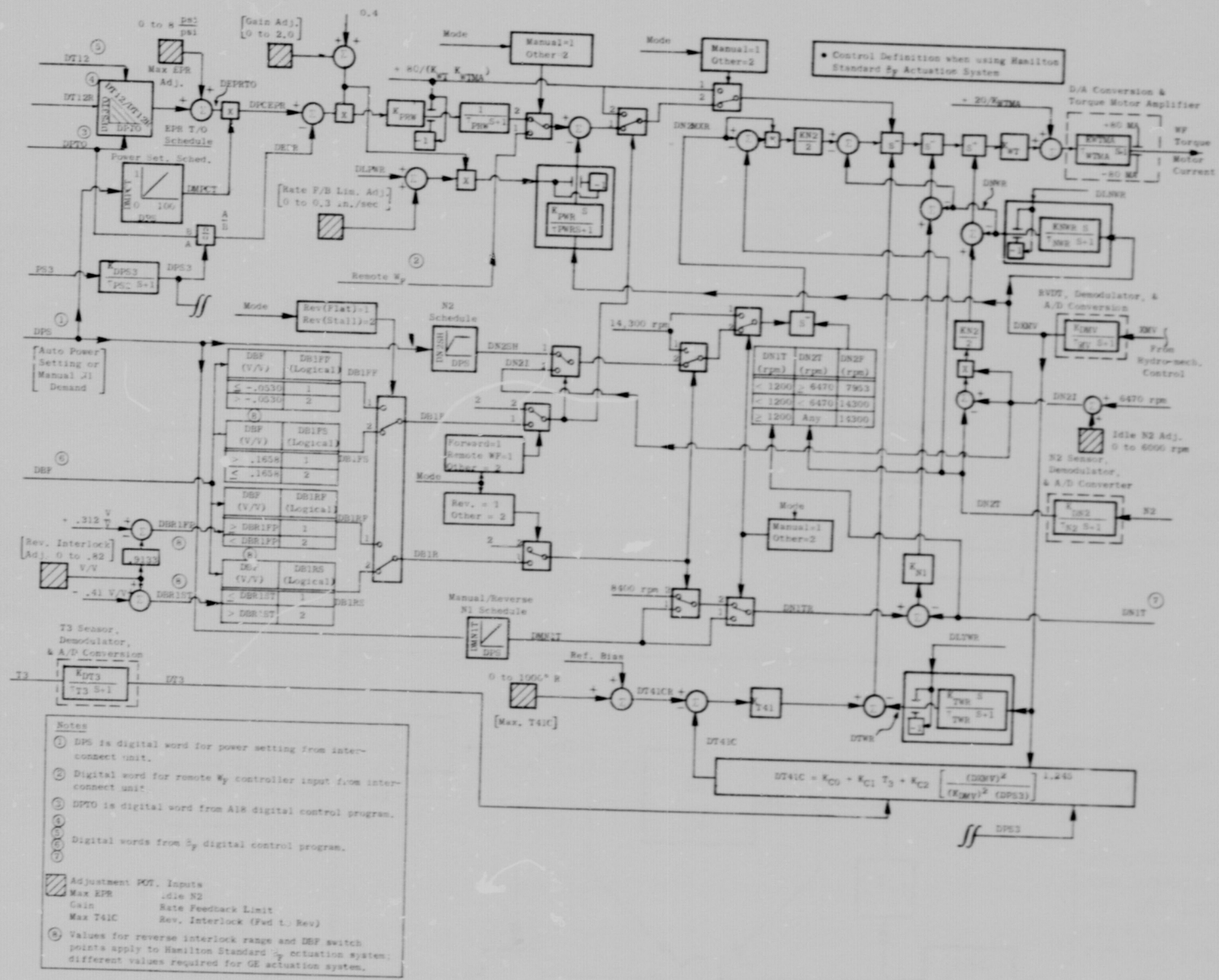

Figure 35. Digital Electronic Engine Pressure Ratio Control.

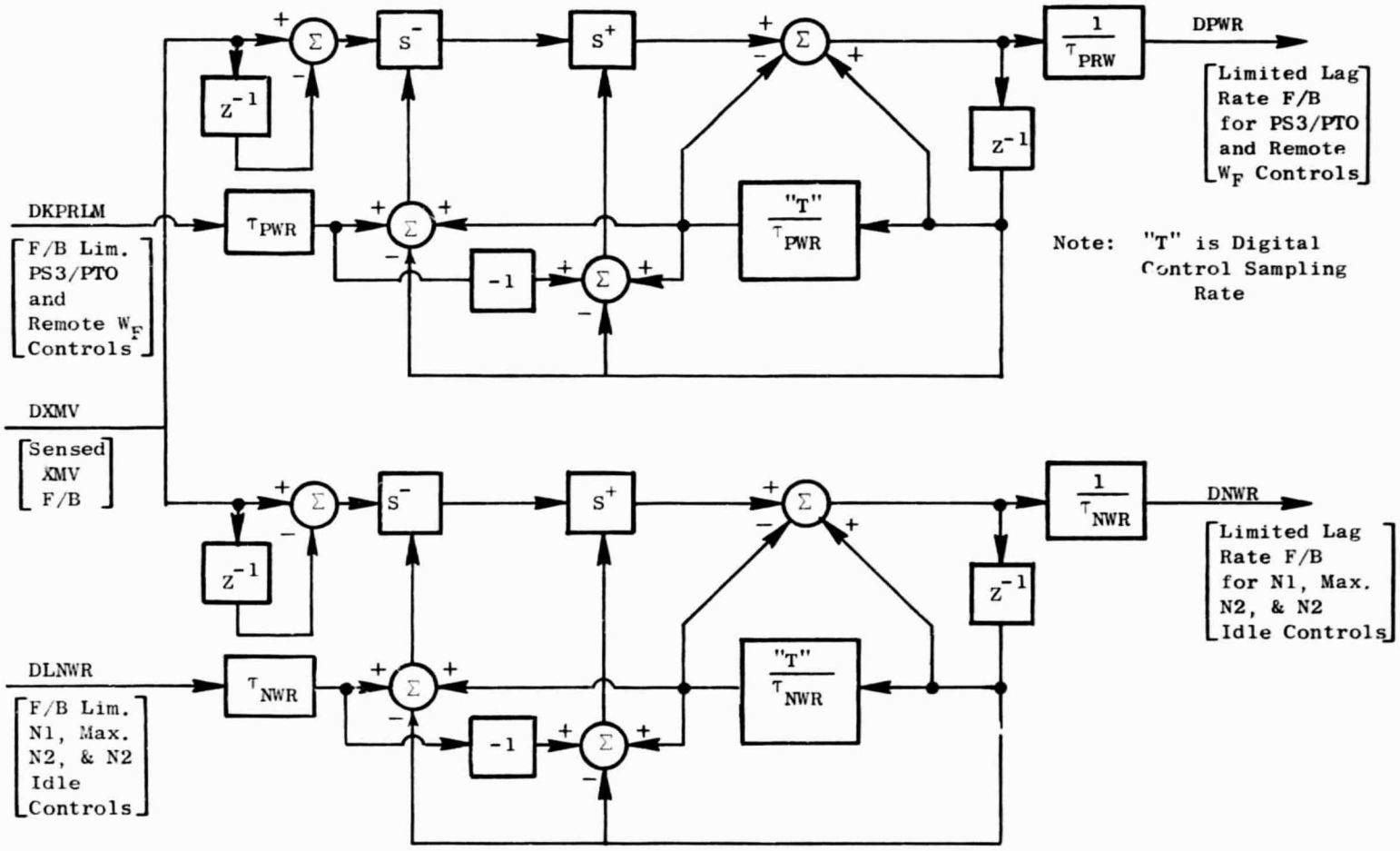

Figure 36. Detail Block Diagrams for Lag Rate Feedbacks with Rate Limits in Digital Electronic Engine Pressure Ratio Control.

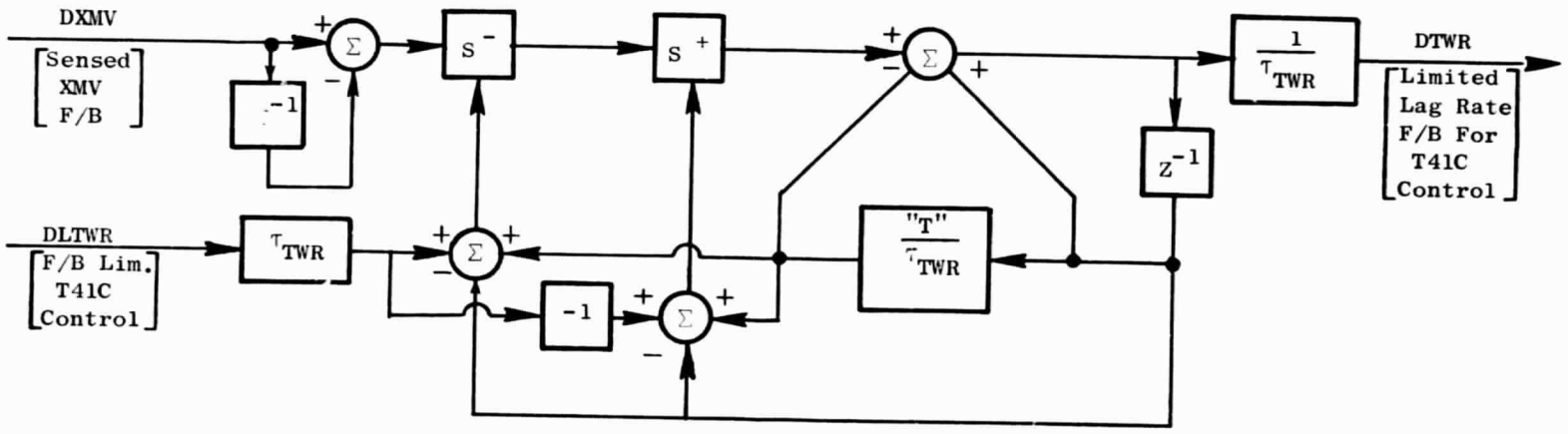

Figure 36. Detail Block Diagrams for Lag Rate Feedbacks with Rate Limits in Digital Electronic Engine Pressure Ratio Control (Concluded).

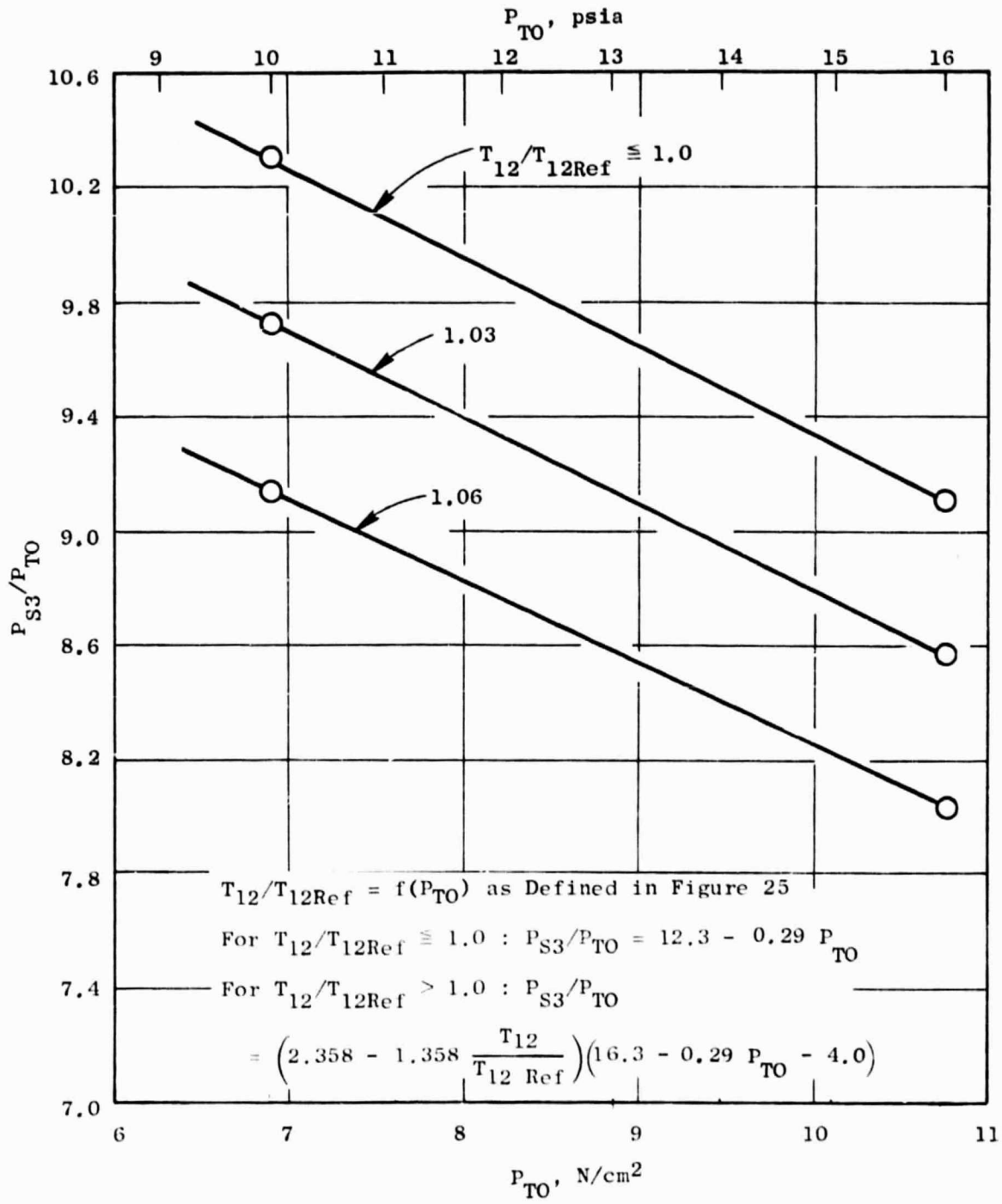

Figure 37. Digital Electronic Engine Pressure Ratio Control Takeoff Power Schedule (for Experimental Engine).

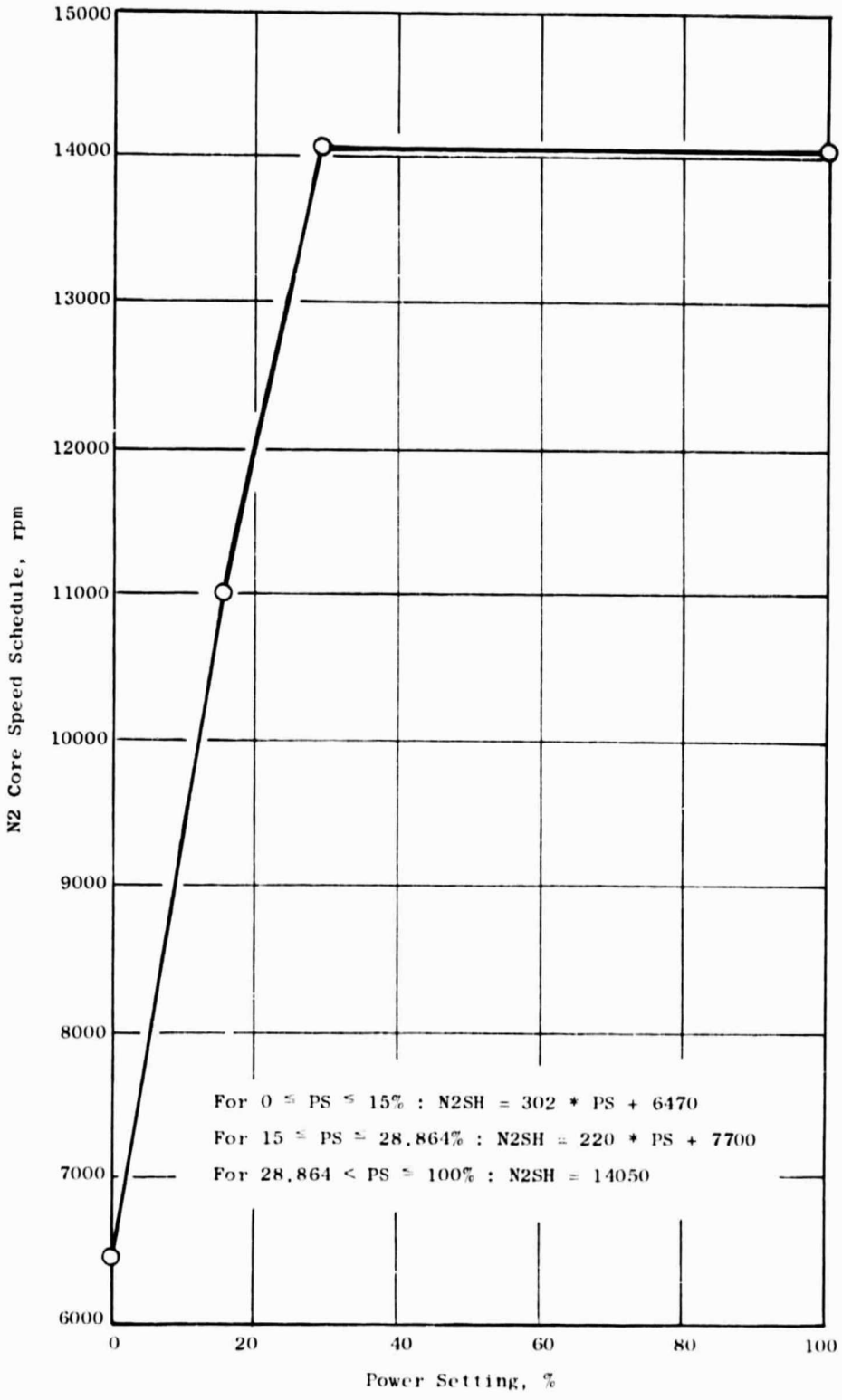

Figure 39. Digital Electronic Control Maximum Core Speed Schedule, Experimental Engine.

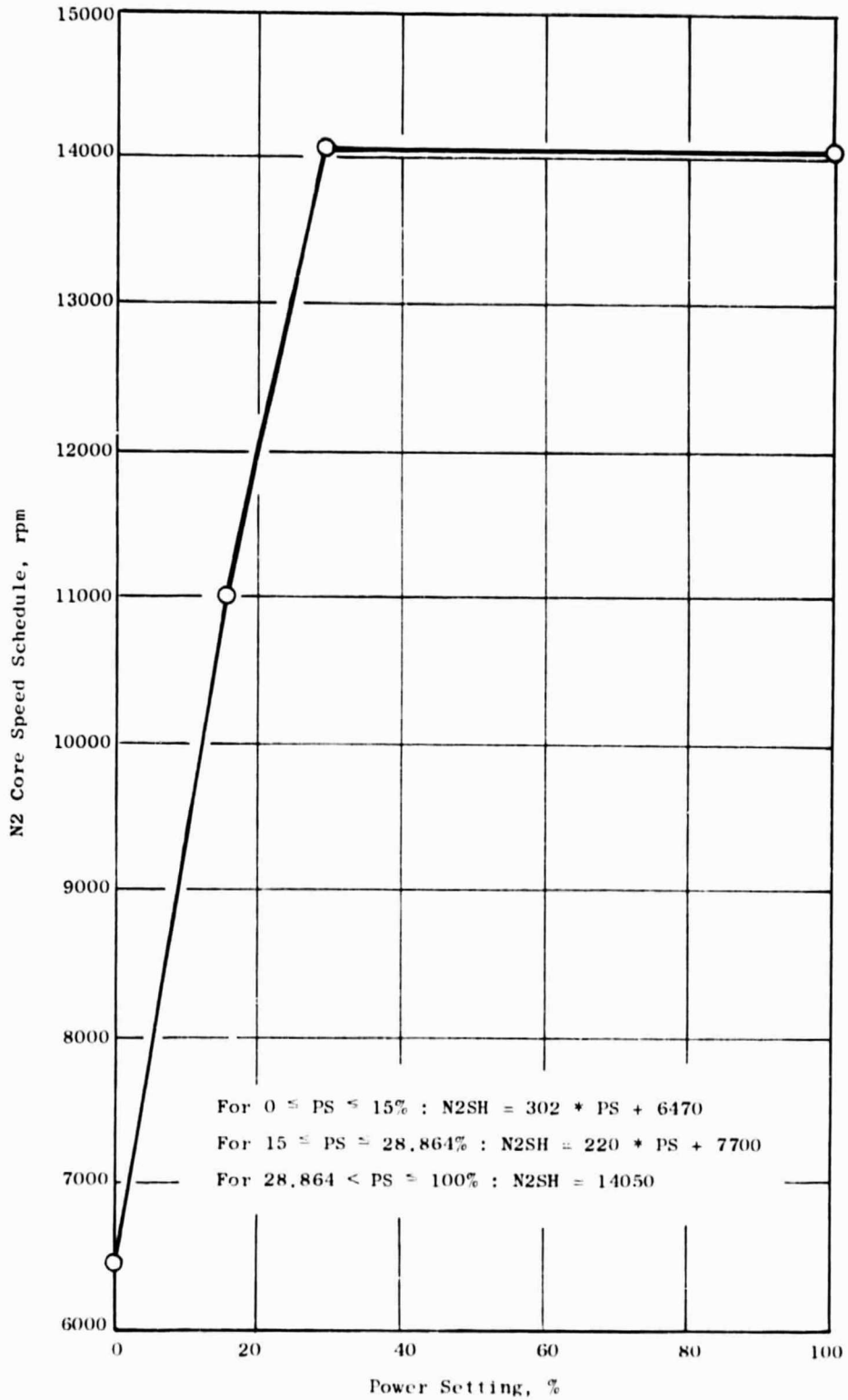

Figure 39. Digital Electronic Control Maximum Core Speed Schedule, Experimental Engine.

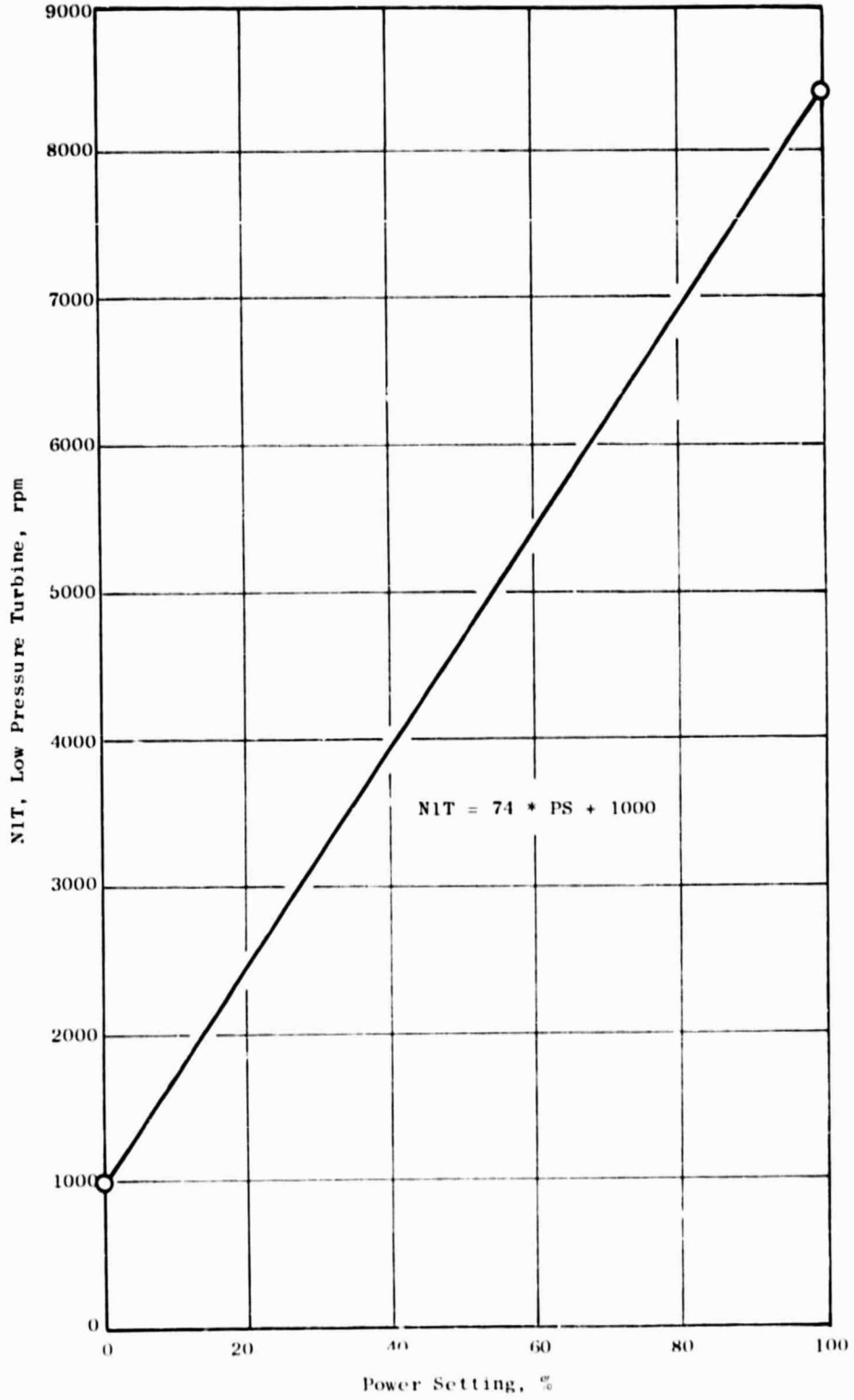

Figure 40. Digital Electronic Control Manual/Reverse Fan Speed Schedule, Experimental Engine.

Table XII. Digital Electronic Engine Pressure Ratio Control Gains.

$\left(\frac{K_{DPS3}}{K_{DPTO}}\right) K_{PRW} K_{WT} K_{WTMA}$	12.00 $\frac{ma}{N/cm^2/N/cm^2}$ $\left(17.40 \frac{ma}{psi/psi}\right)$
$K_{DMV} K_{PWR} K_{WT} K_{WTMA}$	309.1 $\frac{ma}{cm/sec}$ $\left(121.7 \frac{ma}{in./sec}\right)$
$(K_{DN2})^2 K_{N2} K_{WT} K_{WTMA}$	$6.118 \times 10^{-6} \frac{ma}{rpm^2}$
$K_{DMV} K_{NWR} K_{WT} K_{WTMA}$	567.9 $\frac{ma}{cm/sec}$ $\left(223.6 \frac{ma}{in./sec}\right)$
$K_{DNIT} K_{N1} K_{WT} K_{WTMA}$	0.089 $\frac{ma}{rpm}$
$K_{T41} K_{WT} K_{WT} K_{WTMA}$	0.01987 ma/K $\left(0.03576 \text{ ma/}^\circ \text{R}\right)$
$K_{DMV} K_{TWR} K_{WT} K_{WTMA}$	113.59 $\frac{ma}{cm/sec}$ $\left(44.72 \frac{ma}{in./sec}\right)$

Digital Gain Distribution*

$K_{WT} K_{WTMA}$	10.3
$\frac{K_{DPS3}}{K_{DPTO}} K_{PRW}$	1.689
$K_{DMV} K_{PWR}$	11.815
$K_{DN2}{}^2 K_{N2}$	5.940×10^{-7}
$K_{DMV} K_{NWR}$	21.709
$K_{DNIT} K_{N1}$	8.641×10^{-3}
K_{T41}	3.472×10^{-3}
$K_{DMV} K_{TWR}$	4.3417

*The above digital gain distribution is required for the lag rate feedback limits specified in table of digital constants.

Table XIV. Digital Electronic Engine Pressure Ratio Control Constants

Symbol	Description	Value
DLPWR	WF Metering Valve Rate Feedback Limit In EPR/Remote WF Controls	0.010 kg/sec (0.04 in/sec)
DLNWR	WF Metering Valve Rate Feedback Limit In N1 and N2 Speed Controls	0.244 kg/sec (0.096 in/sec)
DLTWR	WF Metering Valve Rate Feedback Limit in T41C Control	0.183 kg/sec (0.072 in/sec)

Table XV. Digital Electronic Engine Pressure Ratio Control Sensors.

Symbol	Description	Range
DN2	Sensed Core Engine Speed	0 to 15492 rpm
DPS3	Sensed Compressor Discharge Pressure	0 to 207 N/cm^2 (0 to 300 psia)
DT3	Sensed Compressor Discharge Temperature	2.19 to 861 K (395° to 1550° R)
DXMV	Sensed Metering Valve Position	0 to 2.065 cm (0 to .813 in.)

APPENDIX D

SYMBOLS

A18	Bypass jet nozzle actual area - cm^2 (sq in.)
A_{BV}	Servovalve area - cm^2 (sq in.)
A_H	Total head area for nozzle actuators - cm^2 (sq in.)
A_{LM}	Effective area to represent hydraulic motor leakage - cm^2 (sq in.)
ALTK	Altitude - m (feet)
A_R	Total rod area for nozzle actuators - cm^2 (sq in.)
A_{SV}	Servovalve area - cm^2 (sq in.)
BETA	HP compressor stator angle - deg.
BETAID	Steady-state HP compressor stator angle - deg.
DLBETA	HP compressor stator error - deg.
DLTO	Adder on free stream total temperature - K (°R.)
F	Force - N (lbs)
FDT_S	Sensed compressor inlet temperature - K (°R)
FN	Net thrust - N (lb)
GR	Gear ratio
HCL42	HP turbine discharge cooling flow enthalpy - J/kg (Btu/lb)
HCL555	LP turbine discharge cooling flow entahlpy - J/kg (Btu/lb)
I_A	Inlet duct Mach number control servo valve amplifier current - mA
I_B	Fan speed control servovalve amplifier current - mA
I_W	Engine pressure ratio control servovalve amplifier current - mA
K	Gain
K_C	Integration gain proportional to reciprocal of core rotor inertia
K_F	Integration gain proportional to reciprocal of total rotor inertia for fan, gearbox, and fan turbine
NIT	Fan turbine speed - rpm
N2REF	Maximum core speed schedule - rpm
NHD	Maximum core speed limit in hydromechanical fuel control - rpm
NHS	Sensed core rotor speed - rpm
N_M	Hydraulic motor speed - rpm
PO	Free stream total pressure - N/cm^2 (psia)
P11	Inlet throat total pressure - N/cm^2 (psia)

C-2

P12	Fan tip inlet total pressure - N/cm^2 (psia)
P13	Fan tip discharge total pressure - N/cm^2 (psia)
P23	Fan hub discharge total pressure - N/cm^2 (psia)
P25	HP compressor inlet total pressure - N/cm^2 (psia)
P3	HP compressor discharge total pressure - N/cm^2 (psia)
P4	HP turbine 1st stage nozzle inlet total pressure - N/cm^2 (psia)
P49	LP turbine inlet total pressure - N/cm^2 (psia)
P5	LP turbine discharge total pressure - N/cm^2 (psia)
PLA	Power lever angle - deg.
PS11	Inlet throat static pressure - N/cm^2 (psia)
PS3	HP compressor discharge static pressure - N/cm^2 (psia)
PS3MEC	Control sensed PS3 - N/cm^2 (psia)
PTO	Engine nacelle probe total pressure (assumed equal to P11) - N/cm^2 (psia)
PW12	Fan tip power - W (hp)
PW2	Fan hub power - W (hp)
PW25	HP compressor power - W (hp)
PW41	Core turbine power - W (hp)
PW49	Fan turbine power - W (hp)
PWPXH	HP rotor power loss - W (hp)
PWPXL	LP rotor power loss - W (hp)
Q_{BV}	Servovalve flow - cm^3/sec ($in.^3$/sec)
Q_{LM}	Hydraulic motor leakage flow - cm^3/sec ($in.^3$/sec)
Q_{VH}	Servovalve flow to head side of nozzle actuators - cm^3/sec ($in.^3$/sec)
Q_{VR}	Servovalve flow to rod side of nozzle actuators - cm^3/sec ($in.^3$/sec)
ROPDEG	Fan rotor pitch angle -deg.
S	Laplace variable - sec^{-1}
SM12	Percent fan stall margin - % @ constant flow
SM25	Percent HP compressor stall margin - % @ constant flow
TO	Free stream total temperature - K (°R)
T11	Inlet throat total temperature - K (°R)
T12	Fan tip inlet total temperature - K (°R)

T13	Fan tip discharge total temperature - K (°R)
T23	Fan hub discharge total temperature - K (°R)
T3	HP compressor discharge total temperature - K (°R)
T4	HP turbine 1st stage nozzle inlet total temperature - K (°R)
T41	HP turbine rotor inlet total temperature - K (°R)
T41C	Control calculated T41 - K (°R)
T42P	HP turbine discharge total temperature before mixing - K (°R)
T49	LP turbine rotor inlet total temperature - K (°R)
T55	LP turbine frame discharge total temperature - K (°R)
T5P	LP turbine discharge total temperature before mixing - K (°R)
T8	Primary jet nozzle throat total temperature - K (°R)
TBLD	Fan blade aero load - cm-N/blade (in.-lb/blade)
TCBETH	Time constant approximation for core compressor stator control - sec.
T_L	Total load torque - cm-N (in.-lb)
W18	Bypass jet nozzle throat total flow - kg/sec (lb/sec)
W25	HP compressor inlet airflow - kg/sec (lb/sec)
W2A	Fan front face total flow - kg/sec (lbs/sec)
W3	HP compressor discharge flow - kg/sec (lb/sec)
W4	Combustor discharge gas flow - kg/sec (lb/sec)
W41	HP turbine rotor inlet gas flow - kg/sec (lb/sec)
W55	LP turbine frame discharge total gas flow - kg/sec (lb/sec)
W6	Primary jet nozzle airflow - kg/sec (lb/sec)
WC41	HP turbine rotor inlet cooling flow - kg/sec (lb/sec)
WFM	Engine fuel flow -kg/hr (lb/hr)
X18	Nozzle actuator position - cm (in)
XMO	Flight Mach number
XM11	Inlet throat Mach number
XMV	Fuel metering valve power position - cm (in.)
XMVACC	Main fuel control valve accel schedule limit - cm (in.)
XMVDEC	Main fuel control valve decel schedule limit - cm (in.)
XNH	HP compressor physical speed - rpm
XNL	Fan physical speed - rpm

Z^{-1}	Z transform
ΔP_M	Hydraulic motor pressure drop - N/cm^2 (psi)
τ	Time constant - sec
θ_M	Hydraulic motor position - revs.
θ_C	Position at downstream side of flex shaft - revs.
θ_i	Position at hydraulic motor side of flex shaft - revs.
(P_S-P_O)	Servovalve pressure drop (supply to return) - N/cm^2 (psi)
β_T	Fan rotor pitch angle (same as ROPDEG) - deg.

REFERENCES

1. Advanced Engineering & Technology Programs Department, Group Engineering Division, General Electric Company, "Quiet Clean Short-Haul Experimental Engine (QCSEE) Under-the-Wing Digital Control System Design Report," National Aeronautics & Space Admininstration, Contract Report No. CR134920.

2. Kuo, Benjamin C., Automatic Control Systems, Prentice-Hall, Inc.; C 1962; pages 419 - 422.